# Modular control analysis and its application to glucose metabolism in *Plasmodium falciparum*-infected erythrocytes

by

Joel Chanse Fisher

*Thesis presented in partial fulfilment of the requirements for the degree of Master of Science (Biochemistry) in the Faculty of Science at Stellenbosch University*

Supervisor: Prof. J.L. Snoep
Co-supervisor: Dr. D.D van Niekerk

December 2021

The financial assistance of the National Research Foundation (NRF) towards this research is hereby acknowledged. Opinions expressed and conclusions arrived at, are those of the author and are not necessarily to be attributed to the NRF.

# Declaration

By submitting this thesis electronically, I declare that the entirety of the work contained therein is my own, original work, that I am the sole author thereof (save to the extent explicitly otherwise stated), that reproduction and publication thereof by Stellenbosch University will not infringe any third party rights and that I have not previously in its entirety or in part submitted it for obtaining any qualification.

Date: 2021/10/07 .....

# Abstract

Disease treatment is achieved through the administration of medication acting at the molecular level which results in changes at the physiological level. These changes are caused by molecular interactions which are usually complex and not well understood. Research often focuses on the mechanism of action of the drug as well as the specificity and binding affinity for the drug target. Such research is important, however, understanding and analysing the drug effects at the physiological level are equally important. The analysis and quantification of these effects can be difficult in large, complex systems. Consequently, such systems are mostly analysed from a broad perspective, often with the implementation of computational techniques including mathematical modelling. Analyses can then be performed using specialised mathematical frameworks, such as modular control analysis. These frameworks often focus on determining the control of groups of reactions (modules) and are usually complex, requiring detailed knowledge of the framework prior to implementation. To this end, modular control analysis was formulated in Mathematica and a software package was constructed to automate the application of the analysis framework. Use of the package was demonstrated on a model of glucose metabolism in *Plasmodium falciparum*-infected erythrocytes. The control of the whole parasite was determined, with the control of the parasite on the flux through itself and the infected erythrocyte determined to be near complete. Use of the package to analyse models with multiple modules was also demonstrated. In this way, use of the modular control analysis framework has been simplified, with only fundamental knowledge required to perform analyses with the software package.

# Opsomming

Siektes word behandel deur die toediening van medikasie wat op molekulêre vlak werk en veranderinge op fisiologiese vlak tot gevolg het. Hierdie veranderinge word veroorsaak deur molekulêre interaksies wat gewoonlik kompleks is en nie goed verstaan word nie. Navorsing fokus dikwels op die werkingsmeganisme van die geneesmiddel sowel as die spesifisiteit en bindingsaffiniteit vir die geneesmiddelteiken. Sulke navorsing is belangrik, maar om die geneesmiddeleffekte op fisiologiese vlak te verstaanen te ontleed is ewe belangrik. Die ontleding en kwantifisering van hierdie effekte kan moeilik wees in groot, komplekse stelsels. Gevolglik word sulke stelsels meestal vanuit 'n breë perspektief ontleed, dikwels deur die implementering van berekeningstegnieke, insluitend wiskundige modellering. Ontledings kan dan uitgevoer word met behulp van gespesialiseerde wiskundige raamwerke, soos modulêre kontrole-analise. Hierdie raamwerke fokus dikwels op die bepaling van die beheer van groepe reaksies (modules) en is gewoonlik kompleks, wat gedetailleerde kennis van die raamwerk vereis voor implementering. Vir hierdie doel is modulêre kontrole-analise in Mathematica geformuleer en 'n sagtewarepakket is saamgestel om die toepassing van die ontledingsraamwerk te outomatiseer. Gebruik van die pakket is gedemonstreer op 'n model van glukosemetabolisme in *Plasmodium falciparum*-geïnfekteerde rooibloedselle. Die beheer van die hele parasiet is bepaal, en dit is gevind dat die parasiet byna volledig beheer op die fluksie deur homself en die besmette rooibloedsel het. Die gebruik van die pakket om modelle met veelvuldige modules te ontleed is ook gedemonstreer. Op hierdie manier is die gebruik van die modulêre kontrole-analise raamwerk vereenvoudig, met slegs fundamentele kennis wat nodig is om ontledings met die sagtewarepakket uit te voer.

# Acknowledgements

I would like to express my sincere gratitude to the following people and organisation:

- my supervisor, Prof. Jacky Snoep, for his guidance throughout the project,
- my co-supervisor, Dr Dawie Van Niekerk, for his input and support,
- Ms Kathleen Green for her input and support,
- the JJJ lab,
- the NRF for their financial support and
- my family and friends for their encouragement and support.

# Contents

# List of Figures

# List of Tables

# Chapter 1

# General Introduction

## 1.1 Motivation

The treatment of diseases is frequently achieved through the administration of medication acting at the molecular level which results in changes at the physiological level. This phenomenon is the foundation of modern medicine and is often taken for granted. These physiological changes are the result of numerous molecular interactions that are usually complex and not well understood. Improving the understanding of these interactions is of particular importance as it can provide insight into possible treatments of disease states through the identification of drug targets. Research often focuses on the mechanism of action of drug candidates and the effects at the molecular level, i.e. the specificity and affinity of binding to the target, however, analysing and understanding the drug effects at the physiological level is equally important. The quantification of these effects can be difficult due to the size and complexity of the biochemical systems involved. Such systems are mostly analysed from a broad perspective, such as a hierarchical approach, often with the implementation of computational techniques including mathematical modelling. A number of mathematical models describing glucose metabolism and regulation at the whole-body level have been constructed. Kang and colleagues [2] discuss a number of these models, each including varying degrees of scope and detail. A whole-body model of glycogen regulation [4] has also been constructed with incorporation into a more detailed hierarchical whole-body model proposed by Snoep and colleagues [3]. The hierarchical approach aims to describe a biochemical system in terms of a number of organisational 'levels', such as reactions within cells and the role of tissues and organs. Mathematical models of such systems are subsequently constructed with detailed reaction kinetics included for cellular reactions/processes, while less detail is included for the 'higher' levels such as that of organs. This simplification into detailed compartments at the molecular level and less detailed compartments at the tissue or organ level enables the effect of the molecular level on the physiolog-

ical level to be quantified. This is achieved as the mathematical model links components at the physiological level to molecular components, directly or indirectly, enabling changes at the molecular level to be associated with corresponding changes at the physiological level. Subsequently, our understanding of the regulatory processes involved is improved, enabling us to better understand how the medication is able to achieve the sought after changes observed at the physiological level. In this way, the mechanisms through which medications are able to alleviate symptoms and treat conditions can be analysed in an appropriate mathematical framework.

The effects of interactions between the drug and the drug target, resulting in changes observed both at the molecular level and the physiological level, can be quantified using metabolic control analysis (MCA). MCA is an analysis framework that quantifies the extent to which fluxes or metabolites are controlled by the components within a system [5]. Subsequently, MCA results in the identification of enzymes that may be suitable drug targets due to their considerable control on the fluxes or metabolites of interest. Drug development strategies can then focus on designing drugs capable of efficiently interacting with the identified target enzymes. In this way, MCA acts as a powerful tool for focusing drug design on specific enzymes known to control the component of interest. While this greatly benefits drug development as well as improves the understanding of the regulatory network within biochemical systems, enzymes determined to exert considerable control may yet prove to be inopportune drug targets due to similarity in host and pathogen enzymes and control distributions. Medication is often designed to target unique enzymes of the target organism, however, this is not always possible. In situations where enzymes with a high degree of similarity with host enzymes are targeted, a number of side-effects may be observed. A prevalent example of this is chemotherapy, which successfully targets cancer cells, however, host cells are also negatively affected. This results in severe side-effects experienced by patients. For this reason, treatment approaches are sought which minimise the negative impact on the host.

Two factors determine the response of a system to an alteration. The first is the control coefficient quantifying system wide effects of the change and the second is the elasticity coefficient which quantifies local effects of the change on reaction rates. Similarity between host and pathogen enzymes, which is likely in conserved pathways such as glycolysis, implies similarity in elasticity coefficients. For this reason, emphasis is often placed on determining the control coefficients of enzymes, however, treatment of diseases usually requires knowledge of the healthy/host enzyme as well as that of the target enzyme. This is necessary as the host and pathogen (target organism) may have comparable control coefficients for the identified target enzyme, targeting of which may lead to undesirable side-effects. It is possible to mitigate the risk of side-

effects when targeting enzymes with a high degree of similarity with a host enzyme. This is achieved by analysing the control coefficients determined for the target enzyme on pathogen metabolism to that of the host enzyme on host metabolism. If the control of the host enzyme on host metabolism is considerably smaller than that of the target enzyme on pathogen metabolism, then the target enzyme may still act as a good drug target. In this way, it is possible that drug interactions with both the target enzyme and the host enzyme may have different effects on the target and host pathways. This is due to a small inhibition of the target enzyme having a considerable effect on pathogen metabolism if the target enzyme exerts a large degree of control, while similar inhibition of the host enzyme could result in a lesser effect on the host/healthy cells if the control of the host enzyme on the pathway is small. In this way, comparison of the control of host and pathogen enzymes provides insight into the viability of the pathogen enzymes as potential drug targets.

The application of MCA to biochemical systems provides insight into the regulatory mechanisms and subsequent interactions, however, such analyses may be difficult to perform on large systems. For this reason, extensions to MCA have been developed that simplify the analysis of large biochemical systems. This is achieved through the determination of the control of groups of reactions as opposed to that of individual enzymes. As such, biochemical systems are often simplified prior to performing analyses. One such technique for analysing large biochemical systems is through the decomposition of the system into a number of blocks/modules consisting of multiple reactions. The control of these groups of reactions can then be determined. Such analyses are considerably easier to perform due to the reduced number of components within the decomposed system. A number of extensions to MCA have been developed enabling such analyses to be performed, including top-down control analysis, hierarchical control analysis, and modular control analysis [6; 7; 1]. The application of such a framework to large, complex biochemical systems may improve our understanding of the interactions within the molecular level as well as the subsequent effects at the whole-body level. To this end, modular control analysis was selected for implementation in a software package automating the application of the framework to models of biochemical systems. This will aid the analysis of large, complex biochemical systems such as those of disease states, where molecular interactions cause the development and maintenance of the disease state. Such models will likely be hierarchical in nature, consisting of both fine and coarse grained components. Modular control analysis would then aid the description of the interactions between the organisational levels (cellular, tissue, or organ) through the determining of overall control coefficients for groups of reactions. In this way, the control of the selected groups of reactions, such as cell or tissue types or even different organs, on components at the physiological level may be quantified. While such an analysis could be performed on models of a number of different disease

states, malaria was selected as an example analysis.

An excess of 228 million malaria cases were reported in 2018, with 93% in Africa [8]. This highlights the severity of the disease both globally and in Africa. For this reason, the malaria disease state was chosen to be analysed using modular control analysis. Glucose metabolism in malaria is an ideal case study for the application of the framework as the parasite, infected erythrocytes, or even tissues and organs may be designated as modules for which the overall control coefficients may be determined. Glucose metabolism is of importance when considering the malaria disease state as the malaria parasite is reliant on glycolysis for survival. Hypoglycaemia and lactic acidosis are also prevalent amongst patients with severe malaria infections and are indicators of poor prognosis [9]. While it is understood that the parasite contributes to the development of lactic acidosis, the contribution is considered to be minor due to the biomass of the parasite being considerably smaller than that of the host [10]. Analysing a whole-body model of glucose metabolism in malaria patients could provide insight into and quantify the contribution of various components of glucose metabolism. In this way, the contribution of the parasite and infected erythrocytes to the development and maintenance of lactic acidosis and hypoglycaemia could be quantified. To this end, modular control analysis was applied to models pertaining to malaria, including a model of glycolysis in the malaria parasite, *Plasmodium falciparum* [11], and glucose metabolism in *P. falciparum*-infected erythrocytes [12]. These analyses acted as demonstrations of the possible applications and benefits of modular control analysis, particularly in the context of analysing glucose metabolism in malaria patients. The application of modular control analysis to models of other disease states may be similarly insightful.

## 1.2 Research Question

Can the contribution of organs and molecular compartments of interest to disease states be quantified using modular control analysis? Diseases often manifest at the whole-body level, however, the underlying causes are generally molecular. An example of such a disease is cancer, where whole-body symptoms are experienced by the individual, yet the cause is a molecular mechanism, such as a mutated gene, which alters the molecular environment to such an extent that the disease state develops. In this way, application of modular control analysis to whole-body models of disease states may improve the understanding of the molecular mechanisms involved in the development of the disease states at the whole-body level. This may aid the treatment of diseases through the identification of compartments (modules) warranting further research due to a high degree of control on the pathway flux. Determining the control of compartments may also improve the understanding of the con-

trol that large structures, such as organs, have on fluxes and metabolites of interest. A software package enabling the automation of such analyses was developed in the Wolfram Mathematica ® coding environment. The package was then used to analyse complex, biologically relevant models of glycolysis in *P. falciparum* as well as glucose metabolism in *P. falciparum*-infected erythrocytes. These analyses demonstrate the computational application of modular control analysis on models of large biochemical systems such that analyses of larger, whole-body models may be performed in future studies.

## 1.3 Aims and Objectives

The aim of this thesis was to construct a software package enabling the application of modular control analysis to mathematical models of biochemical systems and demonstrate its use in a model of a disease state. A model of glucose metabolism in *P. falciparum*-infected erythrocytes was selected to demonstrate the application of the package. The aim was achieved through the completion of five objectives:

The first objective was to identify possible theoretical frameworks that could be used to perform the analysis of the model and select the most appropriate one. Secondly, modular control analysis, the chosen framework, was formulated in a manner that may be easily used to perform analyses. Thirdly, modular control analysis was applied to core models to improve understanding of the application of the framework as well as to identify possible difficulties that may arise during analyses of more complex pathways. Fourth, a software package enabling the automation of modular control analysis was developed such that analyses of large, complex models may be performed in a simplified, streamlined manner. Lastly, complex, biologically relevant models were analysed, including the model of glucose metabolism in *P. falciparum*-infected erythrocytes.

Chapter two provides a review of appropriate literature. Systems Biology is introduced, followed by a review of metabolic control analysis as well as several extensions of the framework which may be suitable for addressing the research question. Extensions of MCA involving modularisation of biochemical systems are prioritised. Whole-body modelling is introduced with emphasis on its application to malaria. Malaria is briefly discussed, providing context supporting it as the focus for application of the package in this study. In this way, the potential theoretical frameworks are reviewed with modular control analysis selected to perform the desired analyses as well as for incorporation into a software package.

Chapter three provides a detailed description of modular control analysis as

well as the application of the framework following formulation in the Wolfram Mathematica® coding context. The application of the framework to simple linear and branched pathways is discussed as they were performed prior to the development of a package automating such analyses.

Chapter four provides demonstrations of the application of the developed package to simple and complex core models. Analyses of models of glycolysis in the *P. falciparum* parasite as well as glucose metabolism in *P. falciparum*-infected erythrocytes were performed using the developed package, with the results of these analyses discussed in the final section of chapter four.

Chapter five provides a general discussion of how the aim of this study was addressed and subsequent objectives achieved. Concluding remarks regarding the benefits of both the framework as well as the developed package are made, as well as possible focuses of future research.

# Chapter 2

# Literature Review

## 2.1 Introduction

The purpose of this literature review is to provide background information on systems biology and introduce several theoretical frameworks as possible approaches to address the research question. In this way, the first objective, selection of an appropriate theoretical framework to perform the desired analyses, will be achieved. The basic principles of systems biology will be introduced with emphasis on mathematical modelling and the applications of such models. Approaches to control analysis will be discussed beginning with traditional metabolic control analysis followed by top-down, hierarchical, and modular approaches. Whole-body modelling will be discussed and its application to the malaria disease state, with a focus on glucose metabolism. The examples provided serve to illustrate the respective concepts and approaches discussed in this chapter.

## 2.2 Systems Biology

Systems biology focuses on studying the relationship between components at the molecular level and effects observed at the physiological level [13]. One of the aims of systems biology is to identify the emergent properties of biological systems. Emergent properties are biological functions resulting from interactions between components of systems that cannot be identified through analysis of the components of the system in isolation [14]. These interactions are studied in a quantitative manner using mathematical models, which differs from qualitative approaches implemented in molecular biology where hypotheses are often based on verbal models [14]. Systems biology can be approached in two ways, namely the bottom-up and top-down approaches. The bottom-up approach involves detailed analysis of individual components and their interaction within the system. This approach is often used to analyse specific reaction pathways using detailed models to describe the specific system, or

portion thereof, under study. The top-down approach is more applicable to linking cellular functions, or other larger scale processes, to the whole-body or genome. As such, the top-down approach involves the use of models encompassing entire cells, tissues, or whole organisms/genomes, which, while less detailed than those of the bottom-up approach, provide insight into the interactions between larger components of systems [14]. It should be noted that the two approaches are complementary, with the bottom-up approach analysing systems in a detailed manner from interactions between individual components progressing towards understanding systems on a larger scale, while the top-down approach begins analysing interactions on a larger scale with less detail and progresses towards interactions between finer grained system components.

### 2.2.1 Mathematical models

Mathematical models are used in systems biology to describe the system and the associated interactions in a quantitative manner. Models are inherently simplifications of the systems being studied with the simplification aiding the analysis and comprehension of the system [14]. While models are constructed based on simplifications of systems, varying levels of detail are required depending on the aim of the analysis. The aim of the analysis is relevant as it determines whether details such as kinetics of each reaction within the system should be included in the model, or whether the stoichiometry of the reactions will be sufficient. Another consideration constraining the detail of the model is the size of the system being analysed. Detailed kinetic models, while beneficial for quantitative analysis of the components of a pathway, may prove difficult to construct for large biochemical systems such as whole-cells, genomes, or whole organisms such as for whole-body models. As such, there are two main types of models used in systems biology, firstly kinetic and secondly stoichiometric models [14].

The complexity of biochemical systems is due to the multitude of interactions between components of systems. Enzymes are components of particular importance as they determine the rates of reactions they catalyse, however, the rate at which these reactions occur is influenced by substrate and product concentrations. It is through the consumption and production of shared metabolites that enzymes interact and, in doing so, exert a degree of control on different components of the system [13]. The dependence of reaction rates on the concentrations of metabolites is described by enzyme kinetics. The kinetics of the enzymes, and therefore of the reactions, can be determined experimentally and then compiled into a mathematical model of the system [13] using e.g. ordinary differential equations to describe the time dependent change in metabolite concentrations as a function of enzyme catalysed reaction rates. These detailed kinetic models can be beneficial for a number of reasons. Firstly, the time course data generated by the model can be compared to ex-

perimental observation to test our biochemical understanding. Secondly, in silico experiments can be performed on the model testing the effect of perturbations of system components enabling, for example, analysis of the control distribution via metabolic control analysis. Analogous 'wet' experiments, may prove infeasible due to the difficulty of performing the required perturbations or due to the associated costs [13].

While kinetic models offer a variety of benefits including the ability to perform quantitative analyses, such as metabolic control analysis, the construction of detailed kinetic models of large biochemical systems is challenging. Nielsen [14] describes a form of stoichiometric models applied to the study of metabolism at a larger scale than is usually analysed by kinetic models. The models are termed Genome-Scale Metabolic Models (GEMs) and describe the entirety of metabolism in an organism, using multiple sources of information. The models are primarily based on the stoichiometry of the reactions with each reaction linked to an enzyme [14] and associated with the presence of a gene. GEMs, and stoichiometric models in general, enable the determination of functional metabolic routes through flux balance analysis using steady state constraints, or structural analyses such as elementary flux mode analysis. Flux balance analysis (FBA) identifies the flux distribution within a metabolic network [15]. FBA can be performed to predict growth rate or production of a metabolite of interest following gene knockout(s) and other imposed constraints during in silico experiments. Elementary flux mode analysis identifies minimal, unique reaction sets at steady state, termed elementary flux modes (EFM) [16]. EFM analysis enables the identification of reactions critical to the metabolism of metabolites of interest, enabling potential gene knockout candidates to be identified. These analyses can be performed computationally and can provide insight into the differences between metabolism of different organisms as well as aiding in the metabolic engineering of organisms beneficial for biotechnological applications [14]. A limitation to stoichiometric models is the inability to perform quantitative analyses, such as metabolic control analysis, due to the limited kinetic information included in the models. This limitation can be addressed by the inclusion of reaction kinetics [14], however, this can prove difficult to achieve for all reactions in the system and is the reason kinetic models are usually limited to smaller biochemical systems. The analysis of mathematical models provides insight into the systems being studied, which would otherwise be difficult to achieve using experimentation and observation alone [13]. As such, several methods of analysing mathematical models of biochemical systems, which can be performed computationally, have been formulated, including metabolic control analysis.

## 2.3 Metabolic Control Analysis

Metabolic control analysis (MCA) is a sensitivity analysis framework that can be used to quantify the control exerted by individual enzymes on steady state system variables, such as pathway fluxes and metabolite concentrations [17]. Subsequently, MCA enables the distribution of control among the components of a system to be quantitatively determined, thereby elucidating the relative importance of each component within the system [18]. An important component of MCA is the elasticity coefficient, which represents the local effect of a perturbation of an effector on a reaction rate. The elasticity coefficient considers solely local effects, as opposed to the control coefficients where system-wide effects are taken into account. As such, an enzyme has as many elasticity coefficients as there are parameters directly affecting it, such as the substrates, products, and effectors of the reactions catalysed by the enzyme [13]. Experimentally elasticity coefficients are determined by perturbing individual metabolite concentrations and measuring the change in the rate of the reactions. Computationally, such as when performing MCA on mathematical models of biochemical systems, the elasticity coefficients can be determined by calculating the partial derivatives of reaction rate equations with respect to the individual metabolite concentrations [19], shown in equation 2.1.

$$\epsilon_{s_j}^{v_k} = \frac{\partial v_k}{\partial s_j} \tag{2.1}$$

with $\epsilon_{s_j}^{v_k}$ the unnormalised elasticity coefficient for metabolite j on reaction k, $v_k$ the rate of reaction k and $s_j$ the concentration of metabolite j. The elasticity coefficients are normalised by multiplying the inverse of the steady state flux of reaction k, ${v_k}^{-1}$, with the unnormalised elasticity coefficient $\epsilon_{s_j}^{v_k}$ and the steady state concentration of metabolite j, $s_j$, as shown,

$$\varepsilon_{s_j}^{v_k} = {v_k}^{-1} \times \epsilon_{s_j}^{v_k} \times s_j \tag{2.2}$$

with $\varepsilon_{s_j}^{v_k}$ the normalised elasticity coefficient for metabolite j on reaction k. The elasticity coefficients described here concern changes in metabolite concentrations, however, elasticity coefficients of parameters, $\varepsilon_p^{v_k}$, may also be determined in a similar manner. The degree of control is expressed as flux and concentration control coefficients, which represent the effect of a perturbation of an enzyme activity, or reaction rate, on a specific flux or metabolite at steady state, respectively. This is expressed as the percentage change in the flux or metabolite concentration at steady state following a 1% perturbation to an enzyme activity [13]. The normalised flux control coefficients can then be expressed as

$$C_{v_k}^{J_i} = \frac{\partial J_i}{\partial v_k} \times \frac{v_k}{J_i} \tag{2.3}$$

with $C_{v_k}^{J_i}$ the normalised flux control coefficient of reaction k on flux i. The normalised concentration control coefficients are defined in a similar manner,

$$C_{v_k}^{S_j} = \frac{\partial S_j}{\partial v_k} \times \frac{v_k}{S_j} \tag{2.4}$$

with $C_{v_k}^{S_j}$ the normalised concentration control coefficient of reaction k on metabolite j. The product of the elasticity and control coefficient is the response coefficient, a quantification of the effect of a parameter change on a steady state variable,

$$R_p^x = C_{v_k}^x \varepsilon_p^{v_k} \tag{2.5}$$

with x a steady state flux or metabolite concentration and p the parameter being perturbed. If the parameter being perturbed affects multiple reactions, the response of a flux to the parameter perturbation is equivalent to the sum of elasticity and control ceofficient products of affected reactions.

MCA can be beneficial for a variety of reasons, as discussed by Moreno-Sânchez and colleagues [20], including i) drug design, specifically identification of drug targets for the treatment of diseases and ii) genetic engineering, such as for the production of compounds of interest. Kacser & Burns [5] and Heinrich & Rapoport [21] originally defined MCA and since its development and formalisation, MCA has been extensively utilised for the purposes of identifying enzymes exhibiting 'significant' control over fluxes and intermediate concentrations of biological or industrial importance.

### 2.3.1 Examples of Application

The examples given in the following and subsequent sections serve as demonstrations and are selected rather arbitrarily, they are not necessarily the most relevant, and certainly do not form a complete set of applications. MCA has been applied extensively to biochemical systems for a variety of purposes, with an example of its application to drug target identification presented by Bakker *et al* [22], where metabolic control analysis was applied to the glycolytic pathway of bloodstream form *Trypanosoma brucei*. The application of MCA established that the control over the glycolytic flux was distributed among several enzymes, namely aldolase (ALD), glyceraldehyde-3-phosphate dehydrogenase (GAPDH), phosphoglycerate kinase (PGK), and glycerol-3-phosphate dehydrogenase (GDH), as well as the glucose transporter. The study by Bakker *et al* [22] also highlighted that the control coefficients determined during the analysis are specific to the conditions under which the analysis was performed. This was emphasised by the altering of the control properties of the enzymes and glucose transporter across different external glucose concentrations. The authors determined that while the glucose transporter exerts the majority of

control over glycolytic flux at low (4 mM) external glucose concentrations, with a flux control coefficient of 0.95, the control gradually shifts to the enzymes ALD, GAPDH, PGK and GDH at higher glucose concentrations, although the majority of flux control is still exerted by the glucose transporter at 8 mM external glucose, with a flux control coefficient of 0.63. In this way, Bakker *et al* [22] determined possible drug targets for the treatment of *Trypanosoma brucei* infection with the glucose transporter being the prominent target, followed by ALD, GAPDH, PGK and GDH. Bakker and colleagues also highlight another consideration that must be evaluated after performing a control analysis to identify possible drug targets. The similarity of the host enzymes or proteins to the identified drug targets must be considered as well as the degree of control that such host enzymes or proteins exert over appropriate host metabolic pathways [22]. This is an important consideration as identifying drug targets in a parasite or pathogen based solely on its flux control is not sufficient and, for instance, the similarity between host and pathogen enzymes as well as the control of the homologous enzyme in the host must be considered.

Metabolic control analysis has also been applied to study glycolysis in *Saccharomyces cerevisiae* through the construction of a kinetic model based on the consistent characterisation of all enzymes involved in the pathway [23]. The authors [23] noted that often mathematical models of biochemical systems are generated using information gathered from different sources. This method can, however, be problematic owing to the characterisation of the enzymes being performed under different conditions. This discrepancy may affect the accuracy of the kinetic models produced as well as the outputs of analyses performed on such models, such as the control coefficients determined during MCA [23]. The authors also discuss the fact that isoenzymes present in pathways are often overlooked during enzyme characterisation and subsequent model construction. As such, the authors aimed to construct a detailed kinetic model of yeast glycolysis, specifically of *S. cerevisiae*, through the consistent characterisation of each enzyme in the glycolytic pathway. An initial model of yeast glycolysis was constructed using information gathered from published data as well as pre-existing models. This allowed MCA to be applied to this preliminary kinetic model such that the control distribution of the pathway was computationally determined. The authors then experimentally measured the kinetics of the reaction determined to be the most controlling on glycolytic flux. This was done such that the turnover number, ($k_{cat}$), enzyme concentration, and affinity constants for each isoenzyme were measured, with the values used to refine the model. This process was repeated until each enzyme and related isoenzymes had been kinetically characterised with the determined values used to improve the model. While the objective was to use experimental data to refine each reaction, if this was not possible then data from literature was used. The refined model was then used to predict the steady state fluxes and intermediate concentrations which were subsequently compared to

experimental values. Adjustments were made to the model parameters where appropriate to minimise discrepancies between the predicted and measured values. MCA was then performed following validation of the model. The application of MCA to the refined model provided insight into the distribution of control in the pathway, which was not obvious upon performing MCA on the initial model. The majority of control on glucose uptake in the initial model was by glucose transport, hexokinase, and ATPase. Along with PFK, these reactions accounted for 95% of the flux control in the initial model. The control distribution in the final model, however, was considerably wider with 10 reactions accounting for 95% of flux control, although the same three enzymes exerted the highest control on glucose uptake.

### 2.3.2 Advantages and limitations

There are a variety of benefits to using metabolic control analysis, including the quantification of control enzymes have on fluxes and metabolites of interest. In this way, MCA provides a quantitative description of why the up-regulation of a single enzyme seldom results in a significant increase in the flux through the pathway, while the up-regulation of multiple enzymes determined to exhibit large flux control coefficients results in a more notable increase in the pathway flux [17]. MCA also enables the determination of the mechanism through which a flux or metabolite concentration is regulated. This is achieved through the determination of elasticity, control and subsequent response coefficients.

While there are many benefits to applying metabolic control analysis to biochemical pathways, there are limitations that must be considered. MCA is constructed based on assumptions that may be difficult to satisfy depending on the specific metabolic pathway to be analysed, as well as the metabolite concentrations and fluxes required for the analysis. Fell [17] discusses the assumptions of MCA with one of the important assumptions being that the system to be analysed must be able to achieve a stable steady state. This is achieved by fixation of the source and sink metabolites preventing the system from reaching equilibrium. In this way, the fluxes and metabolite concentrations in the system remain constant at the steady state as the rates of formation and degradation of the metabolites are equal. Another assumption inherent to MCA is that the metabolite concentrations must be uniform/homogenous such that the metabolites are equally available to enzymes catalysing their reactions [17]. This does not apply to compartments within a cell, for example, where the metabolite 'pools' are separated. In this case, the internal metabolites of the compartment must have a homogenous distribution, with the distribution of metabolites external to the compartment also being homogenous, where the internal and external steady state concentrations need not be identical [17]. While the determination of control coefficients for each enzyme in a pathway

can provide insight into the mechanisms through which flux or metabolite concentrations may be modified, through the use of inhibitors or genetic manipulation among others, this can prove difficult to achieve with large, complex biochemical networks. The difficulty arises during the experimental determination of the metabolite concentrations, steady state fluxes, and the kinetic characterisation of the enzymes in the pathway. The measurement may be difficult to achieve experimentally, or expensive particularly when many reactions are to be analysed. This limitation is compounded by the perturbations that need to be made to the system to determine the desired control and elasticity coefficients. The impact of these experimental limitations can be reduced by performing MCA on a subset of enzymes, fluxes and metabolites.

Extensions to traditional MCA have, however, been developed which enable the system under study to be grouped such that the experimental requirements are reduced, enabling the analysis of large, complex biochemical networks. These extensions are not necessarily replacements to traditional MCA for application to larger networks, but rather alternatives. One such extension of traditional MCA, which allows the treatment of a biochemical system such that a group of reactions (enzymes) may be analysed, is top-down control analysis.

## 2.4 Top-Down Control Analysis

Top-down control analysis is a useful extension to traditional metabolic control analysis as it allows complex metabolic networks to be simplified through the grouping of reactions into reaction 'blocks'. Control analysis can then be performed on the simplified version of the metabolic network consisting of various blocks of reactions and connecting metabolites. A notable contribution to the formalisation of this approach to metabolic control analysis was provided by Brown and colleagues in 1990 [6]. They provide a detailed description of the mathematical derivation as well as application of this method to a linear pathway. Top-down control analysis differs from traditional MCA primarily as the analysis yields overall control coefficients of the reaction blocks. This is in contrast to the control coefficients of individual enzymes determined by traditional MCA. In this way, the two methods are complementary, with successive top-down control analyses determining control coefficients from a broad perspective progressing towards a finer perspective, such as determining control coefficients of individual enzymes. This is achieved by reducing the size of the reaction blocks until only a single enzyme remains within a reaction block at which point the individual control coefficients of each enzyme would have been determined. Traditional control analysis, however, determines control coefficients of individual enzymes, allowing the progressive determination of the control of multiple enzymes on a specific flux or metabolite. As such,

traditional MCA has also been referred to as a 'bottom-up' approach [24].

### 2.4.1 Examples of application

Top-down control analysis has been applied to various biochemical systems illustrating the ease with which this approach to control analysis can be performed experimentally, although traditional MCA is still one of the most applied control analysis frameworks. Simpson and colleagues [25] applied top-down control analysis to the biosynthesis of lysine in *Corynebacterium glutamicum*. This was achieved by grouping a simplified lysine production pathway around the PEP/pyruvate branch point. In this way, three modules were selected with the first encompassing the reactions converting glucose to PEP/pyruvate, the second module encompassing the reactions involved in the TCA cycle and the third and final module encompassing the reactions converting PEP/pyruvate to lysine [25]. During this analysis PEP/pyruvate were treated as a single metabolite due to uncertainty of the anaplerotic pathway reactions stoichiometry regarding the production of lysine from PEP and pyruvate [25]. The authors noted that this grouping results in the equivalent assumption that the pyruvate kinase reaction is at equilibrium as this reaction is responsible for the conversion of PEP to pyruvate. Subsequently, the flux control coefficients resulting from perturbations in pyruvate kinase activity are assumed to be zero [25]. Large perturbations were used to determine the group/overall flux control coefficients through the use of a method described by Small and Kacser [26] allowing the determination of flux control coefficients despite such coefficients being defined on the basis of infinitesimally small perturbations. The group control coefficients determined in this study showed that the control of lysine synthesis resided primarily with the lysine synthesis reactions encompassed in the third module. The analysis also determined that the TCA cycle, the second module, primarily controls itself. As such, the authors noted that the PEP/pyruvate branch point can be considered a rigid branch point as the downstream branches weakly affect one another, while strongly affecting themselves as quantified by the large group control coefficients for the modules on their own fluxes [25].

Top-down control analysis has also been applied to oxidative phosphorylation in liver mitochondria of rats fed with a high-fat diet [27]. The aim of the study was to determine whether the inhibition of mitochondrial adenine nucleotide translocator (ANT) by long chain acyl-CoA (LCAC) is an underlying mechanism linking obesity with type 2 diabetes. The authors addressed this aim firstly by determining whether mitochondrial adaptation occurred as a result of the diet-induced inhibition of ANT, resulting in a reduction of this inhibition. Secondly, the control of ANT on aspects of oxidative phosphorylation was determined, as a high control of ANT on oxidative phosphorylation supports the role of ANT inhibition by LCAC linking obesity with type 2 dia-

betes [27]. Top-down control analysis was performed following decomposition of the oxidative phosphorylation system into 5 modules, a substrate oxidation module, proton leak module, ATP synthesis module, ANT and hexokinase [27]. These modules were considered to be connected by three intermediates, specifically membrane potential ($\Delta\psi$), intra- and extra- mitochondrial ATP/ADP ratios [27]. Although the approach used was top-down control analysis, it is referred to as modular control analysis in the study. This is likely due to top-down control analysis requiring modular decomposition of the system prior to performing the analysis, similar to that of modular control analysis. However, while both methods involve decomposition of the system into modules, there are considerable differences between these two approaches, with modular control analysis being discussed in section 2.6 and differences between the two methods discussed in section 2.6.2.

In their study the high fat diet induced an increase in hepatic LCAC concentration as well as accumulation of the oxidative stress marker $N^{\varepsilon}$ - (carboxymethyl) lysine. The authors determined that there was not a significant change in mitochondrial number between the low-fat and high-fat diets. Aspects of the mitochondrial composition of the hepatocytes from the low and high fat diets were then tested. The authors determined there was a significant reduction in cytochromes c + $c_1$ in the high-fat diet treated group [27]. The respiratory activity of the mitochondria was determined not to be significantly different between the high and low fat diet treated groups. Lastly, modular kinetic analysis was performed to determine if functional components of mitochondrial oxidative phosphorylation were altered between the two diet-treated groups, with no significant difference being determined [27]. The control of ANT on oxidative phosphorylation in mitochondria was determined to be similar in rats of both treatment groups. This supports the role of ANT linking obesity with type 2 diabetes. As such, ANT plays an important role in the development of type 2 diabetes in rats brought on by a high-fat diet resulting in the increase in LCAC, with LCAC inhibiting ANT. This inhibition of ANT is significant due to the considerable control exerted by ANT on mitochondrial oxidative phosphorylation, which suggests inhibition of ANT will have significant effects on mitochondrial function. Prolonged exposure to a high fat diet did not result in metabolic alterations to combat the effects of increased LCAC and associated ANT inhibition [27]. The results of this study may be applicable to humans such that high-fat diets may be linked to the development of type 2 diabetes in humans through the accumulation of LCAC and subsequent inhibition of ANT.

Top-down control analysis is a powerful tool for performing control analysis on large, complex biochemical networks. This method enables the simplification of such networks into a number of reaction blocks (modules) linked by a small number of intermediates, which aides its experimental application. As

with all forms of control analysis, however, this method has both advantages and limitations that must be considered prior to its application.

### 2.4.2 Advantages and limitations

There are several benefits to applying top-down control analysis to a biochemical network, the most evident being the simplification of the network being analysed. The simplification of the network, while decreasing the difficulty of performing the required experiments, results in the quantification of the control that a group of reactions, such as within the mitochondria or other such compartment, exert on a flux or metabolite of interest [24]. This can be particularly beneficial as it allows one to determine, quantitatively, portions of a pathway that exert significant control on the fluxes or metabolites of interest in control coefficients termed overall flux/concentration control coefficients that quantify the control of all reactions in the reaction block on the flux/metabolite of interest. In this way, top-down control analysis can be used as a tool to quantitatively compare portions of a pathway (network) to determine which portions should be further investigated due to those portions exerting significant control. The analysis of these blocks of reactions may provide considerable insight into the importance of cellular structures, tissues, or even organs, on fluxes of interest. Another advantage of top-down control analysis is the ability to determine overall flux control coefficients through the measurement of only fluxes. This can be achieved by the kinetic modification of reaction blocks or the incorporation of new branches [24]. Overall elasticity coefficients (elasticities of the reaction block) can be determined through perturbation of the flux through a reaction block, not the reaction block for which the overall elasticity is being determined, resulting in a change in the steady state concentration of the linking metabolite as well as a change in the flux through the reaction block for which the overall elasticity is being determined. For instance, if two reaction blocks were linked by a single linking metabolite, one could increase the flux through the upstream reaction block enabling the determination of the overall elasticity of the linking metabolite to the downstream reaction block. A similar perturbation may be performed to determine the overall elasticity coefficient for the linking metabolite to the upstream reaction block by perturbing the flux through the downstream reaction block [6]. The flux perturbations can be performed by increasing the concentration of an enzyme in the appropriate reaction block or by introducing a branch which directly affects the concentration of the linking metabolite. While this method for determining the overall elasticities is beneficial, it can only be used if the activity of the reaction block for which the overall elasticity is being determined is not affected by any means other than through the linking metabolite.

As this is a method of control analysis, the assumption that the system is able to reach a stable steady state is inherent and can prove to act as an

experimental limitation. The time scale of the reactions involved must also be considered as there may be significant differences in the time scales of the reactions that can result in control coefficients varying over time [6]. A limitation of top-down control analysis is that the overall control coefficients determined during the analysis do not provide insight into the individual control coefficients of the enzymes within the reaction blocks. As such, the distribution of control among the individual enzymes is unknown. Further analysis of a reaction block determined to have a large control coefficient could reveal small individual control coefficients which sum to the large overall control coefficient of the reaction block. In contrast, a small overall control coefficient may be the result of a large negative control coefficient and multiple small positive control coefficients for the enzymes in the reaction block (or *vice versa*). As a result, while overall control coefficients are useful indicators of the control of reaction blocks, the limitations of these coefficients should be considered. Another limitation to top-down control analysis is the number of independent fluxes that may be present in a reaction block. A single independent flux must be present for each reaction block [28]. While this may appear to be a considerable limitation, it is generally possible to restructure the reaction blocks such that each consists of a single independent flux. An alternative to the proposed restructuring is provided by modular control analysis which will be discussed in section 2.6.

An alternative to traditional MCA and top-down control analysis is hierarchical control analysis. Hierarchical control analysis is similar to the top-down approach in that the biochemical system to be studied is separated into groups of reactions. These groups are, however, not linked by net mass flow. In this way, hierarchical control analysis can be considered an extension of the top-down approach for application to hierarchical systems, such as signal transduction networks [24; 29].

## 2.5 Hierarchical Control Analysis

Hierarchical control analysis, like top-down control analysis, is a tool for performing control analysis on large, complex biochemical networks. Hierarchical control analysis, however, specifically addresses biochemical systems consisting of groups of reactions (or modules) regulating other modules solely by regulatory effects. In this way, there is no net mass flow between the modules, which are subsequently referred to as the levels of the system [29]. An important contribution to the development and formalisation of hierarchical control analysis was by Kahn and Westerhoff in 1991 [29] where they initially referred to the method as the cascade control theorem. In their publication they provide the mathematical development of the method while also applying the method to an example system, the regulatory cascade controlling glutamine-synthetase in

enteric bacteria. Cascade control theory was progressively expanded in their paper [29], with the initial cascade control theorem being applicable to linear cascades lacking feedback loops. A linear cascade without any feedback loops is characterised by a system containing multiple modules, with module 1 regulating itself and module 2, module 2 regulating itself and module 3, in a linear fashion, progressing until the last module in the cascade which regulates only itself. In this form, the theorem could describe how the control of the modules in a linear cascade was regulated in terms of the control of the modules on themselves as well as on one another. This form of the theorem was then generalised such that non-linear cascades could be analysed providing no feedback loops were present in the cascade. In this way, the theory was extended such that a module in the cascade could regulate any number of modules downstream of itself, such as module 1 being able to regulate modules 2,3,4,5...n with n denoting the last module in the cascade [29]. While this was a considerable improvement to the applicability of the theorem, the authors noted that the inability to apply the theorem to biological systems consisting of one or more feedback loops would act as a considerable limitation. As such, the authors further developed the theory into a two-module control theorem which allowed for a feedback loop in a two-module system [29]. This was then extended to a cascade system consisting of a cyclic feedback loop. This form of the theorem, termed the cyclic feedback control theorem by the authors, could be applied to regulatory cascades where each module only regulated itself and the module immediately downstream, such that module 1 regulates only itself and module 2, with the final module in the cascade regulating itself and the first module and in this way completing the cycle of feedback. The final extension discussed by Kahn and Westerhoff in their publication [29], concerned their feedback loop control theorem. This form of their control theorem for regulatory cascades allowed the control analysis of a linear regulatory cascade consisting of a single feedback loop. As such, only one module in the cascade could regulate an upstream module, with an example being an 8 module cascade where module 5 regulates both module 6 as well as an upstream module such as module 2. The cascade control theorems presented by Kahn and Westerhoff were later extended by Hofmeyr and colleagues [7] such that a more general theorem was developed. The method presented by Hofmeyr and colleagues allowed for the existence of multiple feedback loops within a multi-level (or multi-module) biochemical system. However, repeated application of the two-module control theorem [29] enabled application of the theorem to systems consisting of multiple feedback loops, resulting in a similar analysis to that which would be achieved by the method presented by Hofmeyr and colleagues [7].

### 2.5.1 Examples of application

Hierarchical control analysis has been experimentally applied to DNA supercoiling in *Escherichia coli* with a focus on the regulatory role of gyrase and topoisomerase I [30]. Snoep and colleagues [30] determined the inherent control coefficients of both gyrase and topoisomerase I on DNA supercoiling to be 0.17 ($\pm$0.01) and -0.14 ($\pm$0.03) respectively. The inherent control coefficients represent the control of each enzyme on DNA supercoiling following a modulation to the transcription level of the enzyme after which the enzyme concentration is fixed. The system is then allowed to attain a new steady state. These inherent control coefficients are equivalent to the local or intramodular control coefficients described by Hofmeyr and Westerhoff [7], where each level is considered in isolation [18]. Snoep and colleagues [30] then determined the global control coefficients, termed integral control coefficients by Hofmeyr and Westerhoff [7], of gyrase and topoisomerase I to be 0.13 and -0.13 respectively. The summation of the inherent control coefficients of gyrase and topoisomerase I on DNA supercoiling is equivalent to 0, within the bounds of experimental error, as is the summation of the global control coefficients for gyrase and topoisomerase I on DNA supercoiling. This consistency, noted by the authors [30], provides evidence supporting the authors assumption that gyrase and topoisomerase I are the main contributors to the degree of wild-type supercoiling at steady state. The authors also determined the distribution of the homeostasis of DNA supercoiling in wild-type *E. coli* at the activity level and at the gene expression level, with 72% of the homeostasis occurring at the level of enzyme activity and 28% at the gene expression level. In this way, the contribution of the regulation of gene expression as well as of the regulation of enzyme activities was determined. The authors also determined the individual contribution of the regulation of gene expression for both gyrase and topoisomerase I on homeostatic control. The regulation of gyrase expression contributed 21%, while the regulation of topoisomerase I contributed 7% to the homeostasis of DNA supercoiling [30]. This application of hierarchical control analysis provides an indication of the appropriateness of the method to determining, in a quantitative manner, the distribution of control in a multi-level biochemical network.

Another example of the application of hierarchical control analysis is provided by Westerhoff and colleagues [31], where hierarchical control analysis is applied to an example ecosystem, that of the production of acetic acid from glucose such as occurs during the souring of wine. The purpose of this study is to demonstrate the application of hierarchical control analysis to microbial ecological systems. This is possible with the example ecosystem analysed in the publication, however, it may also be possible to apply hierarchical control analysis to other ecological systems provided the system can attain a stable steady state and the degree of coupling between the feeding and growth rates is treated explicitly, as stated by the authors. The analysis of the ecosystem

under study demonstrates the similarity between the ecosystem and that of a biochemical network [31]. As such, the species for which control is determined can be biological or chemical, with regards to the hierarchical control analysis of an ecological system. In this way, yeast and *Acetobacter* were both treated as species during the analysis, along with ethanol. The system is considered hierarchical as it is analysed from the perspective of three levels being present, one each for yeast, ethanol, and *Acetobacter*, which regulate one another indirectly, noting that there is no conservation of mass in this system. In this way, the system analysis is comparable to that of hierarchical control analysis and was analysed accordingly. While the authors noted the magnitude of the elasticities used during the analysis may not be correct, it is stated that the elasticities chosen may be realistic enough for any observations made based on the results of the analysis to still be pertinent [31]. In light of this, the authors noted the analysis yielded interesting results regarding the control on ethanol concentration, with yeast exerting no control over the concentration of ethanol. It was also observed that *Acetobacter* exerts strong control over the yeast concentration, which is of interest due to the pH and acetic acid concentrations being buffered. This application of hierarchical control analysis demonstrates that this approach, while applicable to large, complex biochemical systems such as those of signal transduction, may also be used to analyse ecosystems under steady state conditions and in doing so improve understanding of the distribution of control in ecological systems [31].

### 2.5.2 Advantages and limitations

Hierarchical control analysis is a powerful extension to traditional MCA as it enables the determination of control distribution in biochemical systems consisting of multiple levels that are not connected by mass flow. This is particularly advantageous as traditional control analysis does not address the distribution of control over multi-level systems such that the control different levels exert over one another could be quantified. In this way, hierarchical control analysis extends the scope of application for control analysis to systems of biological importance including gene expression and signal transduction. While this is itself a significant advantage of the method, another is the reduction of complexity resulting from the decomposition of the system into levels (or modules). The degree of complexity can then be increased upon successive analyses if more detail is sought, similar to successive analyses using top-down control analysis.

While there are various benefits to the use of hierarchical control analysis, there are limitations. One such limitation is that the levels may only regulate one another through effectors such that the effectors are not converted during the regulation of other levels in the system [32]. This limitation is based on assumptions, which while generally applicable to biochemical systems, may

prove limiting. One such assumption is that the concentration of the effector is much higher than that of the enzyme it regulates, with the resulting enzyme-effector complex being negligible relative to the total effector concentration [32]. Another assumption is that enzymes acting as catalysts are not altered by the reactions they catalyse. While these assumptions are generally applicable, each should be validated prior to hierarchical control analysis being performed [32]. Each level in the system may not exchange net mass flow while at steady state, as has been previously mentioned, however, another limitation is inherent in hierarchical control analysis regarding conserved moieties. Conserved moieties may not be shared between levels thereby linking them. They can, however, be present within individual levels [32].

## 2.6 Modular Control Analysis

Both hierarchical and top-down control analysis are useful extensions of traditional MCA, each with their advantages and limitations, and we now introduce modular control analysis, a third approach to perform control analysis on complex biochemical systems. Modular control analysis, as suggested by the name, involves the decomposition of the system being analysed into modules. This decomposition differs from that used in the hierarchical approach as modular control analysis, similar to top-down control analysis, allows for net mass flow between modules. Modular control analysis, while similar to the top-down approach, differs in two main aspects. Firstly, modular control analysis allows for metabolites within a module to affect reactions within other modules, provided the interactions conform to specific constraints, whereas the top-down approach does not allow for metabolites within modules to interact with components in other modules [24]. Secondly, this method allows for the presence of multiple independent bridging fluxes linking modules, as opposed to the top-down approach where only a single independent bridging flux is permitted [24]. As such, modular control analysis is considered a more general approach than top-down control analysis.

A notable contribution to the formalisation of modular control analysis was by Schuster and colleagues [1]. A detailed mathematical derivation of the formalisation of the approach was provided, with aspects of the formalism applied to biochemical pathways. The formalism describes the decomposition of the system to be analysed into modules of two types. Type 1 modules (module 1) are considered 'black-boxes' where detailed information regarding the reactions and metabolites within the module are assumed to be unknown and are not considered during the analysis [33]. Modules of type 2 (module 2) are considered to be under observation such that the reactions and metabolites are known and any changes are observable [33]. This decomposition of the system results in reactions being partitioned such that they can be considered

module 1 or module 2 reactions, however, reactions linking modules of type 1 with modules of type 2 are termed bridging reactions [1]. A generalised schematic of this decomposition is shown in Figure 2.1 [1].

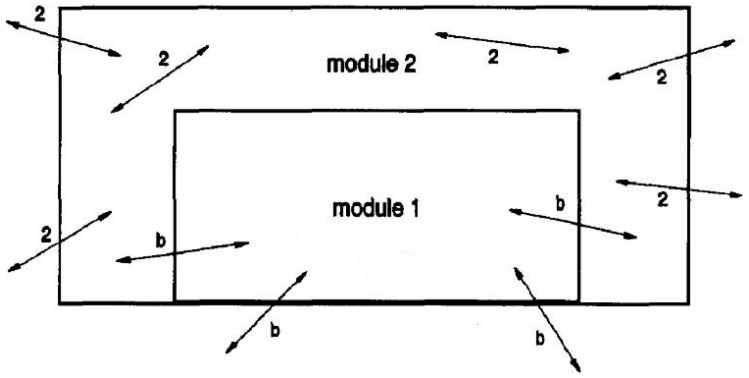


**Figure 2.1:** Schematic of the generalised modular decomposition of a metabolic network, adapted from the publication by Schuster and colleagues [1], with module 1 and 2 representing type 1 and 2 modules respectively. The arrows indicate the reactions in the network. Arrows labelled with a "b" indicate reactions bridging module 1 with module 2 or the external environment, and arrows labelled with a "2" indicate the reactions present in module 2.

Following determination of the independent bridging reactions, the analysis is performed such that the control of the modules on the bridging reactions, as well as on components of module 2, are determined. Schuster and colleagues [1] demonstrated the extension of the method where a system can be analysed with two modules of type 1. While the example demonstrated in the publication represents a simple decomposition such that only metabolites link the two type 1 modules, shown in Figure 2.2, the authors describe how the method can be applied to a system decomposed into any number of type 1 modules connected by both metabolites and reactions, such that the type 2 module consists of both reactions and metabolites [1]. Modular control analysis was then applied to a system consisting of glycolysis, the TCA cycle and oxidative phosphorylation where oxidative phosphorylation was considered as a type 1 module. Modular control analysis was subsequently applied to a model of metabolic regulation including gene expression [1]. This is of particular importance as previously such analyses were performed in terms of unconnected modules, such as by the application of hierarchical control analysis, whereas the authors demonstrate that this approach enables the substrates for protein synthesis to be considered as metabolites, therefore affecting the regulatory process [1].

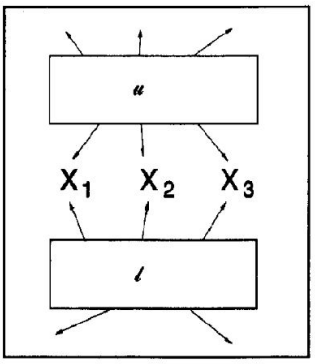


**Figure 2.2:** Simplified schematic of a biochemical network decomposed such that two type 1 modules are defined, modules u and l [1]. Internal reactions of the type 1 modules are not shown. This decomposition is such that the type 2 module does not contain any reactions, as such the arrows indicate the bridging reactions of the two type 1 modules. The two type 1 modules are linked by metabolites $X_1, X_2,$ and $X_3$.

### 2.6.1 Examples of application

Modular control analysis has been applied to slipping enzymes by Schuster and Westerhoff [34]. Slipping enzymes are enzymes that catalyse two (or more) incompletely coupled reactions. The authors noted that although the modular approach was initially formulated for the determination of the control of modules consisting of groups of reactions at a larger scale, the approach could be applied to slipping enzymes as the slipping enzyme could be considered a type 1 module with multiple independent bridging fluxes. Modular control analysis was subsequently applied to a system of non-phosphorylating mitochondria at steady state with the respiratory chain considered a type 1 module. The application describes how control coefficients can be defined for slipping enzymes following modular control analysis, however, for this approach to be applicable to the specific slipping enzymes to be studied, enzyme-intermediate complexes may not directly affect reactions catalysed by other enzymes and conservation relations may not link different modules as this allows the two conditions of modular control analysis to be fulfilled. The authors noted that measuring slip rates may prove difficult experimentally, however, the theoretical application described may prove beneficial for future studies aimed at determining the control of slipping enzymes.

Modular control analysis has also been applied to experimentally determine the control of membranes and cytosol on the growth of the yeast *Kluyveromyces marxianus* [35]. This study was performed to test and quantify the extent of control that membrane processes exert over the specific growth rate of *K. marxianus* using modular control analysis. It was assumed that if the control on maximal growth rate resided primarily in membrane-located enzymes, an increase in cell surface area relative to cell volume should result in an in-

crease in growth rate. This could be caused by spacial limitations affecting the membrane-located enzymes. A pH-auxostat was used to provide a selective pressure for yeast cells with a higher specific growth rate. The authors observed an increase in the surface area relative to the volume of cells with a higher growth rate. Despite this observation supporting the assumption that the control on growth rate resides largely in membrane surface area and associated membrane processes, a quantitative determination was sought. The authors therefore proceeded to perform the analysis such that all membrane-located enzymes were considered components of module 1, while the intracellular enzymes were considered components of module 2. The cells were cultivated such that two steady states were achieved with a difference of approximately 30%. The steady states used in this study refer to the situation where the pH-auxostat is left unchanged for a minimum of 7 generations. Microscopy was used to estimate surface to volume ratios with relevant measurements made to determine approximate cell surface area and volume. The cell volumes were approximately equal despite the observed cell morphology changes, with the first steady state, with a lower growth rate, comprising of spherical cells and the second steady state, with a higher growth rate, comprising of elongated cells. The overall control coefficient of the membrane surface was then determined to be approximately 0.9. As such, this study quantitatively determined the control that the cell membrane surface has on the maximal growth rate of *K. marxianus*.

### 2.6.2 Advantages and limitations

Modular control analysis is a tool for analysing large, complex biochemical pathways where the application of traditional MCA would prove difficult. There are several advantages to this method of analysis, including the modular decomposition that can be applied to biochemical systems. This approach to control analysis allows for modules of type 1 to be defined such that the components of these modules need not be considered during the analysis [1]. This can prove advantageous as it allows the analysis to be performed on systems where components of the system are difficult to measure, provided they can be considered components of a type 1 module. Another advantage is that the components of module 2 are able to affect reactions in modules of type 1, as opposed to top-down control analysis where metabolites within a module could not affect reactions within a different module [1]. Modular control analysis allows for a system to be decomposed such that modules may have multiple independent bridging fluxes, which eases the constraints imposed by top-down control analysis. This allows for more components of biochemical systems to be considered part of 'black-box' modules, such as is demonstrated by Schuster and colleagues [1] where oxidative phosphorylation was considered a type 1 module during their analysis, with the module having multiple bridging fluxes and more than one independent bridging flux being identified.

Modular control analysis, while a powerful tool for analysing complex biochemical systems, makes use of several constraints and assumptions which may act as limitations during its application. There are two constraints imposed during the modular decomposition that may act as limitations. The first constraint imposed is that no conservation relations may link metabolites in a type 1 module to the metabolites in a type 2 module [28]. The second constraint is that metabolites in type 1 modules may not act as effectors of reactions in a type 2 module [28]. While these conditions may limit the application of modular control analysis to biochemical systems, it may be possible to structure the modular decomposition such that these conditions are adhered to, similar to what may be required to perform the top-down control analysis as has been discussed previously. Another limitation concerns an aspect of modular control analysis inherent to most approaches to control analysis, the reliance on linear approximations [28]. As with most other forms of control analysis, modular control analysis results in the determination of control coefficients, including overall control coefficients, which quantify the effect infinitesimal changes in reaction rates (or enzyme activities) at steady state will have on the system. As a result, the control coefficients may not accurately describe the effect that large changes will have on the system. Another limitation to this modular approach is that although type 1 modules are considered 'black-boxes', where information regarding components within the module is not used during the analysis, some level of detail is required. This becomes evident during the modular decomposition of a system where the decomposition must fulfil the two aforementioned conditions [28]. In this way, at least limited information regarding the components of type 1 modules must be known despite such information not being explicitly used to perform the analysis. Another aspect of the components of type 1 modules that is generally required is the stoichiometry of the reactions within the module [1]. The stoichiometry of the reactions enables the determination of the independent bridging fluxes, which are required for the analysis. While this is a limitation, Heinrich and Schuster [33] describe an alternative if the stoichiometry of the reactions within a type 1 module are unknown. The required information may be determined by observation such as by determining the balance of influx and efflux of atoms for the type 1 module. This approach to control analysis is an extension of the previously discussed top-down control analysis addressing several limitations, however, this results in increased complexity that may make experimental application of the method difficult [24]. Consequently, this approach to control analysis has not been extensively used.

The frameworks that have been discussed can be used to analyse suitable experimental data or mathematical models. In this thesis, mathematical models of glycolysis in the malaria parasite as well as glucose metabolism in infected erythrocytes will be analysed, with future research focused on the analysis of a

whole-body model of glucose metabolism in malaria patients, as well as other large models such as whole-body models of other disease states.

## 2.7 Whole-body modelling

Mathematical models used in systems biology provide quantitative descriptions of their respective systems. The detail included in such models varies depending on the goals of the analysis to be performed. Whole-body models are often coarse grained with limited molecular information. A number of whole-body models have been constructed with many focused on glucose metabolism. Kang and colleagues [2] discuss a number of mathematical models of whole-body glucose regulation. The dynamics of blood glucose are the focus of these models, with the inclusion of insulin and glucagon components incorporated into more detailed models. One of the simpler models discussed is that of a minimal model consisting of limited glucose and insulin kinetics and a remote insulin compartment. This model was then extended to include an insulin distribution space. While these models reproduced observed plasma glucose and insulin dynamics, the effects of glucagon were not included and the limited kinetic information prevented the detailed dynamics of glucose and insulin from being simulated. Consequently, more comprehensive models have been constructed, an example of which is illustrated by Figure 2.3, a schematic of a combined model of whole-body glucose regulation.

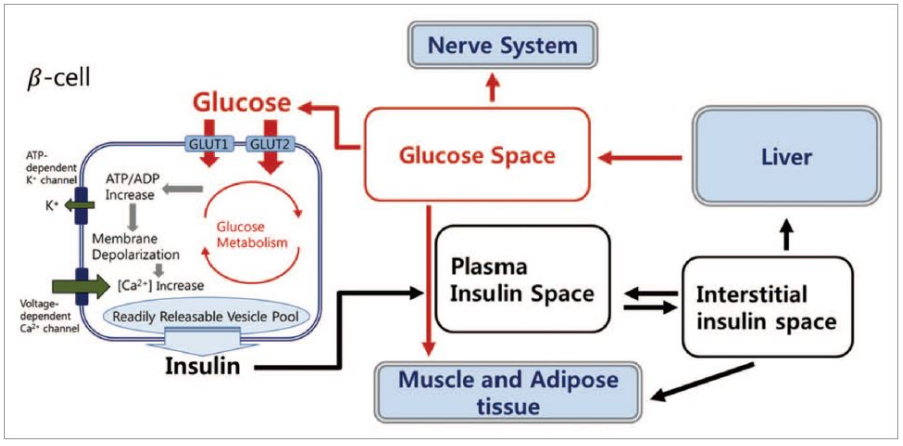


**Figure 2.3:** Schematic of a whole-body glucose regulation and insulin secretion model [2].

The incorporation of detailed enzyme kinetics into whole-body models could improve the simulation and predictive capabilites of the models. Subsequently, Snoep and colleagues [3] describe the construction of a model consisting of detailed reaction kinetics for certain compartments, while other compartments are modelled in less detail, termed coarse-grained compartments.

The construction of such a model on a whole-body level, such as of a disease state, could be described as a multi-level model owing to multiple biological levels being included in the model [3]. Whole-body models constructed in this manner enable quantification of the effect of molecular effects on the physiological level. This is of great importance for disease states, with type 2 diabetes and malaria examples of disease states for which whole-body modelling would be beneficial. Modelling of the insulin signalling cascade at the whole-body level would be ideal for investigating diabetes, with glucose metabolism at the whole-body level ideal for investigating malaria. For the purposes of this review as well as this research project, malaria has been selected as an illustrative example. Snoep and colleagues [3] discussed the construction of a model for glucose metabolism in malaria patients owing to the metabolic changes occurring in patients as a result of the disease warranting quantitative analysis of the disease state at a whole-body level aiming to further understanding of the disease.

### 2.7.1 Malaria

Malaria is a severe disease of global significance with an estimated 228 million cases globally in 2018 [8]. Malaria has a particularly severe impact on Africa with 93% of the cases in 2018 occurring in Africa and the majority of remaining cases occurring in the South-East Asia and Eastern Mediterranean regions with 3.4% and 2.1% of global cases, respectively [8]. Malaria was responsible for 405 000 deaths globally in 2018, with Africa accounting for 380 000 (94%) of the fatalities. This represents a considerable decrease from the 533 000 fatalities observed in Africa in 2010, however, the rate of decrease of malaria mortality has reduced since 2016 [8]. Malaria is caused by an intracellular parasite from the genus *Plasmodium* of which there are five species capable of infecting humans, namely *P.malariae*, *P.vivax*, *P.ovale*, *P.knowlesi* and *P.falciparum* [36]. The species responsible for the majority of infections is *P.falciparum*, which accounts for 99.7% of the estimated malaria cases in Africa, 50% of the cases in the South-East Asia region, 71% of Eastern Mediterranean cases and 65% of Western Pacific region cases in 2018 [8].

The life cycle of *P. falciparum* includes three stages, specifically the mosquito stage and the human stage, which is separated into liver and blood stages [9]. The cycle within the human host begins following blood feeding of a human host by a female *Anopheles* mosquito infected with *P. falciparum* sporozoites. The sporozoites within the mosquito must be located in the salivary glands to be transferred into the human host. Upon successful infection of the human, the sporozoites travel to the hepatocytes where they invade the cells and begin multiplication. An individual sporozoite that has successfully invaded a hepatocyte can produce from 10 000 to more than 30 000 merozoites in $5.5 - 8$ days [9]. This rapid reproduction eventually results in the rupturing of the

infected hepatocytes, termed hepatic schizonts, releasing the merozoites into the bloodstream where they invade host erythrocytes. The asexual life cycle for the *Plasmodium* species in the blood differs, with *P. knowlesi* taking just 24 hours, *P. falciparum, vivax* and *ovale* taking 48 hours and *P. malariae* 72 hours [9]. Following infection of the host erythrocytes, consumption of the erythrocyte cell contents begins, as does the altering of the cell membrane to facilitate transport of nutrients into the cell. The merozoites result in the formation of a haem waste product which is transported out of the erythrocyte as haemozoin, often referred to as malaria pigment [9]. The merozoites replicate and then cause the rupturing of the infected erythrocytes, termed erythrocytic schizonts, releasing between 6 and 30 merozoites that can proceed to repeat the asexual blood stage life cycle, eventually resulting in the development of the malaria disease state [9]. Merozoites may develop into gametocytes capable of infecting *Anopheles* mosquitoes that feed on the blood of an infected individual. Within the mosquito, the gametocytes develop and migrate to the salivary glands where they are able to enter another human host during blood feeding.

The clinical symptoms of malaria include headache, fatigue, anaemia and fever, among others. Characteristics of severe cases include jaundice, acidosis, coma, renal failure, severe anaemia, convulsions, and shock. The likelihood of the development of jaundice and renal failure in severe cases increases with the age of the patient, while convulsions and severe anaemia occur more frequently in children [9]. Acidosis is caused by an accumulation of lactic acid, among other organic acids, and is an important indicator of poor prognosis in severe malaria cases. Lactic acidosis is considered largely the result of anaerobic glycolysis in body tissues, where parasite sequestration has limited blood flow by the blocking of capillaries and venules. Lactate production by the *Plasmodium* cells contributes to lactate acidosis, although this contribution is considered minor [10], as does the impairment of clearance mechanisms of lactate by the kidneys and liver [9]. Hypoglycaemia is a condition commonly associated with the presentation of lactic acidosis as a result of malaria. This association is due to the conversion of glucose to lactate occurring during glycolysis. Subsequently, if the concentration of lactate in the blood is elevated this often coincides with a reduced concentration of glucose in the blood.

Penkler and colleagues [11] constructed a detailed kinetic model of the Embden-Meyerhof-Parnas glycolytic pathway for *P. falciparum* trophozoites. The model was constructed from experimental determination of the kinetics of the individual enzymes and transporters involved in the pathway, with the resulting model determining accurate steady state intermediate concentrations and fluxes for the glycolytic pathway. A detailed kinetic model describing the glycolytic pathway in uninfected human erythrocytes has been constructed and validated by Mulquiney *et al* [37; 38; 39]. These two independent kinetic

models were then compiled into a single, multi-compartmental model such that glucose metabolism in a *P. falciparum*-infected erythrocyte is described [12]. Validation using experimental data confirmed the ability of the combined model to predict steady state fluxes and intermediate concentrations.

While this enables a quantitative determination of the control of each enzyme and transporter on the steady state flux through an infected erythrocyte, the hierarchical whole-body model proposed by Snoep and colleagues [3] would provide quantitative determination of the extent to which molecular mechanisms affect the whole-body level. This is possible as detailed enzyme kinetics of *P. falciparum*-infected erythrocytes, as available from the du Toit model [12], are included along with less detailed information regarding the contribution of organs to glucose metabolism. Figure 2.4 illustrates the hierarchical, whole-body model of glucose metabolism [3]. Several organs and tissues are incorporated into the model, including the liver and muscle tissue, while detailed kinetic information is included for (un)infected erythrocytes.

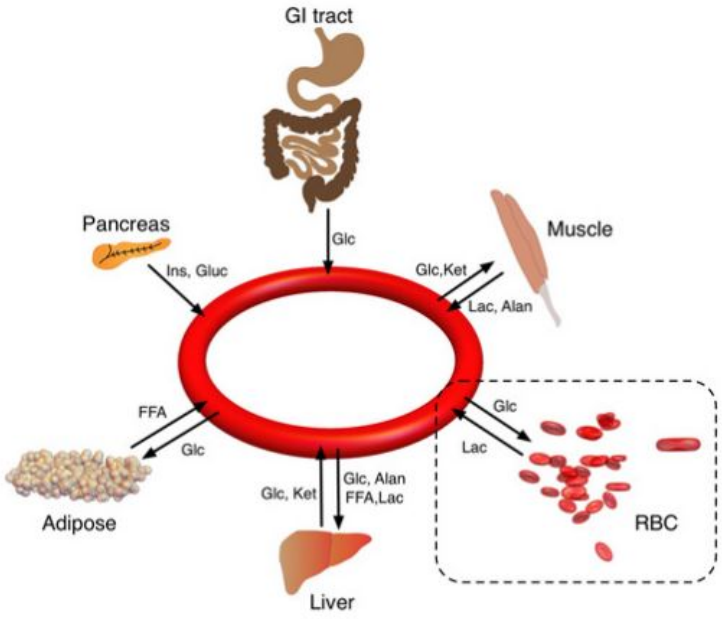


**Figure 2.4:** Schematic of hierarchical whole-body model of glucose metabolism [3].

This multi-level model incorporates both fine-grained models of molecular components and coarse-grained models of the organ and tissue level. In this way, the molecular/enzyme level may be linked to the whole-body level such that the contribution of different compartments, such as infected erythrocytes and organs, to glucose metabolism can be quantitatively determined.

## 2.8 Summary

The purpose of this literature review was to introduce several theoretical frameworks that could be applied to whole-body models such that an appropriate framework could be selected, subsequently achieving the first objective. To address the research question, the advantages and limitations of each of these methods were considered. While MCA provides the ability to quantify the contribution of different aspects of a biochemical system to the control on system components, application to large models would prove difficult. As such, extensions of MCA focusing on quantifying the contribution of groups of reactions, rather than solely individual reactions, were reviewed. Top-down control analysis, while enabling the desired determination of the control of groups of reactions, proved limiting regarding the requirements of the modules. Notably, the limitations regarding the number of independent bridging fluxes permitted through a module, as well as the limited linking metabolites generally allowed, may prove restrictive regarding the application of the framework. Adaptations of this approach may be used to circumvent these limitations, however, such adaptations increase the complexity of the application of top-down control analysis. Hierarchical control analysis proved incompatible owing to the constraint that no net mass flow is permitted between the different 'levels' of the model being analysed. This constraint would limit the general application of the framework to whole-body models as such models may exhibit net mass flow between the levels of the model. Modular control analysis provides a more general method for the analysis of whole-body models when compared to both top-down and hierarchical control analysis frameworks, owing to the modules allowing multiple independent bridging fluxes as well as allowing specific interactions between modules as opposed to the top-down approach which does not allow for any interactions between modules other than those mediated by the connecting metabolites. These additional allowances expand what may be considered a type 1 module when analysing biochemical systems and as such improves the applicability of the framework. For this reason, modular control analysis has been selected as the theoretical framework to be used to address the research question. Whole-body modelling and its application to malaria were briefly introduced. Modular control analysis will be applied to models of glycolysis in the malaria parasite as well as glucose metabolism in *P. falciparum*-infected erythrocytes, with the analysis of the whole-body model of glucose metabolism in malaria patients to be performed in a future study.

# Chapter 3

# Modelling software package

## 3.1 Modular Control Analysis Formalisation

### 3.1.1 Introduction

Metabolic control analysis is a technique for quantifying the control distribution within a biological system or pathway. MCA is typically used to determine the extent of control that individual enzymes exert over the metabolic pathway, using control coefficients, which can be estimated through experimental methods, such as through the application of specific inhibitors [6]. While this approach to MCA is useful for identifying specific enzymes that exhibit significant control over, for example, the steady state flux of a metabolic pathway, there are limitations that can reduce the possible applications of this technique. Identifying the control coefficients of each enzyme involved in a complex biochemical network/pathway experimentally could be both difficult as well as expensive. It may be desirable to determine the control of a group of reactions within a pathway on a flux or metabolite of interest, as opposed to the control of each of the individual reactions.

An alternative to traditional MCA is that of modular control analysis. Modular control analysis, an early version of which was proposed by Westerhoff *et al* in 1983 [40], aims to identify the overall flux control coefficients of a metabolic pathway, tissue, or other functional unit, termed a module [6]. This can be particularly useful when performing control analysis on large biochemical networks. Modular control analysis is performed by simplifying the network to be studied into two types of modules, namely type 1, referred to as module 1, and type 2, referred to as module 2. Type 1 modules are portions of the network where only reactions linking the modules to their surroundings are considered. The internal reactions and metabolites are not considered during the analysis. Type 2 modules are portions of the network where each reaction and metabolite is considered during the analysis [28]. These modules can be structurally or functionally defined. In this way, the control module 1 exerts

on the pathway flux can be determined without requiring detailed information of the internal reactions and metabolites. As such, modular control analysis can be applied to models of complex biochemical pathways/networks, such as glucose metabolism in malaria patients [3], where portions of the network to be studied are considered as type 1 modules and overall control coefficients can be determined [28]. Subsequently, information regarding the internal reactions of what has been defined as module 1 is not required for the analysis. As such, modular control analysis enables the quantification of the degree of control that module 1 exerts on the flux through the pathway. It can then be determined whether the control exerted by the module is large enough to warrant further investigation. The overall control coefficients provide a quantitative description of the control of the type 1 module, which may be desirable, particularly when analysing complex pathways. In the example of malaria that will be treated in a subsequent chapter, the overall control of the whole parasite within infected erythrocytes will be determined rather than the control of specific enzymes within the parasite. In this way, the control of the percentage parasitaemia on the pathway flux may be quantified.

This chapter contributes to the formalisation of modular control analysis such that analyses may be performed in a simplified manner, the second objective of this thesis. The formalisation of modular control analysis is discussed alongside application to a simple linear core model, i.e. an application of the framework to core models, the third objective.

### 3.1.2 Modular Decomposition

Modular control analysis is applied to biochemical networks following decomposition into modules of two types as described by Schuster *et al* [1]. Type 1 modules are considered "black box" modules where the internal reactions,$\mathbf{V^1}$, are not considered during the analysis, only the reactions bridging type 1 modules with modules of type 2 are considered. These reactions are termed bridging reactions, $\mathbf{V^B}$. Type 2 modules consist of reactions and metabolites that will be explicitly observed [1], with $\mathbf{V^2}$ representing the internal reactions in module 2 as well as the reactions connecting module 2 with the surroundings. The decomposition of a biochemical pathway into these 2 types of modules is illustrated in a generalised manner in Figure 3.1.

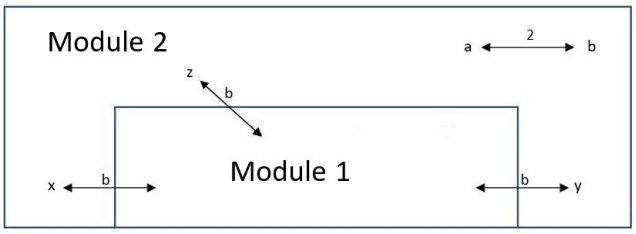


**Figure 3.1:** Schematic representation of the modular decomposition of a metabolic network. The arrows represent the bridging reactions (b) and reactions in module 2 (2) respectively. Metabolites in module 2 are denoted by symbols a, b, x, y, and z.

The vectors used during the analysis are $\mathbf{V}$ representing the reaction rates, $\mathbf{J}$, the vector of steady state fluxes and $\mathbf{S}$ representing the concentration of all metabolites, excluding sink and source metabolites which are considered constant and included in the parameter vector, $\boldsymbol{p}$, as described by Schuster *et al* [1].

A simple linear pathway, which has been decomposed into one module of type 1 and one of type 2, as shown in Figure 3.2, will be used to demonstrate aspects of the formalisation of modular control analysis. When applicable, equations applied to this linear pathway will be displayed to three significant digits, however, calculations are performed with the unrounded numbers. In this pathway, S and P are the fixed source and sink metabolites, respectively. A detailed description of the model components; ODEs, rate equations, parameters, and initial values, are located in appendix A.1.

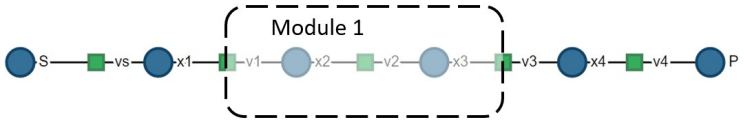


**Figure 3.2:** Schematic of the modular decomposition of a simple linear pathway with module 1 shown. S and P are fixed source and sink metabolites, respectively.

The stoichiometry matrix, $\mathbf{N}$, relates the change in metabolite concentrations to the reaction rates:

$$\frac{d\mathbf{S}}{dt} = \mathbf{N} \cdot \mathbf{V} \tag{3.1}$$

A submatrix of $\mathbf{N}$ can be chosen, $\overline{\mathbf{N}}$, such that it consists of the maximum number of linearly independent rows. This is achieved as follows:

$$\mathbf{N} = \mathbf{L} \cdot \overline{\mathbf{N}} \tag{3.2}$$

with $\mathbf{L}$ the link matrix. The link matrix describes the relationship between the stoichiometry matrix and the reduced stoichiometry matrix, enabling the analysis to be performed on as few rows (metabolites) as possible. The link

matrix can be determined using the method described by Hofmeyr [19]. Subsequently, $\mathbf{S}$ can be written in terms of the independent metabolites using the link matrix, $\mathbf{S} = \mathbf{L} \cdot \overline{\mathbf{S}}$. The modules are defined such that there are no conservation relations linking module 1 to module 2 then the link matrix can be represented as:

$$\mathbf{L} = \begin{bmatrix} \mathbf{L}^1 & \mathbf{0} \\ \mathbf{0} & \mathbf{L}^2 \end{bmatrix} \tag{3.3}$$

where $\mathbf{L}$ is the link matrix and $\mathbf{L}^1$ and $\mathbf{L}^2$ represent the link matrices of module 1 and module 2 respectively. In this way, link matrices of module 1 and of module 2 can be determined separately. The link matrices for the linear pathway shown in Figure 3.2 are

$$\mathbf{L}^1 = \begin{array}{c} \\ x_2 \\ x_3 \end{array} \begin{array}{c} \begin{array}{cc} x_2 & x_3 \end{array} \\ \begin{pmatrix} 1 & 0 \\ 0 & 1 \end{pmatrix} \end{array} \tag{3.3a}$$

$$\mathbf{L}^2 = \begin{array}{c} \\ x_1 \\ x_4 \end{array} \begin{array}{c} \begin{array}{cc} x_1 & x_4 \end{array} \\ \begin{pmatrix} 1 & 0 \\ 0 & 1 \end{pmatrix} \end{array} \tag{3.3b}$$

where the link matrices are identity matrices due to the lack of dependent metabolites in the pathway. The row and column headers of $\mathbf{L}^1$ are the components of $\mathbf{S}^1$ with the row and column headers of $\mathbf{L}^2$ the components of $\mathbf{S}^2$. Equations with alphabetical sub-numbering, as demonstrated by the link matrices 3.3a and 3.3b, indicate application to the linear pathway depicted in Figure 3.2.

The stoichiometry matrix, concentration and rate vectors are partitioned relative to the modular decomposition of the network [1],

$$\mathbf{N} = \left[\begin{array}{c|c|c} \mathbf{N_{1,1}} & \mathbf{N_{1,B}} & 0 \\ \hline 0 & \mathbf{N_{2,B}} & \mathbf{N_{2,2}} \end{array}\right] \tag{3.4}$$

$$\mathbf{S} = \begin{bmatrix} \mathbf{S}^1 \\ \mathbf{S}^2 \end{bmatrix} \tag{3.5}$$

$$\mathbf{V} = \begin{bmatrix} \mathbf{V}^1 \\ \mathbf{V}^B \\ \mathbf{V}^2 \end{bmatrix} \tag{3.6}$$

where the superscript indicates to which module (or portion of the pathway) the subvector pertains. In this way, $\mathbf{S}^1$ denotes the metabolites within module 1 and $\mathbf{V}^1$ the reactions within module 1. The subscript of the stoichiometry submatrices indicates the metabolites and reactions, respectively. In this way, $\mathbf{N}_{2,B}$ is the stoichiometry submatrix of module 2 metabolites and the bridging reactions.

For the purpose of demonstration, the stoichiometry in module 1 is included but this is not strictly a requirement for the analysis, the stoichiometry of

module 1 will, however, be used to determine the Q matrix, discussed in section 3.1.3. The stoichiometry matrix for the linear pathway is then partitioned as

$$\mathbf{N} = \begin{array}{c} \\ x_2 \\ x_3 \\ \hline x_1 \\ x_4 \end{array} \begin{array}{c} \begin{array}{cc|cc|cc} v_2 & & v_1 & v_3 & & v_s & v_4 \end{array} \\ \left(\begin{array}{cc|cc|cc} -1 & & 1 & 0 & & 0 & 0 \\ 1 & & 0 & -1 & & 0 & 0 \\ \hline 0 & & -1 & 0 & & 1 & 0 \\ 0 & & 0 & 1 & & 0 & -1 \end{array}\right) \end{array}$$

where $\mathbf{S}^1 = (x_2,\ x_3)$ and $\mathbf{S}^2 = (x_1,\ x_4)$ as shown in the stoichiometry matrix with $\mathbf{S}^1$ and $\mathbf{S}^2$ separated by a horizontal line. Similarly, the reactions of this linear pathway are partitioned as $\mathbf{V}^1 = (v_2)$, $\mathbf{V}^B = (v_1,\ v_3)$, and $\mathbf{V}^2 = (v_s,\ v_4)$ as can be seen in the partitioning of the stoichiometry matrix. Reaction subvectors can be distinguished from individual reactions as the subvectors are denoted by a superscript, such as $\mathbf{V}^1$, while individual reactions are denoted by a subscript, such as the first reaction in the pathway shown in Figure 3.2 denoted as $v_s$, as shown in the stoichiometry matrix for this pathway. A vector of fluxes is partitioned similarly to the reactions, with $\mathbf{J}$ used in place of $\mathbf{V}$ such that $\mathbf{J}^2$ denotes the module 2 fluxes at steady state.

In general, the partitioning of the stoichiometry matrix results in $\mathbf{N}_{1,2}$ $\mathbf{N}_{2,1}$ to 0, as shown in equation 3.4, due to the nature of the modular decomposition. This is the result of metabolites in module one not being metabolised by reactions in module two and *vice versa*.

### 3.1.3 Choosing the independent bridging flux

When module 1 is at steady state the input and output fluxes must balance, suggesting the bridging fluxes are linearly dependent. Linearly independent bridging fluxes, $\mathbf{J}^R$, can then be determined [1]:

$$\mathbf{J}^B = \mathbf{Q} \cdot \mathbf{J}^R \tag{3.7}$$

If knowledge regarding the stoichiometry within module 1 is known, the $\mathbf{Q}$ matrix can be determined by performing a null-space analysis of module 1, with $(\mathbf{N}_{1,1} \quad \mathbf{N}_{1,B})$ the components of module 1, collectively termed $N^1$. This is possible as the influx and efflux through module 1 at steady state must be of equivalent magnitudes and subsequently the vector of bridging fluxes can be described by a subset of bridging fluxes termed the independent bridging fluxes. This can be done in a manner similar to that which is performed during standard MCA where the K matrix is determined, enabling the quantification of the relationship between independent and dependent fluxes. In the case of the linear pathway shown in Figure 3.2, the linearly independent bridging flux,

$\mathbf{J}^R$, could be selected as either $v_1$ or $v_3$ with equation 3.7 reading

$$\overbrace{\begin{bmatrix} v_1 \\ v_3 \end{bmatrix}}^{\mathbf{J}^B} = \overbrace{\begin{pmatrix} 1 \\ 1 \end{pmatrix}}^{\mathbf{Q}} \cdot \overbrace{\begin{bmatrix} v_1 \end{bmatrix}}^{\mathbf{J}^R} \tag{3.7a}$$

with $v_1$ selected as the independent bridging flux and this $\mathbf{Q}$ matrix the result of the pathway being linear. An asterisk is included in the notation of fluxes to indicate the situation when module 1 is in steady state with module 2 metabolite concentrations fixed, module 1 metabolite concentrations are not fixed. In this way, ${}^*\mathbf{J}^R$ is used to denote the vector of reduced bridging fluxes attained when module 1 is at steady state with only module 2 metabolite concentrations, $\mathbf{S}^2$ fixed. Schuster and colleagues [1] note that the inclusion of the asterisk is necessary only when derivatives are being considered. Both the fluxes in module 2 as well as the reduced bridging fluxes of module 1 can be expressed in terms of $p$, $\mathbf{S}^1$, and $\mathbf{S}^2$ [33]. The assumption that module 1 can attain a steady state on its own implies module 1 metabolites are a function of the module 2 metabolites. Subsequently, ${}^*\mathbf{J}^R$ and ${}^*\mathbf{J}^2$ can be expressed as functions of parameters and metabolites in module 2:

$${}^*\mathbf{J}^R = \mathbf{V}^R(\mathbf{S}^1(\mathbf{S}^2), \mathbf{S}^2, p) \tag{3.8}$$

$${}^*\mathbf{J}^2 = \mathbf{V}^2(\mathbf{S}^1(\mathbf{S}^2), \mathbf{S}^2, p) \tag{3.9}$$

While the parameter vector $p$ should also be transformed such that the parameters from module 1 are replaced by overall parameters that are observable, this is not necessary for this analysis [1].

The matrix of non-normalised elasticities, $\epsilon$, can be partitioned as such [1]:

$$\epsilon = \frac{\partial \mathbf{V}}{\partial \mathbf{S}} = \begin{bmatrix} \epsilon_{1,1} & \epsilon_{1,2} \\ {}^*\epsilon_{B,1} & {}^*\epsilon_{B,2} \\ \epsilon_{2,1} & {}^*\epsilon_{2,2} \end{bmatrix} \tag{3.10}$$

with the asterisk superscript indicating when module 1 is allowed to attain steady state with only the concentrations of metabolites in module 2 clamped. Module 1 metabolites are permitted to reach a new steady state, as opposed to the determination of standard elasticities where all metabolite concentrations are fixed except for the concentration of the metabolite for which the elasticity is being determined. The submatrix ${}^*\epsilon_{B,2}$ consists of overall (block) elasticities for module 1. The elasticity submatrix $\epsilon_{2,1}$ consists of allosteric influences due to $\mathbf{N}_{1,2} = 0$. It is, however, assumed that the network is decomposed such that the concentrations of metabolites in module 1 do not influence the reactions in module 2. It then follows that $\epsilon_{2,1} = 0$. This method of analysis does not require explicit knowledge of the components of module 1. As such, it is assumed that this knowledge is not available during the analysis. In this way, the

elasticity submatrices $\epsilon_{1,1}$, $\epsilon_{1,2}$, and $\epsilon_{B,1}$ are not required. The stoichiometry submatrices $\mathbf{N}_{1,1}$ and $\mathbf{N}_{1,B}$ may also not be known, however, in this analysis it is assumed this knowledge is available [1].

The ${}^*\epsilon_{B,2}$ submatrix can be determined as such

$$ {}^*\epsilon_{B,2} = \frac{\partial {}^*\mathbf{J}^B}{\partial \mathbf{S}^2} \tag{3.11} $$

The matrix ${}^*\epsilon_{B,2}$ for the linear pathway depicted in Figure 3.2 is partitioned as

$$ {}^*\epsilon_{B,2} = \begin{array}{c} \\ v_1 \\ v_3 \end{array} \begin{array}{c} \begin{array}{cc} x_1 & x_4 \end{array} \\ \begin{pmatrix} {}^*\epsilon_{x_1}^{v_1} & {}^*\epsilon_{x_4}^{v_1} \\ {}^*\epsilon_{x_1}^{v_3} & {}^*\epsilon_{x_4}^{v_3} \end{pmatrix} \end{array} \tag{3.11a} $$

with the overall elasticities determined by clamping metabolites $x_1$ and $x_4$ and individually perturbing them, while measuring the change in reactions $v_1$ and $v_3$.

Differentiation of equation 3.9 in terms of $\mathbf{S}^2$ yields, as a result of $\epsilon_{2,1} = 0$,

$$ {}^*\epsilon_{2,2} = \frac{\partial {}^*\mathbf{J}^2}{\partial \mathbf{S}^2} = \epsilon_{2,1}\frac{\partial \mathbf{S}^1}{\partial \mathbf{S}^2} + \epsilon_{2,2} = \epsilon_{2,2} \tag{3.12} $$

with ${}^*\epsilon_{2,2}$ describing the local effect of changes in module 2 metabolite concentrations on module 2 reaction rates. The elasticity submatrix, $\epsilon_{2,2}$, for the linear pathway shown in Figure 3.2 can then be partitioned as such

$$ \epsilon_{2,2} = \begin{array}{c} \\ v_s \\ v_4 \end{array} \begin{array}{c} \begin{array}{cc} x_1 & x_4 \end{array} \\ \begin{pmatrix} \epsilon_{x_1}^{v_s} & \epsilon_{x_4}^{v_s} \\ \epsilon_{x_1}^{v_4} & \epsilon_{x_4}^{v_4} \end{pmatrix} \end{array} \tag{3.12a} $$

The matrix of overall elasticities, ${}^*\epsilon_{R,2}$, which pertains to ${}^*\mathbf{J}_R$, can be linked to ${}^*\epsilon_{B,2}$ using equation 3.7 as described by Schuster *et al* [1]:

$$ {}^*\epsilon_{B,2} = \mathbf{Q} \cdot {}^*\epsilon_{R,2} \tag{3.13} $$

which can be applied to the linear pathway shown in Figure 3.2 such that the equation reads

$$ \overbrace{\begin{array}{c} \\ v_1 \\ v_3 \end{array} \begin{array}{c} \begin{array}{cc} x_1 & x_4 \end{array} \\ \begin{pmatrix} 1.64 & -0.0909 \\ 1.64 & -0.0909 \end{pmatrix} \end{array}}^{{}^*\epsilon_{B,2}} = \overbrace{\begin{pmatrix} 1 \\ 1 \end{pmatrix}}^{\mathbf{Q}\text{ matrix}} \cdot \overbrace{\begin{array}{c} \\ v_1 \end{array} \begin{array}{c} \begin{array}{cc} x_1 & x_4 \end{array} \\ \begin{pmatrix} 1.64 & -0.0909 \end{pmatrix} \end{array}}^{{}^*\epsilon_{R,2}} \tag{3.13a} $$

The values populating the ${}^*\epsilon_{B,2}$ and ${}^*\epsilon_{R,2}$ submatrices for the linear pathway were determined by fixing the concentrations of all module 2 metabolites,

leaving the module 1 metabolites unfixed. The concentrations of the module 2 metabolites were then individually perturbed, while measuring the resulting change in the bridging fluxes.

Further analysis is performed with the assumption that detailed knowledge of the components of module 2 is available such that $\mathbf{N}_{2,2}$, $\mathbf{N}_{2,B}$, $\mathbf{S}^2$ and $\mathbf{V}^2$ are known, as well as the elasticity submatrices $\epsilon_{2,2}$, ${}^*\epsilon_{B,2}$ and ${}^*\epsilon_{R,2}$ [1].

### 3.1.4 Overall control expressed in terms of overall elasticity properties

The control of a system can be calculated in terms of the overall elasticity properties of the system's modules [1]. This can be achieved through the use of $N^2 = (N_{2,B} \quad N_{2,2})$, with $N^2$ the stoichiometry matrix of module 2, and equations 3.2 and 3.3, from which it follows that

$$\mathbf{N^2} = \mathbf{L^2} \cdot \overline{\mathbf{N^2}} \tag{3.14}$$

The stoichiometry of module 2 can then be described in terms of the module 2 link matrix and the reduced stoichiometry submatrices:

$$(\mathbf{N}_{2,B} \quad \mathbf{N}_{2,2}) = \mathbf{L}^2 \cdot (\overline{\mathbf{N}}_{2,B} \quad \overline{\mathbf{N}}_{2,2}) \tag{3.15}$$

Using equations 3.1 and 3.15 the steady state condition of module 2 can then be described by

$$\frac{d\overline{\mathbf{S}^2}}{dt} = (\overline{\mathbf{N}}_{2,B} \quad \overline{\mathbf{N}}_{2,2}) \cdot \begin{pmatrix} {}^*\mathbf{J}^B \\ {}^*\mathbf{J}^2 \end{pmatrix} \tag{3.16}$$

Equation 3.7 allows this steady state condition to be expressed by [33]

$$\frac{d\overline{\mathbf{S}^2}}{dt} = \overbrace{\overline{\mathbf{N}}_{2,B} \cdot \mathbf{Q} \cdot {}^*\mathbf{J}^R}^{\text{module 1 interacting with module 2}} + \overbrace{\overline{\mathbf{N}}_{2,2} \cdot {}^*\mathbf{J}^2}^{\text{interactions within module 2}} = \mathbf{0} \tag{3.17}$$

This can be demonstrated through application of the steady state condition to the linear pathway as follows,

$$\overbrace{\begin{bmatrix} -1 & 0 \\ 0 & 1 \end{bmatrix}}^{\overline{\mathbf{N}}_{2,B}} \cdot \overbrace{\begin{bmatrix} 1 \\ 1 \end{bmatrix}}^{\mathbf{Q}} \cdot \overbrace{[1.21]}^{{}^*\mathbf{J}^R} + \overbrace{\begin{bmatrix} 1 & 0 \\ 0 & -1 \end{bmatrix}}^{\overline{\mathbf{N}}_{2,2}} \cdot \overbrace{\begin{bmatrix} 1.21 \\ 1.21 \end{bmatrix}}^{{}^*\mathbf{J}^2} = \begin{bmatrix} 0 \\ 0 \end{bmatrix} \tag{3.17a}$$

The reaction rates at steady state were determined using the FindRoot function available in Wolfram Mathematica®, with these values used to populate ${}^*\mathbf{J}^R$ and ${}^*\mathbf{J}^2$ in equation 3.17a.

Equation 3.17 can be differentiated with respect to any parameter vector $\boldsymbol{p}$ to yield

$$\overline{\mathbf{N}}_{2,B} \cdot \mathbf{Q} \cdot \left[ \frac{\partial^* \mathbf{J}^R}{\partial p} + {}^*\epsilon_{R,2} \cdot \frac{\partial \mathbf{S}^2}{\partial p} \right] + \overline{\mathbf{N}}_{2,2} \cdot \left[ \frac{\partial^* \mathbf{J}^2}{\partial p} + \epsilon_{2,2} \cdot \frac{\partial \mathbf{S}^2}{\partial p} \right] = \mathbf{0} \tag{3.18}$$

Due to equation 3.3, resulting from the assumption that no conservation relations link module 1 to module 2, as well as equation 3.5, which specifies the partitioning of the metabolites, the change in a metabolite due to a change in a parameter can be described as

$$\frac{\partial \mathbf{S}^x}{\partial p} = \mathbf{L}^x \cdot \frac{\partial \overline{\mathbf{S}^x}}{\partial p} \tag{3.19}$$

with x either 1 or 2. Equations 3.18 and 3.19 can then be combined [33]:

$$\overline{\mathbf{N}}_{2,B} \cdot \mathbf{Q} \cdot \frac{\partial^* \mathbf{J}^R}{\partial p} + \overline{\mathbf{N}}_{2,2} \cdot \frac{\partial^* \mathbf{J}^2}{\partial p} + \mathbf{M}^* \cdot \frac{\partial \overline{\mathbf{S}^2}}{\partial p} = \mathbf{0} \tag{3.20}$$

with

$$\mathbf{M}^* = \left( \overline{\mathbf{N}}_{2,B} \cdot \mathbf{Q} \cdot^* \epsilon_{R,2} + \overline{\mathbf{N}}_{2,2} \cdot \epsilon_{2,2} \right) \cdot \mathbf{L}^2 \tag{3.21}$$

where $\mathbf{M}^*$ is the Jacobian matrix of module 2 accounting for the effects of module 1 on the regulation of module 2 metabolites [1]. Equation 3.20 is valid for both parameters affecting only the bridging reactions and only the reactions present in module 2, however, not for parameters affecting only module 1. This allows the concentration control coefficients to be calculated. Traditional MCA defines concentration control coefficients as [19]

$$\mathbf{\Gamma}_k^j = \left( \frac{\partial \mathbf{S}_j}{\partial p_k} \right) \cdot \left( \frac{\partial \mathbf{V}_k}{\partial p_k} \right)^{-1} \tag{3.22}$$

with $\Gamma$ the unnormalised concentration control coefficient, $S_j$ metabolite j, $V_k$ reaction k, and $p_k$ parameter k which only affects reaction k. Hofmeyr [19] describes the importance of the jacobian matrix as well as its use in determining the matrix of concentration control coefficients as such

$$\mathbf{\Gamma} = -\mathbf{L} \cdot (\mathbf{M})^{-1} \cdot \overline{\mathbf{N}} \tag{3.23}$$

with $\Gamma$ the matrix of unnormalised concentration control coefficients, $M$ the jacobian matrix, and $\overline{N}$ the row-reduced stoichiometry matrix. The unnormalised concentration control coefficient matrices for module 1 and module 2 can be defined similarly to equation 3.22:

$${}^*\mathbf{\Gamma}_{2,R} = \left( \frac{\partial \mathbf{S}^2}{\partial p^R} \right) \cdot \left( \frac{\partial^* \mathbf{J}^R}{\partial p^R} \right)^{-1} \tag{3.24}$$

$$\mathbf{\Gamma}_{2,2} = \left(\frac{\partial \mathbf{S}^2}{\partial p^2}\right) \cdot \left(\frac{\partial \mathbf{V}^2}{\partial p^2}\right)^{-1} \tag{3.25}$$

with ${}^*\Gamma_{2,R}$ and $\Gamma_{2,2}$ the unnormalised concentration control coefficient matrices of module 1 and module 2, respectively. $p^2$ is a vector of parameters with the matrix $\partial \mathbf{V}^2 \,/\, \partial p^2$ being a non-singular square matrix, $S^2$ the module 2 metabolites, $V^2$ the module 2 reactions, and ${}^*J^R$ the reduced bridging fluxes. The concentration control coefficient matrices can then be determined in a manner similar to that shown in equation 3.23 and as stated by Schuster and colleagues [1]:

$${}^*\mathbf{\Gamma}_{2,R} = -\mathbf{L}^2 \cdot (\mathbf{M}^*)^{-1} \cdot \overline{\mathbf{N}}_{2,B} \cdot \mathbf{Q} \tag{3.26}$$

$$\mathbf{\Gamma}_{2,2} = -\mathbf{L}^2 \cdot (\mathbf{M}^*)^{-1} \cdot \overline{\mathbf{N}}_{2,2} \tag{3.27}$$

The matrices of symbolic concentration control ceofficients for the linear pathway would then be

$${}^*\mathbf{\Gamma}_{2,R} = \begin{matrix} \\ x_1 \\ x_4 \end{matrix} \overset{\text{Module 1}}{\begin{pmatrix} \mathbf{C}^{x_1}_{\text{Module 1}} \\ \mathbf{C}^{x_4}_{\text{Module 1}} \end{pmatrix}} \tag{3.26a}$$

$$\mathbf{\Gamma}_{2,2} = \begin{matrix} \\ x_1 \\ x_4 \end{matrix} \overset{\begin{matrix} v_s & v_4 \end{matrix}}{\begin{pmatrix} \mathbf{C}^{x_1}_{v_s} & \mathbf{C}^{x_1}_{v_4} \\ \mathbf{C}^{x_4}_{v_s} & \mathbf{C}^{x_4}_{v_4} \end{pmatrix}} \tag{3.27a}$$

The concentration control coefficients can then be normalised

$${}^*\mathbf{C}^S_{2,R} = (dg\mathbf{S}^2)^{-1} \cdot {}^*\mathbf{\Gamma}_{2,R} \cdot (dg\mathbf{J}^R) \tag{3.28}$$

$$\mathbf{C}^S_{2,2} = (dg\mathbf{S}^2)^{-1} \cdot \mathbf{\Gamma}_{2,2} \cdot (dg\mathbf{J}^2) \tag{3.29}$$

with dg denoting the construction of a diagonal matrix. The ${}^*\mathbf{C}^S_{2,R}$ matrix for the linear pathway is then determined by

$${}^*\mathbf{C}^S_{2,R} = \overbrace{\begin{bmatrix} 1.27 & 0 \\ 0 & 1.17 \end{bmatrix}}^{dg\,(\mathbf{S}^2)^{-1}} \cdot \overbrace{\begin{matrix} \\ x_1 \\ x_4 \end{matrix} \overset{\text{Module 1}}{\begin{pmatrix} -0.373 \\ 0.186 \end{pmatrix}}}^{{}^*\mathbf{\Gamma}_{2,R}} \cdot \overbrace{\begin{bmatrix} 1.21 \end{bmatrix}}^{dg\,\mathbf{J}^R} = \begin{matrix} \\ x_1 \\ x_4 \end{matrix} \overset{\text{Module 1}}{\begin{pmatrix} -0.573 \\ 0.264 \end{pmatrix}} \tag{3.28a}$$

with ${}^*\mathbf{\Gamma}_{2,R}$ determined using equation 3.26. ${}^*\mathbf{C}^S_{2,2}$ for the linear pathway is then determined in a similar manner using $\Gamma_{2,2}$ and a diagonal matrix of the fluxes in module 2. The flux control coefficients in traditional MCA can be defined as [19]

$$\mathbf{\Phi}^i_k = \left(\frac{\partial \mathbf{J}_i}{\partial p_k}\right) \cdot \left(\frac{\partial \mathbf{V}_k}{\partial p_k}\right)^{-1} \tag{3.30}$$

with $\Phi^i_k$ the unnormalised flux control coefficient of reaction k on flux i. Hofmeyr [19] describes how the matrix of flux control coefficients can be described in terms of elasticity and concentration control coefficients:

$$\mathbf{\Phi} = \mathbf{I} + \epsilon_s \cdot \mathbf{\Gamma} \tag{3.31}$$

with $\Phi$ the matrix of unnormalised flux control coefficients, $I$ an identity matrix of appropriate dimensions, $\epsilon_s$ the unnormalised elasticity coefficient matrix, and $\Gamma$ the unnormalised concentration control coefficient matrix.

The flux control coefficients for module 2 can be defined as

$$\mathbf{\Phi}_{R,2} = \left(\frac{\partial \mathbf{J}^R}{\partial p^2}\right) \cdot \left(\frac{\partial \mathbf{V}^2}{\partial p^2}\right)^{-1} \tag{3.32}$$

$$\mathbf{\Phi}_{2,2} = \left(\frac{\partial \mathbf{J}^2}{\partial p^2}\right) \cdot \left(\frac{\partial \mathbf{V}^2}{\partial p^2}\right)^{-1} \tag{3.33}$$

with $\Phi_{R,2}$ and $\Phi_{2,2}$ the unnormalised flux control coefficients for module 2 reactions on the independent bridging fluxes and module 2 fluxes, respectively. Application to the linear pathway expresses these matrices as

$$\mathbf{\Phi}_{R,2} = v_1 \begin{array}{c} \begin{array}{cc} v_s & v_4 \end{array} \\ \begin{pmatrix} \mathbf{C}^{v_1}_{v_s} & \mathbf{C}^{v_1}_{v_4} \end{pmatrix} \end{array} \tag{3.32a}$$

$$\mathbf{\Phi}_{2,2} = \begin{array}{c} \begin{array}{cc} v_s & v_4 \end{array} \\ \begin{array}{c} v_s \\ v_4 \end{array} \begin{pmatrix} \mathbf{C}^{v_s}_{v_s} & \mathbf{C}^{v_s}_{v_4} \\ \mathbf{C}^{v_4}_{v_s} & \mathbf{C}^{v_4}_{v_4} \end{pmatrix} \end{array} \tag{3.33a}$$

Similarly, the overall flux control coefficients for module 1 are defined as

$${}^*\mathbf{\Phi}_{R,R} = \left(\frac{\partial \mathbf{J}^R}{\partial p^R}\right) \cdot \left(\frac{\partial^* \mathbf{J}^R}{\partial p^R}\right)^{-1} \tag{3.34}$$

$${}^*\mathbf{\Phi}_{2,R} = \left(\frac{\partial \mathbf{J}^2}{\partial p^R}\right) \cdot \left(\frac{\partial^* \mathbf{J}^R}{\partial p^R}\right)^{-1} \tag{3.35}$$

with ${}^*\Phi_{R,R}$ and ${}^*\Phi_{2,R}$ the unnormalised overall flux control coefficients for module 1 on the independent bridging fluxes and on module 2 fluxes, respectively. The overall flux control coefficient matrices for the linear pathway can then be expressed as

$${}^*\mathbf{\Phi}_{R,R} = v_1 \begin{array}{c} \text{Module 1} \\ \begin{pmatrix} \mathbf{C}^{v_1}_{\text{Module 1}} \end{pmatrix} \end{array} \tag{3.34a}$$

$${}^*\mathbf{\Phi}_{2,R} = \begin{array}{c} \text{Module 1} \\ \begin{array}{c} v_s \\ v_4 \end{array} \begin{pmatrix} \mathbf{C}^{v_s}_{\text{Module 1}} \\ \mathbf{C}^{v_4}_{\text{Module 1}} \end{pmatrix} \end{array} \tag{3.35a}$$

The flux control coefficients for module 1 and 2 can be obtained through the differentiation of $\mathbf{J}^x(p) = {}^*\mathbf{J}^x(p, \mathbf{S}^2)$, with $x = R$ or 2, with respect to $p$, as described by Schuster *et al* [1]

$$\frac{\partial \mathbf{J}^x}{\partial p} = \frac{\partial^* \mathbf{J}^x}{\partial p} + \frac{\partial^* \mathbf{J}^x}{\partial \mathbf{S}^2} \cdot \frac{\partial \mathbf{S}^2}{\partial p} \tag{3.36}$$

Equation 3.36 allows the determination of the flux control coefficient matrices in a manner similar to that shown in equation 3.31 and as stated by Schuster and colleagues [1]:

$$ {}^{*}\mathbf{\Phi}_{R,R} = \mathbf{I} + {}^{*}\epsilon_{R,2} \cdot {}^{*}\mathbf{\Gamma}_{2,R} \tag{3.37} $$

$$ \mathbf{\Phi}_{2,2} = \mathbf{I} + \epsilon_{2,2} \cdot \mathbf{\Gamma}_{2,2} \tag{3.38} $$

$$ \mathbf{\Phi}_{R,2} = {}^{*}\epsilon_{R,2} \cdot \mathbf{\Gamma}_{2,2} \tag{3.39} $$

$$ {}^{*}\mathbf{\Phi}_{2,R} = \epsilon_{2,2} \cdot {}^{*}\mathbf{\Gamma}_{2,R} \tag{3.40} $$

with $I$ denoting an identity matrix of appropriate dimensions. Equations 3.37 and 3.38 are analogous to equation 3.31 with application to modules 1 and 2 respectively. Equations 3.39 and 3.40, however, lack the addition of an identity matrix due to these matrices expressing the flux control of each module on the other, specifically the control of module 2 reactions on module 1 independent bridging fluxes and the overall control of module 1 on module 2 fluxes. The flux control coefficients are normalised through the application of a general formula as stated by Schuster *et al* [1]

$$ {}^{*}\mathbf{C}^{J}_{\mathrm{x,y}} = (dg\mathbf{J}^{x})^{-1} \, {}^{*}\mathbf{\Phi}_{\mathrm{x,y}} \, (dg\mathbf{J}^{y}) \tag{3.41} $$

with x, y denoting R and/or 2. In this way, the control module 1 exerts on the components of module 2 as well as on the independent bridging fluxes is quantified. The overall control coefficient matrices will have a number of columns equivalent to the number of independent bridging fluxes, representing the degrees of freedom in the flux of module 1 [33]. In the case of the linear pathway, this is a single column as has been shown, however, if more than one linearly independent bridging fluxes are present then the control of the whole module 1 is equivalent to the summation of the columns [1; 33]. In this way, if ${}^{*}\mathbf{C}^{S}_{2,R}$ is a 2 row X 2 column matrix, the controls shown in the matrix can be summed such that the matrix representing the control of module 1 on the metabolites in module 2 would have 2 rows and 1 column.

Application of equations 3.37 and 3.41 to the linear pathway results in the normalised overall flux control coefficients for the reduced bridging fluxes to be determined,

$$ {}^{*}\mathbf{C}^{J}_{R,R} = \left[1.21\right]^{-1} \cdot \left( \left[1\right] + \overbrace{\begin{pmatrix} 1.64 & -0.0909 \end{pmatrix}}^{{}^{*}\epsilon_{R,2}} \cdot \overbrace{\begin{pmatrix} -0.373 \\ 0.186 \end{pmatrix}}^{{}^{*}\mathbf{\Gamma}_{2,R}} \right) \cdot \left[1.21\right] \tag{3.41a} $$

$$ = \overbrace{v_1 \begin{pmatrix} 0.373 \end{pmatrix}}^{{}^{*}\mathbf{C}^{J}_{R,R}} \quad \text{Module 1} $$

with ${}^{*}\mathbf{C}^{J}_{R,R}$ the normalised overall flux control coefficient matrix for module 1 on the reduced bridging fluxes. The flux control coefficients of the dependent bridging fluxes can be calculated through the multiplication of the normalised $\mathbf{Q}$ matrix. The $\mathbf{Q}$ matrix can be normalised by

$$\mathbf{Q}_{\text{norm}} = (dg\mathbf{J}^{B})^{-1} \cdot \mathbf{Q} \cdot (dg\mathbf{J}^{R}) \tag{3.42}$$

with $\mathbf{Q}_{\text{norm}}$ the normalised Q matrix. The matrix of overall flux control coefficients for module 1 on the bridging fluxes can then be determined by

$${}^{*}\mathbf{C}^{J}_{B,R} = \mathbf{Q}_{\text{norm}} \cdot {}^{*}\mathbf{C}^{J}_{R,R} \tag{3.43}$$

with ${}^{*}\mathbf{C}^{J}_{B,R}$ the matrix of overall flux control coefficients of module 1 on all bridging fluxes. Similarly the control of module 2 reactions on all bridging fluxes can be determined

$$\mathbf{C}^{J}_{B,2} = \mathbf{Q}_{\text{norm}} \cdot \mathbf{C}^{J}_{R,2} \tag{3.44}$$

with $\mathbf{C}^{J}_{B,2}$ the matrix of flux control coefficients of module 2 reactions on the bridging fluxes. Equation 3.43 can be applied to the linear pathway as follows

$${}^{*}\mathbf{C}^{J}_{B,R} = \begin{pmatrix} 1 \\ 1 \end{pmatrix} \cdot \overbrace{v_1 \underbrace{\begin{pmatrix} 0.373 \end{pmatrix}}_{\text{Module 1}}}^{{}^{*}\mathbf{C}^{J}_{R,R}} = \begin{matrix} \\ v_1 \\ v_3 \end{matrix} \underbrace{\begin{pmatrix} 0.373 \\ 0.373 \end{pmatrix}}_{\text{Module 1}} \tag{3.43a}$$

The application of modular control analysis has been described, however, the presence of conserved moiety cycles, and subsequently linearly dependent metabolites, can complicate the determination of the overall elasticities. Schuster and colleagues [1] describe how such overall elasticities can be determined. Overall elasticities are determined by fixing module 2 metabolites, with module 1 metabolites unfixed, and individually perturbing them while observing the changes in the bridging fluxes. The fixation of dependent metabolites could result in numerical errors when solving for the steady state fluxes and concentrations. Consequently, it was decided that analyses will be performed on reduced models. Models are reduced by removing the dependent metabolites from the stoichiometry matrix of the pathway. The dependent metabolites are accounted for by the inclusion of parameters, describing the sum of the concentrations of the metabolites in each conserved moiety cycle, and moiety rules, describing the concentration of the dependent metabolites as a function of the independent metabolites and the parameter of the sum of the concentrations of the metabolites in the moiety conserved cycle.

Following determination of the concentration control coefficients of the reduced model, excluding dependent metabolites, a link matrix for module 2 of

the unreduced model can be used to determine the concentration control coefficients for all module 2 metabolites, inclusive of the dependent metabolites. This link matrix can then be normalised by

$$\mathbf{L}^2_{\text{norm}} = (dg\mathbf{S}^2)^{-1} \cdot \mathbf{L}^2 \cdot (dg\mathbf{S}^2_{indep}) \tag{3.45}$$

with $\mathbf{L}^2_{\text{norm}}$ the normalised link matrix of module 2, $(dg\mathbf{S}^2)^{-1}$ the diagonal matrix of the inverse of module 2 metabolite concentrations at steady state, $\mathbf{L}^2$ the unnormalised module 2 link matrix, and $(dg\mathbf{S}^2_{indep})$ the diagonal matrix of the steady state concentrations of the independent module 2 metabolites. Multiplication of the normalised module 2 link matrix with the normalised concentration control coefficient matrices, $\mathbf{C}^S_{2,2}$ or ${}^*\mathbf{C}^S_{2,R}$, results in the concentration control coefficients of module 2 reactions on all module 2 metabolites, or of module 1 on all module 2 metabolites, respectively.

### 3.1.5 Control Theorems

Following the determination of elasticity and control coefficients, the summation and connectivity theorems for the metabolite concentrations and reaction fluxes can be determined. The unnormalised concentration control coefficients shown in equations 3.26 and 3.27, in conjunction with the steady-state condition described in equation 3.17, imply the summation theorem for the concentration control coefficients [1] can be described as

$$({}^*\mathbf{\Gamma}_{2,R} \quad \mathbf{\Gamma}_{2,2}) \cdot \begin{bmatrix} \mathbf{J}^R \\ \mathbf{J}^2 \end{bmatrix} = \mathbf{0} \tag{3.46}$$

This theorem applies to the normalised concentration control coefficients as

$$({}^*\mathbf{C}^S_{2,R} + \mathbf{C}^S_{2,2}) \cdot \mathbf{1} = {}^*\mathbf{C}^S_{2,R} \cdot \mathbf{1} + \mathbf{C}^S_{2,2} \cdot \mathbf{1} = \mathbf{0} \tag{3.47}$$

where $\mathbf{1}$ denotes a unit vector, $(111...1)^T$, of appropriate length [1]. Equation 3.47 is analogous to the normalised concentration control coefficient summation theorem of traditional MCA [33],

$$\mathbf{C}^S \cdot \mathbf{1} = \mathbf{0} \tag{3.48}$$

with $\mathbf{C}^S$ the matrix of normalised concentration control coefficients. Equation 3.47 can be demonstrated by applying it to the linear pathway,

$$\overbrace{\underset{\text{Module 1}}{\begin{matrix} x_1 \\ x_4 \end{matrix}\begin{pmatrix} -0.573 \\ 0.264 \end{pmatrix}}^{{}^*\mathbf{C}^S_{2,R}} \cdot (1) + \overbrace{\begin{matrix} & v_s & v_4 \\ x_1 & 0.599 & -0.0261 \\ x_4 & 0.432 & -0.696 \end{matrix}}^{\mathbf{C}^S_{2,2}} \cdot \begin{pmatrix} 1 \\ 1 \end{pmatrix} = \begin{pmatrix} 0 \\ 0 \end{pmatrix} \tag{3.47a}$$

Heinrich and Schuster [33] describe how the concentration connectivity theorem can be determined during traditional MCA. The concentration connectivity theorem can be applied to unnormalised concentration control coefficients as

$$\mathbf{\Gamma} \cdot \epsilon \cdot \mathbf{L} = -\mathbf{L} \tag{3.49}$$

with $\Gamma$ the matrix of unnormalised concentration control coefficients, $\epsilon$ the matrix of unnormalised elasticity coefficients, and $L$ the unnormalised link matrix. The concentration connectivity theorem can also be applied to the normalised coefficients [33]:

$$\mathbf{C}^S \cdot \varepsilon \cdot (dg\mathbf{S})^{-1} \cdot \mathbf{L} = -(dg\mathbf{S})^{-1} \cdot \mathbf{L} \tag{3.50}$$

with $C^S$ the matrix of normalised concentration control coefficients, $\varepsilon$ the matrix of normalised elasticity coefficients, and $(dgS)^{-1}$ a matrix with the inverse of the steady state concentrations of the metabolites on the diagonal. The concentration connectivity relationship for the coefficients determined during the modular analysis can be expressed in manners similar to those shown in equations 3.49 and 3.50, with the unnormalised form

$${}^*\mathbf{\Gamma}_{2,R} \cdot {}^*\epsilon_{R,2} \cdot \mathbf{L}^2 + \mathbf{\Gamma}_{2,2} \cdot \epsilon_{2,2} \cdot \mathbf{L}^2 = -\mathbf{L}^2 \tag{3.51}$$

and the concentration connectivity relationship of the normalised coefficients as

$$({}^*\mathbf{C}^S_{2,R} \cdot {}^*\varepsilon_{R,2} + \mathbf{C}^S_{2,2} \cdot \varepsilon_{2,2}) \cdot (dg\mathbf{S}^2)^{-1} \cdot \mathbf{L^2} = -(dg\mathbf{S}^2)^{-1} \cdot \mathbf{L^2} \tag{3.52}$$

where $\varepsilon$ denotes the normalised elasticities [1]. The elasticities can be normalised as follows,

$${}^*\varepsilon_{R,2} = (dg\mathbf{J}^R)^{-1} \cdot {}^*\epsilon_{R,2} \cdot (dg\mathbf{S}^2) \tag{3.53}$$

$$\varepsilon_{2,2} = (dg\mathbf{J}^2)^{-1} \cdot \epsilon_{2,2} \cdot (dg\mathbf{S}^2) \tag{3.54}$$

The summation theorem and connectivity relationships for metabolite concentrations have been determined, however, a summation theorem and connectivity relationships exist for the fluxes in a pathway as well. The flux summation theorem for unnormalised control coefficients determined during MCA can be expressed as [33]

$$\mathbf{\Phi} \cdot \mathbf{J} = \mathbf{J} \tag{3.55}$$

with $\Phi$ the matrix of unnormalised flux control coefficients and $J$ a vector of steady state fluxes. Reder [41] describes the flux summation of normalised coefficients as

$$\mathbf{C}^J \cdot \mathbf{1} = \mathbf{1} \tag{3.56}$$

with $C^J$ the matrix of normalised flux control coefficients and 1 a unit vector of appropriate length. The summation of flux control coefficients can be applied

to the control coefficients determined in the modular analysis in a similar manner, with the flux summation of unnormalised coefficients described as

$$\begin{pmatrix} {}^{*}\mathbf{\Phi}_{R,R} & \mathbf{\Phi}_{R,2} \\ {}^{*}\mathbf{\Phi}_{2,R} & \mathbf{\Phi}_{2,2} \end{pmatrix} \cdot \begin{pmatrix} \mathbf{J}^{R} \\ \mathbf{J}^{2} \end{pmatrix} = \begin{pmatrix} \mathbf{J}^{R} \\ \mathbf{J}^{2} \end{pmatrix} \tag{3.57}$$

with the unnormalised flux control coefficients and fluxes collected in a manner analogous to equation 3.55. The normalised form can then be determined in a manner similar to equation 3.56,

$${}^{*}\mathbf{C}^{J}_{\mathrm{R,R}} \cdot \mathbf{1} + \mathbf{C}^{J}_{\mathrm{R,2}} \cdot \mathbf{1} = \mathbf{1} \tag{3.58}$$

$${}^{*}\mathbf{C}^{J}_{\mathrm{2,R}} \cdot \mathbf{1} + \mathbf{C}^{J}_{\mathrm{2,2}} \cdot \mathbf{1} = \mathbf{1} \tag{3.59}$$

with equation 3.58 the flux summation of normalised flux control coefficients pertaining to module 1, via the reduced bridging fluxes, and equation 3.59 the flux summation of normalised flux control coefficients pertaining to module 2 fluxes. Application of equations 3.58 and 3.59 to the linear pathway results in the following

$$\overbrace{\text{Module 1}}^{{}^{*}\mathbf{C}^{J}_{R,R}} \quad \overbrace{\phantom{v_s \quad v_4}}^{\mathbf{C}^{J}_{R,2}} \\ v_1 \begin{pmatrix} 0.373 \end{pmatrix} \cdot (1) + v_1 \begin{pmatrix} v_s & v_4 \\ 0.610 & 0.0169 \end{pmatrix} \cdot \begin{pmatrix} 1 \\ 1 \end{pmatrix} = (1) \tag{3.58a}$$

$$\overbrace{\text{Module 1}}^{{}^{*}\mathbf{C}^{J}_{2,R}} \quad \overbrace{\phantom{v_s \quad v_4}}^{\mathbf{C}^{J}_{2,2}} \\ \begin{matrix} v_s \\ v_4 \end{matrix} \begin{pmatrix} 0.373 \\ 0.373 \end{pmatrix} \cdot (1) + \begin{matrix} v_s \\ v_4 \end{matrix} \begin{matrix} \begin{matrix} v_s & v_4 \end{matrix} \\ \begin{pmatrix} 0.610 & 0.0169 \\ 0.610 & 0.0169 \end{pmatrix} \end{matrix} \cdot \begin{pmatrix} 1 \\ 1 \end{pmatrix} = \begin{pmatrix} 1 \\ 1 \end{pmatrix} \tag{3.59a}$$

The flux connectivity relationships for traditional MCA are described by Heinrich and Schuster [33] as

$$\mathbf{\Phi} \cdot \epsilon \cdot \mathbf{L} = \mathbf{0} \tag{3.60}$$

for the unnormalised control coefficients, with $\Phi$ the unnormalsied flux control coefficients, $\epsilon$ the matrix of unnormalised elasticity coefficients, and 0 a vector of 0 of appropriate dimensions. The normalised flux connectivity relationship is determined by [33]

$$\mathbf{C}^{J} \cdot \varepsilon \cdot (dg\mathbf{S})^{-1} \cdot \mathbf{L} = \mathbf{0} \tag{3.61}$$

with $C^J$ the matrix of normalised flux control coefficients, $\varepsilon$ the matrix of normalised elasticities and $(dgS)^{-1}$ a diagonal matrix of the inverse of the steady state metabolite concentrations. The unnormalised flux connectivity relationships for the modular control coefficients can be expressed in a manner analogous to equation 3.60 [1]

$${}^{*}\mathbf{\Phi}_{x,R} \cdot {}^{*}\epsilon_{R,2} \cdot \mathbf{L}^{2} + \mathbf{\Phi}_{x,2} \cdot \epsilon_{2,2} \cdot \mathbf{L}^{2} = \mathbf{0} \tag{3.62}$$

where x represents R or 2 [1]. Equation 3.62 illustrates the similarity between the traditional flux connectivity relationships and those of the modular flux connectivity relationships. The flux connectivity relationships of the normalised coefficients can then be read as [1]

$$({}^{*}\mathbf{C}^{J}_{\mathrm{R,R}} \cdot {}^{*}\varepsilon_{\mathrm{R},2} + \mathbf{C}^{J}_{\mathrm{R},2} \cdot \varepsilon_{2,2}) \cdot (dg\mathbf{S^2})^{-1} \cdot \mathbf{L^2} = \mathbf{0} \tag{3.63}$$

$$({}^{*}\mathbf{C}^{J}_{\mathrm{2,R}} \cdot {}^{*}\varepsilon_{\mathrm{R},2} + \mathbf{C}^{J}_{2,2} \cdot \varepsilon_{2,2}) \cdot (dg\mathbf{S^2})^{-1} \cdot \mathbf{L^2} = \mathbf{0} \tag{3.64}$$

with equations 3.63 and 3.64 analogous to equation 3.61 for module 1 and module 2, respectively.

The modular summation and connectivity theorems can be applied to both the normalised and unnormalised control coefficient and elasticity matrices, allowing the validity of the control coefficients determined during the analysis to be ascertained. While these theorems provide support for the validity of the control coefficients, the accuracy of the controls can be confirmed through comparison to appropriate traditional control coefficients. Such an example is that of the confirmation of the ${}^{*}\mathbf{C}^{S}_{2,R}$ matrix determined for the simple linear pathway. This can be achieved through the summation of the control coefficients of the reactions within module 1 with those of the bridging reactions as follows,

$$\overbrace{\begin{array}{c}\text{Module 1}\\ \begin{array}{c}x_1\\x_4\end{array}\begin{pmatrix}-0.573\\0.264\end{pmatrix}\end{array}}^{{}^{*}\mathbf{C}^{S}_{2,R}} = \overbrace{\begin{array}{ccccccc} & v_1 & + & v_2 & + & v_3\\ x_1 & -0.313 & + & -0.208 & + & -0.0521\\ x_4 & 0.144 & + & 0.0960 & + & 0.0240\end{array}}^{\text{Traditional } \mathbf{C}^{S^2}_{V_{module1}}}$$

The control module 1 exerts on the components of module 2, as well as on the independent bridging fluxes, is quantified and is equivalent to the summation of the control coefficients of the reactions within module 1 as well as the bridging reactions linking the two modules. Modular control analysis is a powerful tool with which the control of large complex biochemical networks can be described in terms of modules within the network. This technique can be applied to complex biochemical networks of a hierarchical design with portions of the pathway lacking explicit detail of each reaction. This quantifies the control that the portion of the network lacking explicit detail exerts on the property of interest. On this basis one can decide whether further investigation of this module is warranted.

The application of modular control analysis to a simple linear model has been demonstrated, however, application to a system including branches would be beneficial as this is a common aspect of biochemical systems. As such, the following section demonstrates the application of the framework to a simple branched model.

## 3.2 Modular analysis of a branched pathway

The previous section discussed the formalisation of modular control analysis as well as its application to a simple linear system. The analysis was performed manually in Wolfram Mathematica®, however, without the use of a package automating the analysis. While the analysis of the linear system was beneficial as a first step towards understanding, applying, and automating, the application of the modular control analysis framework, the next logical step was to apply the framework to a branched system. Therefore, this section will describe the 'manual' analysis of a simple branched system. In this way, this section contributes to the completion of the third objective, specifically the application of the framework to core models. The analysis was performed on a simple branched pathway consisting of eight reversible reactions as shown in Figure 3.3. The fixed metabolites in the pathway are s, p1 and p2, the initial substrate and the final products, respectively. Detail regarding the model components, including ODEs, rate equations, parameters, and initial values are located in appendix A.2. Three significant digits will be displayed in relevant equations.

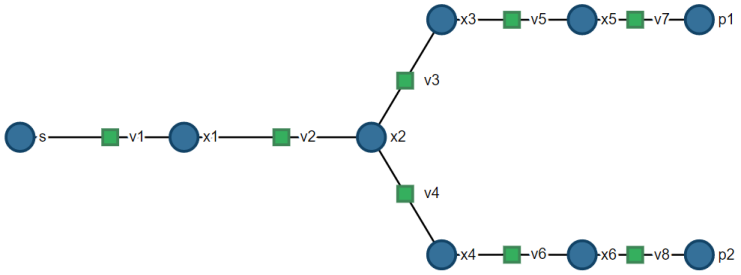


**Figure 3.3:** A schematic of the simple 8 reaction branched pathway as generated by JWS Online (jjj.bio.vu.nl)

The model was arbitrarily decomposed as shown in Figure 3.4, with the reaction and concentration vectors partitioned as follows:

$$\mathbf{V}^1 = \begin{bmatrix} \mathbf{V}_3 \\ \mathbf{V}_4 \end{bmatrix} \qquad \mathbf{V}^B = \begin{bmatrix} \mathbf{V}_2 \\ \mathbf{V}_5 \\ \mathbf{V}_6 \end{bmatrix} \qquad \mathbf{V}^2 = \begin{bmatrix} \mathbf{V}_1 \\ \mathbf{V}_7 \\ \mathbf{V}_8 \end{bmatrix} \tag{3.65}$$

$$\mathbf{S}^1 = \begin{bmatrix} \mathbf{X}_2 \\ \mathbf{X}_3 \\ \mathbf{X}_4 \end{bmatrix} \qquad \mathbf{S}^2 = \begin{bmatrix} \mathbf{X}_1 \\ \mathbf{X}_5 \\ \mathbf{X}_6 \end{bmatrix} \tag{3.66}$$

The vectors of fluxes were partitioned similarly to the reaction rates, with $\mathbf{J}^B$ the bridging fluxes ($\mathbf{V}^B$) at steady state, $\mathbf{J}^R$ the linearly independent bridging

fluxes ($\mathbf{V}^R$) at steady state, and $\mathbf{J}^2$ the steady state fluxes of the reactions in module 2 ($\mathbf{V}^2$).

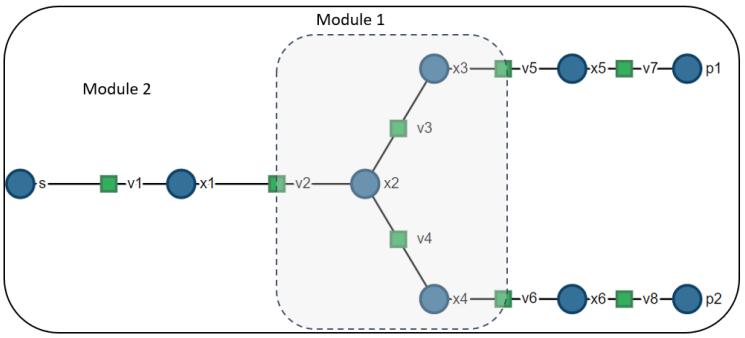


**Figure 3.4:** A schematic of the modular decomposition of the pathway with module 1 shown.

The stoichiometry matrix was then constructed as such,

$$\mathbf{N} = \begin{bmatrix} \mathbf{N_{1,1}} & \mathbf{N_{1,B}} & 0 \\ 0 & \mathbf{N_{2,B}} & \mathbf{N_{2,2}} \end{bmatrix}$$

$$= \begin{array}{c} \\ \mathbf{X}_2 \\ \mathbf{X}_3 \\ \mathbf{X}_4 \\ \mathbf{X}_1 \\ \mathbf{X}_5 \\ \mathbf{X}_6 \end{array} \begin{array}{c} \begin{array}{ccc|ccc|ccc} \mathbf{V}_3 & \mathbf{V}_4 & & \mathbf{V}_2 & \mathbf{V}_5 & \mathbf{V}_6 & & \mathbf{V}_1 & \mathbf{V}_7 & \mathbf{V}_8 \end{array} \\ \left(\begin{array}{ccc|ccc|ccc} -1 & -1 & | & 1 & 0 & 0 & | & 0 & 0 & 0 \\ 1 & 0 & | & 0 & -1 & 0 & | & 0 & 0 & 0 \\ 0 & 1 & | & 0 & 0 & -1 & | & 0 & 0 & 0 \\ \hline 0 & 0 & | & -1 & 0 & 0 & | & 1 & 0 & 0 \\ 0 & 0 & | & 0 & 1 & 0 & | & 0 & -1 & 0 \\ 0 & 0 & | & 0 & 0 & 1 & | & 0 & 0 & -1 \end{array}\right) \end{array} \tag{3.67}$$

The linearly independent bridging fluxes, $\mathbf{J}^R$, were determined such that $\mathbf{J}^B = \mathbf{Q} \cdot \mathbf{J}^R$ as follows,

$$\overbrace{\begin{pmatrix} V_2 \\ V_5 \\ V_6 \end{pmatrix}}^{\mathbf{J}^B} = \overbrace{\begin{pmatrix} 1 & 0 \\ 0 & 1 \\ 1 & -1 \end{pmatrix}}^{\mathbf{Q}} \cdot \overbrace{\begin{pmatrix} V_2 \\ V_5 \end{pmatrix}}^{\mathbf{J}^R} \tag{3.68}$$

The $\mathbf{Q}$ matrix spans 2 columns corresponding to the two independent fluxes of module 1, the fluxes of reactions $V_2$ and $V_5$ at steady state. While these fluxes were selected as independent, any pair of the bridging fluxes could have been selected as the independent bridging fluxes due to the linear interdependence enabling the determination of the third bridging flux. The steady state concentrations for the metabolites in module 2 ($\mathbf{S}^2$) were determined, as

were the fluxes at steady state, using the FindRoot function available in Wolfram Mathematica®. The non-normalised elasticity submatrix ${}^*\epsilon_{R,2}$ was then calculated by fixing metabolites in module 2 ($\mathbf{S}^2$), with module 1 metabolite concentrations unfixed, and perturbing them individually while observing the change in the linearly independent bridging fluxes (${}^*\mathbf{J}^R$),

$$ {}^*\epsilon_{R,2} = \begin{array}{c} \\ V_2 \\ V_5 \end{array} \begin{array}{c} \begin{array}{ccc} X_1 & X_5 & X_6 \end{array} \\ \begin{pmatrix} 0.530 & -0.224 & -0.235 \\ 0.295 & -0.336 & 0.148 \end{pmatrix} \end{array} \tag{3.69} $$

where the asterisk superscript denotes overall (or block) elasticities. The non-normalised elasticity submatrix $\epsilon_{\mathbf{2,2}}$ was determined by calculating the partial derivatives of module 2 reaction rates with respect to module 2 metabolites,

$$ \epsilon_{2,2} = \begin{array}{c} \\ V_1 \\ V_7 \\ V_8 \end{array} \begin{array}{c} \begin{array}{ccc} X_1 & X_5 & X_6 \end{array} \\ \begin{pmatrix} -1 & 0 & 0 \\ 0 & 1 & 0 \\ 0 & 0 & 1 \end{pmatrix} \end{array} \tag{3.70} $$

The link matrix for module 2 ($\mathbf{L^2}$) was determined in a manner similar to that described by Hofmeyr [19] with the matrix being a 3 X 3 identity matrix due to the absence of dependent metabolites. The $\mathbf{M}^*$ matrix was then determined according to the following equation,

$$ \mathbf{M}^* = \left( \overline{\mathbf{N}}_{2,B} \cdot \mathbf{Q} \cdot {}^*\epsilon_{R,2} + \overline{\mathbf{N}}_{2,2} \cdot \epsilon_{2,2} \right) \cdot \mathbf{L}^2 \tag{3.71} $$

with the asterisk superscript indicating the matrix includes the effect of module 1 on module 2. $\overline{\mathbf{N}}_{2,B}$ and $\overline{\mathbf{N}}_{2,2}$, the reduced stoichiometry submatrices, are equivalent to $\mathbf{N}_{2,B}$ and $\mathbf{N}_{2,2}$ respectively, due to the lack of dependent metabolites. The inverse of this matrix, $(\mathbf{M}^*)^{-1}$, was then determined as it is used to calculate the control coefficients,

$$ (\mathbf{M}^*)^{-1} = \begin{array}{c} \\ X_1 \\ X_5 \\ X_6 \end{array} \begin{array}{c} \begin{array}{ccc} X_1 & X_5 & X_6 \end{array} \\ \begin{pmatrix} -0.699 & -0.128 & -0.132 \\ -0.169 & -0.787 & -0.113 \\ -0.132 & -0.0854 & -0.755 \end{pmatrix} \end{array} \tag{3.72} $$

The matrices of unnormalised control coefficients were then determined according to equations 3.26, 3.27 and 3.37 to 3.40 shown in the section 3.1.4. The control coefficients were then normalised, with the concentration control coefficients normalised as shown in 3.28 and 3.29. The flux control coefficients were normalised as described by equation 3.41,

$$ {}^*\mathbf{C}^J_{\mathrm{R,R}} = (dg\mathbf{J}^R)^{-1} \cdot {}^*\mathbf{\Phi}_{\mathrm{R,R}} \cdot (dg\mathbf{J}^R) \tag{3.73} $$

$$ \mathbf{C}^J_{\mathrm{R,2}} = (dg\mathbf{J}^R)^{-1} \cdot \mathbf{\Phi}_{\mathrm{R,2}} \cdot (dg\mathbf{J}^2) \tag{3.74} $$

$$ {}^*\mathbf{C}^J_{\mathrm{2,R}} = (dg\mathbf{J}^2)^{-1} \cdot {}^*\mathbf{\Phi}_{\mathrm{2,R}} \cdot (dg\mathbf{J}^R) \tag{3.75} $$

$$ \mathbf{C}^J_{2,2} = (dg\mathbf{J}^2)^{-1} \cdot \mathbf{\Phi}_{2,2} \cdot (dg\mathbf{J}^2) \tag{3.76} $$

The elasticity submatrices ${}^{*}\epsilon_{R,2}$ and $\epsilon_{2,2}$ were normalised according to equations 3.53 and 3.54. The concentration and flux summation and connectivity theorems described by equations 3.46, 3.47, 3.51, 3.52, and 3.57 to 3.59 were calculated and determined to be upheld, supporting the validity of the normalised modular control coefficients determined during the analysis. The normalised modular control coefficients for module 2 can, however, be compared to normalised control coefficients determined using standard MCA, as these control coefficients should be identical. In this way, the accuracy of the module 2 control coefficients can be tested. The normalised standard control coefficients were determined following a similar procedure to that which is described by Hofmeyr [19]. The comparison of the control of fluxes in module 2 on metabolites in module 2 is as follows,

$$\overbrace{\begin{array}{c} \\ \\ \mathbf{C}^{S}_{2,2} = \end{array}\begin{array}{c} \\ X_1 \\ X_5 \\ X_6 \end{array}\begin{array}{c} \begin{array}{ccc} V_1 & V_7 & V_8 \end{array} \\ \begin{pmatrix} 0.232 & -0.0254 & -0.0177 \\ 0.121 & -0.336 & -0.0324 \\ 0.110 & -0.0423 & -0.252 \end{pmatrix} \end{array}}^{\text{Control coefficients determined through modular analysis}} \tag{3.77}$$

$$= \overbrace{\begin{array}{c} \\ \\ = \end{array}\begin{array}{c} \\ X_1 \\ X_5 \\ X_6 \end{array}\begin{array}{c} \begin{array}{ccc} V_1 & V_7 & V_8 \end{array} \\ \begin{pmatrix} 0.232 & -0.0254 & -0.0177 \\ 0.121 & -0.336 & -0.0324 \\ 0.110 & -0.0423 & -0.252 \end{pmatrix} \end{array}}^{\text{Control coefficients determined through standard MCA}}$$

The comparison of the control of reactions in module 2 on module 2 fluxes is as follows,

$$\overbrace{\begin{array}{c} \\ \\ \mathbf{C}^{J}_{2,2} = \end{array}\begin{array}{c} \\ V_1 \\ V_7 \\ V_8 \end{array}\begin{array}{c} \begin{array}{ccc} V_1 & V_7 & V_8 \end{array} \\ \begin{pmatrix} 0.301 & 0.0765 & 0.0533 \\ 0.283 & 0.213 & -0.0760 \\ 0.329 & -0.127 & 0.245 \end{pmatrix} \end{array}}^{\text{Control coefficients determined through modular analysis}} \tag{3.78}$$

$$= \overbrace{\begin{array}{c} \\ \\ = \end{array}\begin{array}{c} \\ V_1 \\ V_7 \\ V_8 \end{array}\begin{array}{c} \begin{array}{ccc} V_1 & V_7 & V_8 \end{array} \\ \begin{pmatrix} 0.301 & 0.0765 & 0.0533 \\ 0.283 & 0.213 & -0.0760 \\ 0.329 & -0.127 & 0.245 \end{pmatrix} \end{array}}^{\text{Control coefficients determined through standard MCA}}$$

The control of reactions in module 2 on the independent bridging fluxes can be validated by comparing the control coefficients determined during mod-

ular control analysis with the appropriate traditional control coefficients. The matrix of normalised modular flux control coefficients for this comparison is as follows,

$$\mathbf{C}^J_{R,2} = \begin{array}{c} \\ V_2 \\ V_5 \end{array} \overbrace{\begin{array}{ccc} V_1 & V_7 & V_8 \\ 0.301 & 0.0765 & 0.0533 \\ 0.283 & 0.213 & -0.0760 \end{array}}^{\text{Control of module 2 reactions on } \mathbf{J}^R} \tag{3.79}$$

with the matrix of appropriate traditional flux control coefficients as follows,

$$\mathbf{C}^J_V = \begin{array}{c} \\ V_2 \\ V_5 \end{array} \begin{array}{ccc} V_1 & V_7 & V_8 \\ 0.301 & 0.0765 & 0.0533 \\ 0.283 & 0.213 & -0.0760 \end{array} \tag{3.80}$$

The control coefficients describing the control of the reactions in module 2, $\mathbf{V}^2$, on the independent bridging fluxes, $\mathbf{J}^R$, are identical as is expected.

The accuracy of the control of module 1 on the independent bridging fluxes as well as on components of module 2 can be tested through the comparison of the overall control coefficients determined during the modular analysis and appropriate traditional control coefficients.

The control module 1 has on the independent bridging fluxes, $\mathbf{J}^R$, is described by the normalised overall control coefficient matrix ${}^*\mathbf{C}^J_{R,R}$. The accuracy of these control coefficients can be determined by comparing them to the summation of the traditional flux control coefficients for each reaction in module 1 as well as the bridging reactions. These traditional control coefficients quantify the control each reaction has on the independent bridging fluxes. The control of module 1 determined through modular analysis is,

$${}^*\mathbf{C}^J_{R,R} = \begin{array}{c} \\ V_2 \\ V_5 \end{array} \overbrace{\begin{array}{c} \text{Module 1} \\ 0.569 \\ 0.579 \end{array}}^{\text{Control of module 1 on } \mathbf{J}^R} \tag{3.81}$$

The summation of appropriate traditional MCA flux control coefficients is performed as such,

$$\begin{array}{c} \\ V_2 \\ V_5 \end{array} \begin{array}{ccccccccc} V_2 & + & V_3 & + & V_4 & + & V_5 & + & V_6 \\ 0.301 & + & 0.0842 & + & 0.0533 & + & 0.0765 & + & 0.0533 \\ 0.283 & + & 0.235 & + & -0.0760 & + & 0.213 & + & -0.0760 \end{array} \tag{3.82}$$

with the summation of the control coefficients equivalent to the modular control coefficients shown in equation 3.81. Equations 3.81 and 3.82 demonstrate the accuracy of the overall control coefficients determined by modular control

analysis, as the control module 1 exerts on the independent bridging fluxes is equal to the summation of the controls of the individual module 1 and bridging reactions on the independent bridging fluxes connecting module 1 and module 2.

The control of module 1 on the components of module 2 can be validated similarly. The matrix of normalised modular concentration control coefficients, ${}^*\mathbf{C}^S_{2,R}$, is compared to corresponding traditional concentration control coefficients. The comparison is performed by comparing the determined overall concentration control coefficients of module 1 on each metabolite in module 2 to the summation of the control of the individual reactions in module 1, $\mathbf{V}^1$, and the bridging reactions, $\mathbf{V}^B$, on each metabolite in module 2. The normalised modular concentration control coefficients are,

$$ {}^*\mathbf{C}^S_{2,R} = \begin{array}{c} \overbrace{\text{Module 1}}^{\text{Control of module 1 on } \mathbf{S}^2} \\ \begin{array}{c} X_1 \\ X_5 \\ X_6 \end{array} \begin{pmatrix} -0.189 \\ 0.247 \\ 0.185 \end{pmatrix} \end{array} \tag{3.83} $$

The appropriate traditional concentration control coefficients can be summed to determine the control of module 1 as follows,

$$ \begin{array}{c} \quad V_2 \quad + \quad V_3 \quad + \quad V_4 \quad + \quad V_5 \quad + \quad V_6 \\ \begin{array}{c} X_1 \\ X_5 \\ X_6 \end{array} \begin{pmatrix} -0.100 & + & -0.0280 & + & -0.0177 & + & -0.0254 & + & -0.0177 \\ 0.121 & + & 0.100 & + & -0.0324 & + & 0.0911 & + & -0.0324 \\ 0.110 & + & -0.0466 & + & 0.0819 & + & -0.0423 & + & 0.0819 \end{pmatrix} \end{array} \tag{3.84} $$

The control of module 1 determined both through modular control analysis, shown in equation 3.83, as well as through the summation of the traditional control coefficients, shown in equation 3.84, are identical.

The control of module 1 on the fluxes in module 2 can be similarly compared,

$$ {}^*\mathbf{C}^J_{2,R} = \begin{array}{c} \overbrace{\text{Module 1}}^{\text{Control of module 1 on } \mathbf{J}^2} \\ \begin{array}{c} V_1 \\ V_7 \\ V_8 \end{array} \begin{pmatrix} 0.569 \\ 0.579 \\ 0.553 \end{pmatrix} \end{array} \tag{3.85} $$

The appropriate traditional flux control coefficients can be summed to deter-

mine the control of module 1,

$$\begin{array}{c} \\ V_1 \\ V_7 \\ V_8 \end{array} \begin{array}{c} \begin{array}{ccccccccc} V_2 & + & V_3 & + & V_4 & + & V_5 & + & V_6 \end{array} \\ \begin{pmatrix} 0.301 & + & 0.0842 & + & 0.0533 & + & 0.0765 & + & 0.0533 \\ 0.283 & + & 0.235 & + & -0.0760 & + & 0.213 & + & -0.0760 \\ 0.329 & + & -0.139 & + & 0.245 & + & -0.127 & + & 0.245 \end{pmatrix} \end{array} \tag{3.86}$$

The control of module 1 on the fluxes in module 2 determined through modular analysis as well as through the summation of the appropriate traditional control coefficients is identical, as seen in equations 3.85 and 3.86. This, together with the previous comparisons, is a simple test for the validity of the control coefficients determined by the modular control analysis.

Modular control analysis has been successfully formulated in the Wolfram Mathematica® coding context. The framework has also been successfully applied to simple linear and branched models. As such, the first and second objectives have been achieved with the third partially addressed. For this reason, the following section focuses on the development and application of a Mathematica package on a variety of models.

# Chapter 4

# Results and Discussion

## 4.1 Core model analyses with Mathematica package

The development of a package automating the application of modular control analysis on models of biochemical systems is the fourth objective of this thesis. With this we aim to simplify the use of modular control analysis, which may otherwise prove difficult and time consuming for large models. The package also enables users less familiar with modular control analysis to perform analyses, provided limited knowledge of the decomposition is known. Throughout its development, the package was applied to a range of core models to ensure it was capable of correctly and accurately performing modular control analysis on models with a multitude of components that could be present in models of biologically relevant biochemical systems. The models analysed include linear and branched systems as well as models containing conserved moiety cycles. Other aspects were also incorporated into core models and analysed, such as the presence of fluxes with a magnitude of 0 at steady state (as would be present in systems with equilibrium reactions), reactions with near-zero fluxes at steady state, and models with metabolites with zero or near-zero concentrations at steady state. A selection of these analyses will be discussed and, where necessary, the adaptions made to the package which enable the analyses to be performed, or which improve the output provided by the package, will be described. In this way, section 4.1 contributes to the completion of the third and fourth objectives, specifically the analysis of core models and the development of a package for automating the analyses.

The package has been developed such that the function performing the analysis requires two arguments, the first being that of the model specification as obtained from JWS Online, described in Appendix B, and the second argument is a list of lists containing the information of module 1 metabolites and reactions as well as the bridging reactions. The list is structured such that it

contains a number of lists equivalent to the number of type 1 modules. If a single type 1 module is present, the list will contain a single list containing three sublists; the first sublist containing the metabolites in the type 1 module, the second, the reactions within the type 1 module, and the third, the bridging reactions connecting the type 1 module to the type 2 module. Prior to performing modular control analysis using any functions present in the package, the package must be loaded using the *Needs* or *Get* functions in the Wolfram Mathematica® notebook.

### 4.1.1 Linear pathway

Firstly, the package was applied to a model of a linear system as depicted in Figure 4.1 with both S and P fixed metabolites. Once the components of module 1 and the bridging reactions have been identified, the ordering list, the second argument required for the function performing the analysis, can be constructed. In this case, the ordering list is short and as such was saved in a single variable: $orderinglist = \{\{\{x2[t], x3[t]\}, \{v2\}, \{v1, v3\}\}\}$ with the model information saved in the variable *pathway*. This enables the function to be called: **ModularControlAnalysis**[*pathway*, *orderinglist*]. The control coefficient matrices determined by the function can be accessed through a number of variables. An example of such a variable name is *fullnormCj22* which is the matrix containing the flux control coefficients for the module 2 reactions on module 2 fluxes. The matrices containing overall control coefficients are stored in variables with names ending in _*star*, similar to the convention used by Schuster and colleagues [1] where an asterisk was used to denote matrices containing overall control coefficients of the type 1 module.

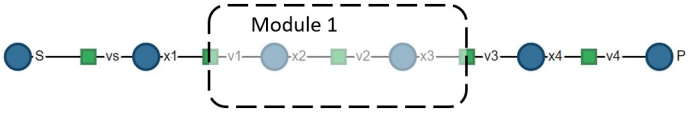


**Figure 4.1:** Schematic of the simple linear pathway being analysed with the modular decomposition indicated.

The initial outputs are the results of the steady state condition and control theorem checks described in section 3.1.5, with the ideal output being "True". The threshold applied to these checks is $10^{-6}$, such that if the output deviates from the expected output by a magnitude of greater than $1 \times 10^{-6}$ the output "False" will be returned as the result of the check. The output will typically be seen as shown in Table 4.1. These control theorem checks were included as the first outputs of the function as they provide an indication as to whether there is an error regarding the modular decomposition and determination of the control coefficients. The normalised flux summation and the flux connenctivity checks

display 2 results, one for each module. The first result corresponds to module 1 and the second to module 2.

**Table 4.1:** The results of the steady state and control theorem checks for the modular control analysis of the simple linear pathway.

```
{{"Steady State Condition"}, {True}}
{{"Concentration Summation-Unnormalised"}, {True}}
{{"Concentration Summation-Normalised"}, {True}}
{{"Concentration Connectivity-Unnormalised"}, {True}}
{{"Concentration Connectivity-Normalised"}, {True}}
{{"Flux Summation-Unnormalised"}, {True}}
{{"Flux Summation-Normalised"}, {True, True}}
{{"Flux Connectivity-Unnormalised"}, {True, True}}
{{"Flux Connectivity-Normalised"}, {True, True}}
```

The control coefficients of the components of module 2 on themselves as well as on the bridging fluxes can be seen in Table 4.2. The function applied to the matrices of control coefficients, *DispMat*, changes the manner in which the matrices are displayed, similar to that achieved by the Mathematica function *MatrixForm*. The changes are aesthetic, intended to improve legibility. The variable names are shown as well as the resulting control coefficients which match those shown in section 3.1, as this pathway was used to demonstrate the application of the framework with an identical modular decomposition being implemented. The control of module 2 reactions on all bridging fluxes are shown, the determination of which is discussed in section 3.1.4. The variable name *fullnormCjBa2* indicates the flux control coefficients of module 2 reactions on the bridging fluxes of module 1. The "Ba" indicates the bridging fluxes of module 1a. This notation is used in preparation for analyses with multiple type 1 modules, where additional type 1 modules are indicated alphabetically proceeding from "b". For control theorem calculations, only the independent control coefficients are included as discussed in section 3.1.5.

**Table 4.2:** Matrices of concentration and flux control coefficients of module 2 reactions on module 2 metabolite concentrations, module 2 fluxes, and on the bridging fluxes.

```
In[7]:= fullnormCs22 // DispMat
        fullnormCj22 // DispMat
        fullnormCjBa2 // DispMat
```

Out[7]//MatrixForm=

| | | | |
|---|---|---|---|
| _ | v4 | vs | _ |
| x1[t] | -0.0261 | 0.599 | x1[t] |
| x4[t] | -0.696 | 0.432 | x4[t] |
| _ | v4 | vs | _ |

Out[8]//MatrixForm=

| | | | |
|---|---|---|---|
| _ | v4 | vs | _ |
| v4 | 0.0169 | 0.61 | v4 |
| vs | 0.0169 | 0.61 | vs |
| _ | v4 | vs | _ |

Out[9]//MatrixForm=

| | | | |
|---|---|---|---|
| _ | v4 | vs | _ |
| v1 | 0.0169 | 0.61 | v1 |
| v3 | 0.0169 | 0.61 | v3 |
| _ | v4 | vs | _ |

Similarly, the matrices of normalised overall control coefficients can be displayed, as shown in Table 4.3, where the control of module 1 on the steady state concentrations of metabolites in module 2 is shown. Module 1 is referred to as "module 1a" in Table 4.3. The control of module 1 on module 2 fluxes and the bridging fluxes are also displayed, with these control coefficients identical to those determined in section 3.1. The overall flux control coefficients of module 1 on the bridging fluxes are contained in the variable *fullnormCjBara_star*, with "ra" indicating the overall control of module 1a on "Ba", the bridging fluxes of module 1a. As such, the output of the package can be considered accurate relative to both the manual modular control analysis as well as the appropriate traditional control coefficients and summations thereof.

**Table 4.3:** Matrices of overall concentration and flux control coefficients for module 1 (module 1a) on module 2 metabolites, module 2 fluxes, and the bridging fluxes.

```
In[10]:= fullnormCs2ra_star // DispMat
         fullnormCj2ra_star // DispMat
         fullnormCjBara_star // DispMat
```

Out[10]//MatrixForm=

| | Control of module 1a | |
|---|---|---|
| x1[t] | -0.573 | x1[t] |
| x4[t] | 0.264 | x4[t] |
| | Control of module 1a | |

Out[11]//MatrixForm=

| | Control of module 1a | |
|---|---|---|
| v4 | 0.373 | v4 |
| vs | 0.373 | vs |
| | Control of module 1a | |

Out[12]//MatrixForm=

| | Control of module 1a | |
|---|---|---|
| v1 | 0.373 | v1 |
| v3 | 0.373 | v3 |
| | Control of module 1a | |

While the control coefficients can be accessed, so too can the Q matrix of module 1, using the variable name *Qmatrices*. Following the analysis of this simple linear pathway, it is evident that the package is able to accurately analyse linear models and as such can be tested on a branched model such as the simple 8 reaction branched pathway which has been manually analysed previously. The model was decomposed in an identical manner to enable direct comparison of the control coefficients from the package analysis to those of the manual analysis.

### 4.1.2 Branched pathway

The package was used to analyse the branched pathway, shown in Figure 4.2, with the components of the module chosen as shown in the figure and as was selected in the manual analysis previously. The steady state condition and modular control theorems were the same as before, with the resulting control coefficients shown in Table 4.4.

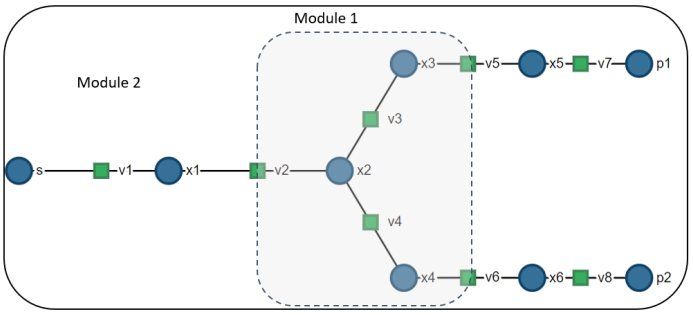


**Figure 4.2:** Schematic of the 8 reaction branched pathway with the modular decomposition as annotated. The bridging reactions are reactions v2, v5 and v6.

**Table 4.4:** Control coefficients determined by the package following analysis of the 8 reaction branched pathway decomposed as annotated.

```
In[7]:= fullnormCs22 // DispMat
        fullnormCj22 // DispMat
        fullnormCjBa2 // DispMat
```

Out[7]//MatrixForm=

| | v1 | v7 | v8 | |
|---|---|---|---|---|
| x1[t] | 0.232 | -0.0254 | -0.0177 | x1[t] |
| x5[t] | 0.121 | -0.336 | -0.0324 | x5[t] |
| x6[t] | 0.11 | -0.0423 | -0.252 | x6[t] |
| | v1 | v7 | v8 | |

Out[8]//MatrixForm=

| | v1 | v7 | v8 | |
|---|---|---|---|---|
| v1 | 0.301 | 0.0765 | 0.0533 | v1 |
| v7 | 0.283 | 0.213 | -0.076 | v7 |
| v8 | 0.329 | -0.127 | 0.245 | v8 |
| | v1 | v7 | v8 | |

Out[9]//MatrixForm=

| | v1 | v7 | v8 | |
|---|---|---|---|---|
| v2 | 0.301 | 0.0765 | 0.0533 | v2 |
| v5 | 0.283 | 0.213 | -0.076 | v5 |
| v6 | 0.329 | -0.127 | 0.245 | v6 |
| | v1 | v7 | v8 | |

**(a)** Module 2 control coefficients

```
In[10]:= fullnormCs2ra_star // DispMat
         fullnormCj2ra_star // DispMat
         fullnormCjBara_star // DispMat
```

Out[10]//MatrixForm=

| | Control of module 1a | |
|---|---|---|
| x1[t] | -0.189 | x1[t] |
| x5[t] | 0.247 | x5[t] |
| x6[t] | 0.185 | x6[t] |
| | Control of module 1a | |

Out[11]//MatrixForm=

| | Control of module 1a | |
|---|---|---|
| v1 | 0.569 | v1 |
| v7 | 0.579 | v7 |
| v8 | 0.553 | v8 |
| | Control of module 1a | |

Out[12]//MatrixForm=

| | Control of module 1a | |
|---|---|---|
| v2 | 0.569 | v2 |
| v5 | 0.579 | v5 |
| v6 | 0.553 | v6 |
| | Control of module 1a | |

**(b)** Module 1 overall control coefficients

The control coefficients determined using the package are identical to those determined manually and therefore correspond to the appropriate traditional control coefficients, or summations thereof, as was shown during the discussion of the manual analysis. The next core model analysis to be discussed is that of a pathway with branches and a conserved moiety cycle present, with the model referred to as the complex core model. The presence of dependent metabolites must be addressed as it is a common component of biochemical systems.

### 4.1.3 Complex core model

The package was used to analyse a core model with both branches and a moiety conserved cycle present. The model analysed is shown in Figure 4.3, with $P_1, P_2, X_0, X_6,$ and $X_7$ fixed metabolites. The model description, including ODEs, parameters, initial values, and rate equations, are located in Appendix A.3 and three significant digits are shown for the determined control coefficients. The components of module 1 are shown in the figure as those components of the model encompassed by the shaded/semi-transparent area. As such, the bridging reactions, $\mathbf{V}^B$, are reactions $v_1, v_4,$ and $v_5$, with the module 1 reaction, $\mathbf{V}^1$, as $v_3$. The module 2 reactions, $\mathbf{V}^2$, include reactions $v_2, v_6, v_7, v_8,$ and $v_9$. The modular decomposition results in the partitioning of the metabolites as such, $\mathbf{S}^1 = X_1$ and $X_4$, and $\mathbf{S}^2 = X_{10}, X_3, X_5, X_8, X_9$ and $X_2$, with $X_2$ the dependent metabolite in module 2 due to the sum of the concentrations of metabolites $X_2$ and $X_3$ equal to a constant.

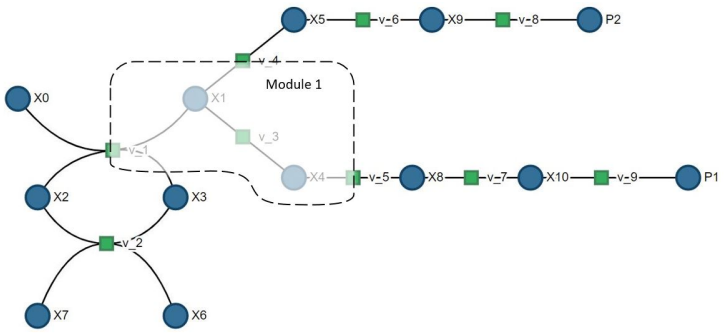


**Figure 4.3:** Schematic of the complex core model with module 1 components encompassed by the shaded area labelled 'Module 1'.

Following the analysis of the model with the package, it was determined that the steady state and control theorems were upheld. The control coefficients for module 2 and module 1 are shown in Table 4.5.

**Table 4.5:** Control coefficients determined by the package following analysis of the complex core pathway.

```
In[7]:= fullnormCs22 // DispMat
        fullnormCj22 // DispMat
        fullnormCjBa2 // DispMat
```

Out[7]//MatrixForm=

| | v_2 | v_6 | v_7 | v_8 | v_9 | |
|---|---|---|---|---|---|---|
| X10[t] | 0.797 | -0.321 | 0.0367 | -0.321 | -0.186 | X10[t] |
| X3[t] | -0.246 | 0.0419 | 0.00329 | 0.0419 | 0. | X3[t] |
| X5[t] | 0.261 | -0.248 | -0.00829 | -0.248 | 0. | X5[t] |
| X8[t] | 0.0957 | -0.0386 | -0.0179 | -0.0386 | 0. | X8[t] |
| X9[t] | 0.228 | 0.156 | -0.00723 | -0.588 | 0. | X9[t] |
| X2[t] | 0.184 | -0.0313 | -0.00246 | -0.0313 | 0. | X2[t] |
| | v_2 | v_6 | v_7 | v_8 | v_9 | |

Out[8]//MatrixForm=

| | v_2 | v_6 | v_7 | v_8 | v_9 | |
|---|---|---|---|---|---|---|
| v_2 | 0.597 | 0.0686 | 0.0054 | 0.0686 | 0. | v_2 |
| v_6 | 0.306 | 0.21 | -0.00972 | 0.21 | 0. | v_6 |
| v_7 | 4.28 | -1.73 | 0.197 | -1.73 | 0. | v_7 |
| v_8 | 0.306 | 0.21 | -0.00972 | 0.21 | 0. | v_8 |
| v_9 | 4.28 | -1.73 | 0.197 | -1.73 | 0. | v_9 |
| | v_2 | v_6 | v_7 | v_8 | v_9 | |

Out[9]//MatrixForm=

| | v_2 | v_6 | v_7 | v_8 | v_9 | |
|---|---|---|---|---|---|---|
| v_1 | 0.597 | 0.0686 | 0.0054 | 0.0686 | 0. | v_1 |
| v_4 | 0.306 | 0.21 | -0.00972 | 0.21 | 0. | v_4 |
| v_5 | 4.28 | -1.73 | 0.197 | -1.73 | 0. | v_5 |
| | v_2 | v_6 | v_7 | v_8 | v_9 | |

**(a)** Module 2 control coefficients

```
In[10]:= fullnormCs2ra_star // DispMat
         fullnormCj2ra_star // DispMat
         fullnormCjBara_star // DispMat
```

Out[10]//MatrixForm=

| | Control of module 1a | |
|---|---|---|
| X10[t] | -0.00519 | X10[t] |
| X3[t] | 0.159 | X3[t] |
| X5[t] | 0.242 | X5[t] |
| X8[t] | -0.000624 | X8[t] |
| X9[t] | 0.211 | X9[t] |
| X2[t] | -0.119 | X2[t] |
| | Control of module 1a | |

Out[11]//MatrixForm=

| | Control of module 1a | |
|---|---|---|
| v_2 | 0.261 | v_2 |
| v_6 | 0.284 | v_6 |
| v_7 | -0.0279 | v_7 |
| v_8 | 0.284 | v_8 |
| v_9 | -0.0279 | v_9 |
| | Control of module 1a | |

Out[12]//MatrixForm=

| | Control of module 1a | |
|---|---|---|
| v_1 | 0.261 | v_1 |
| v_4 | 0.284 | v_4 |
| v_5 | -0.0279 | v_5 |
| | Control of module 1a | |

**(b)** Module 1 overall control coefficients

The traditional control coefficients for the model were then determined and compared to the control coefficients determined by the package. The comparisons were performed through the determination of the maximum absolute difference between the control coefficient matrices as was done during previous analyses. The resulting maximum absolute difference, and subsequently the degree to which the control coefficients determined by the package are accurate, was of magnitude $10^{-9}$. Such a degree of accuracy suggests the package is capable of accurately analysing models with both branches and moiety conserved cycles present. This confirms the package is capable of analysing models with components often present in biologically relevant models. The presence of equilibrium reactions has also been addressed, discussed in Appendix B.4, similarly with presence of metabolites and fluxes with near zero concentrations and fluxes are discussed in Appendix section B.5. The issues observed were general metabolic control analysis issues and not specific to modular control analysis. Subsequently, the package has been shown to correctly and accurately analyse core models with a number of components that may be present in biologically relevant models. Therefore, the next step is the analysis of models of biological systems such as glycolysis in the *P. falciparum* parasite as constructed by Penkler and colleagues [11]. A model of glucose metabolism in *P. falciparum*-infected erythrocytes [12] will also be analysed with these analyses addressing the final objective of this thesis.

## 4.2 Detailed model analyses with Mathematica package

### 4.2.1 Analysis of glycolysis in the *P. falciparum* parasite

Modular control analysis was performed on a model of glycolysis in a *P. falciparum* parasite, constructed and validated by Penkler and colleagues [11], such that the aldolase branch point of the model was designated module 1, as shown in Figure 4.4. The model description is available on JWS Online, with the model name Penkler1. The module was chosen rather arbitrarily but the aldolase branch point is expected to influence redox metabolism structurally and this was tested in the analysis. The metabolites of module 1, $\mathbf{S}^1$, are dhapPF, f16bpPF and gapPF. The inclusion of "PF" in the metabolite and reaction names indicates they are components of the parasite, *P. falciparum*. The bridging reactions, $\mathbf{V}^B$, are vPFvGAPDH, vPFvG3PDH and vPFvPFK, with the internal reactions, $\mathbf{V}^1$, vPFvALD and vPFvTPI. Three significant digits will be displayed for the determined control coefficients.

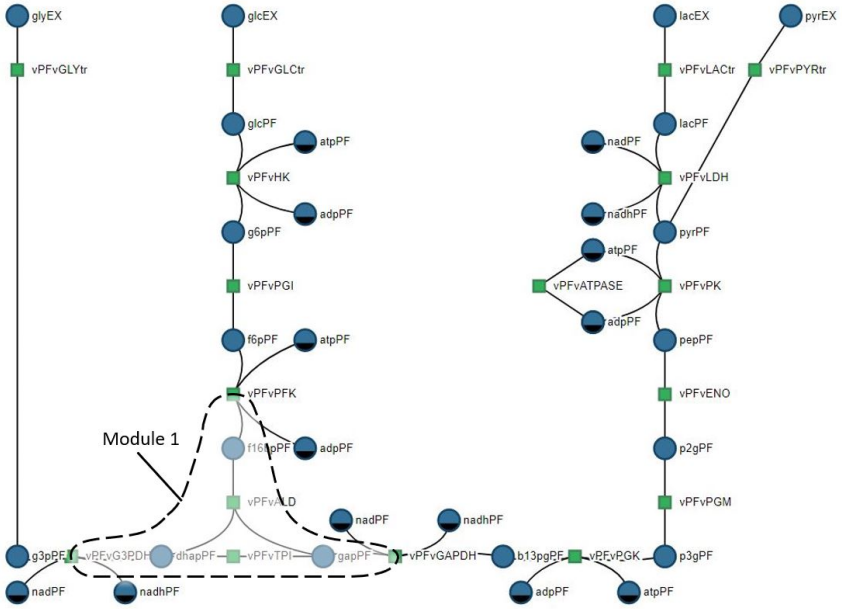


**Figure 4.4:** Schematic of the modular decomposition of the Penkler model for glycolysis in *P. falciparum*. Module 1 is annotated with the components of the module encompassed in the shaded (semi-transparent) area. The bridging reactions are reactions vPFvGAPDH, vPFvG3PDH, and vPFvPFK

Following the analysis with the modular decomposition as shown in Figure 4.4, the control theorems were determined to be upheld, as was the steady state condition. This suggests the control coefficients should be accurate, however, as in the analyses performed on the core models, the control coefficients determined using the package were compared to appropriate traditional control coefficients. The maximum absolute difference between the package control coefficients and the traditional control coefficients was determined to be of magnitude $10^{-8}$, which is a sufficient degree of accuracy. While the control coefficients of module 2 on the metabolites and fluxes in module 2 as well as on the bridging fluxes are of interest, the aim of performing modular control analysis is to determine the control exerted by type 1 modules on the rest of the system. For this reason the control coefficients for module 2 are not shown here but the overall control coefficients of module 1 are shown in Table 4.6. Table 4.6a shows the control of module 1 on the metabolites in module 2. The overall concentration control coefficients for module 1 on the substrates in module 2 were negative, indicating that an upregulation of module 1 would decrease the concentrations of the substrates. The control of module 1 on the concentrations of the products was greater than zero, indicating that upregulation of module 1 will increase the concentrations of the products, with the control on the concentration of b13pgPF complete, with a magnitude of 1. The control of module 1 on the lactate concentration was minimal. The concentration control coefficients of module 2 reactions on the lactate concentration,

not shown here, were also minimal, indicating the control on the concentration of lactate is distributed across a number of fluxes throughout the pathway.

**Table 4.6:** Overall control coefficients of module 1 as determined by the package following analysis of the Penkler model.

```
In[7]:= fullnormCs2ra_star // DispMat
Out[7]//MatrixForm=
```

| | Control of module 1a | |
|---|---|---|
| atpPF[t] | 0.0817 | atpPF[t] |
| b13pgPF[t] | 1.03 | b13pgPF[t] |
| f6pPF[t] | −0.969 | f6pPF[t] |
| g3pPF[t] | 0.521 | g3pPF[t] |
| g6pPF[t] | −0.927 | g6pPF[t] |
| glcPF[t] | −0.451 | glcPF[t] |
| lacPF[t] | 0.0625 | lacPF[t] |
| nadPF[t] | 0.00285 | nadPF[t] |
| p2gPF[t] | 0.514 | p2gPF[t] |
| p3gPF[t] | 0.539 | p3gPF[t] |
| pepPF[t] | 0.654 | pepPF[t] |
| pyrPF[t] | 0.582 | pyrPF[t] |
| adpPF[t] | −0.411 | adpPF[t] |
| nadhPF[t] | −0.146 | nadhPF[t] |
| | Control of module 1a | |

**(a)** Overall concentration control coefficients for module 1.

```
In[8]:= fullnormCj2ra_star // DispMat
        fullnormCjBara_star // DispMat
Out[8]//MatrixForm=
```

| | Control of module 1a | |
|---|---|---|
| vPFvATPASE | 0.388 | vPFvATPASE |
| vPFvENO | 0.402 | vPFvENO |
| vPFvGLCtr | 0.415 | vPFvGLCtr |
| vPFvGLYtr | 0.725 | vPFvGLYtr |
| vPFvHK | 0.415 | vPFvHK |
| vPFvLACtr | 0.388 | vPFvLACtr |
| vPFvLDH | 0.388 | vPFvLDH |
| vPFvPGI | 0.415 | vPFvPGI |
| vPFvPGK | 0.402 | vPFvPGK |
| vPFvPGM | 0.402 | vPFvPGM |
| vPFvPK | 0.402 | vPFvPK |
| vPFvPYRtr | 0.725 | vPFvPYRtr |
| | Control of module 1a | |

```
Out[9]//MatrixForm=
```

| | Control of module 1a | |
|---|---|---|
| vPFvGAPDH | 0.402 | vPFvGAPDH |
| vPFvG3PDH | 0.725 | vPFvG3PDH |
| vPFvPFK | 0.415 | vPFvPFK |
| | Control of module 1a | |

**(b)** Overall flux control coefficients for module 1.

While the concentration control coefficients are of interest, the focus of many MCA studies is on flux control coefficients. With this in mind, there are a number of overall flux control coefficients determined for module 1 which are of interest. The overall flux control coefficients of module 1 on vPFvGLYtr and vPFvPYRtr, the fluxes transporting glycerol and pyruvate out of the parasite, were 0.725. This indicates module 1 exerts considerable control on the efflux of these two metabolites, with the control coefficients identical due to the redox constraints of the pathway. Regarding the control of module 1 on the fluxes in module 2 as a whole, module 1 was determined to exert considerable control on all reactions, with the smallest control coefficient having a magnitude of 0.388. This control coefficient was determined for the fluxes of reactions vPFvATPASE, vPFvLACtr, and vPFvLDH. In this way, despite the module exerting minimal control on the concentration of lactate at steady state, considerable control on both the flux producing lactate, vPFvLDH, as well as on the flux transporting lactate out of the parasite, vPFvLACtr, was determined for module 1. The control of module 1 on the cycling of ATP and ADP, via reaction vPFvATPASE, while among the lowest of the determined overall control coefficients, is still considerable. The control observed for module 1 is likely owing to the bridging reaction vPFvPFK being directly involved

in the production of ADP (adpPF) through the consumption of ATP (atpPF).

The package has been used to analyse the Penkler model of glycolysis in *P. falciparum* with the aldolase branch point of the model selected as the type 1 module. This analysis demonstrated the application of modular control analysis, as well as the possible benefits of applying the framework to models of biochemical systems. The analysis confirmed the high degree of control that the branch point of the system has on the pathway flux. This showcases the possible benefits of applying modular control analysis as it enables the quantification of the control of groups of reactions within a biochemical system. This is beneficial as the overall control may be of interest, such as the degree of control the branch point of glycolysis in the parasite exerts on the other components of the pathway, as opposed to the control of the individual reactions. While overall control coefficients may be determined through the summation of the individual control coefficients, this method enables the overall control to be determined directly, without the determination of the individual control coefficients being required. This analysis demonstrated the application of the package and modular control analysis, however, prior to the application of the package to large, complex whole-body models, such as a whole-body model of glucose metabolism in malaria patients, the package was applied to a model of glucose metabolism in human erythrocytes infected with *P. falciparum* [12].

### 4.2.2 Analysis of glucose metabolism in *P. falciparum*-infected erythrocytes

The model being analysed was constructed by du Toit [12] through the combination of two models. The first model is that of glycolysis in the *P. falciparum* parasite constructed by Penkler and colleagues [11]. The second model is that of glucose metabolism of human erythrocytes including, glycolysis, the 2,3-BPG shunt, and the pentose phosphate pathway [37; 38; 39]. The model by du Toit [12] provides an opportunity to showcase the potential benefits of applying modular control analysis to large, complex biochemical systems as well as to test the application of the package to models with considerably greater complexity than have previously been analysed using the package. The system was decomposed with the parasite, *P. falciparum*, defined as the type 1 module such that the bridging reactions, $\mathbf{V}^B$, connecting module 1 to the type 2 module are reactions vPFvGLCtr, vPFvLACtr, vPFvPYRtr, and vPFvGLYtr. Reaction vPFvGLYtr is not explicitly shown in the schematic of the du Toit model, Figure 4.5, however, the reaction facilitates the transport of glycerol out of the parasite into the external environment, not into the erythrocyte. This is shown in the schematic as the conversion of g3pPF to glyEXT. In this way, the metabolites of the parasite, indicated by the suffix 'PF' in the name of the relevant metabolites, are considered components of module 1, $\mathbf{S}^1$.

The remaining reactions within the parasite, indicated by 'PF' in the reaction name, are considered components of module 1, $\mathbf{V}^1$. The metabolites in module 2, $\mathbf{S}^2$, are indicated by the suffix 'RBCi' in the metabolite name, with RBCi a contraction of Red Blood Cell-infected. The reactions of module 2, $\mathbf{V}^2$, are similarly denoted by the prefix 'vRBCiv'.

This decomposition of the system was chosen as it enables the determination of the control of the parasite on the components of the infected erythrocyte. This is of interest as traditional MCA enables the determination of the control of individual enzymes, however, the control of the parasite as a whole on the metabolism of the infected erythrocyte may be of interest, not necessarily the control of specific enzymes. While the control of specific enzymes is important to identify possible drug targets, the control of the parasite quantifies the contribution of the parasite to erythrocyte metabolism.

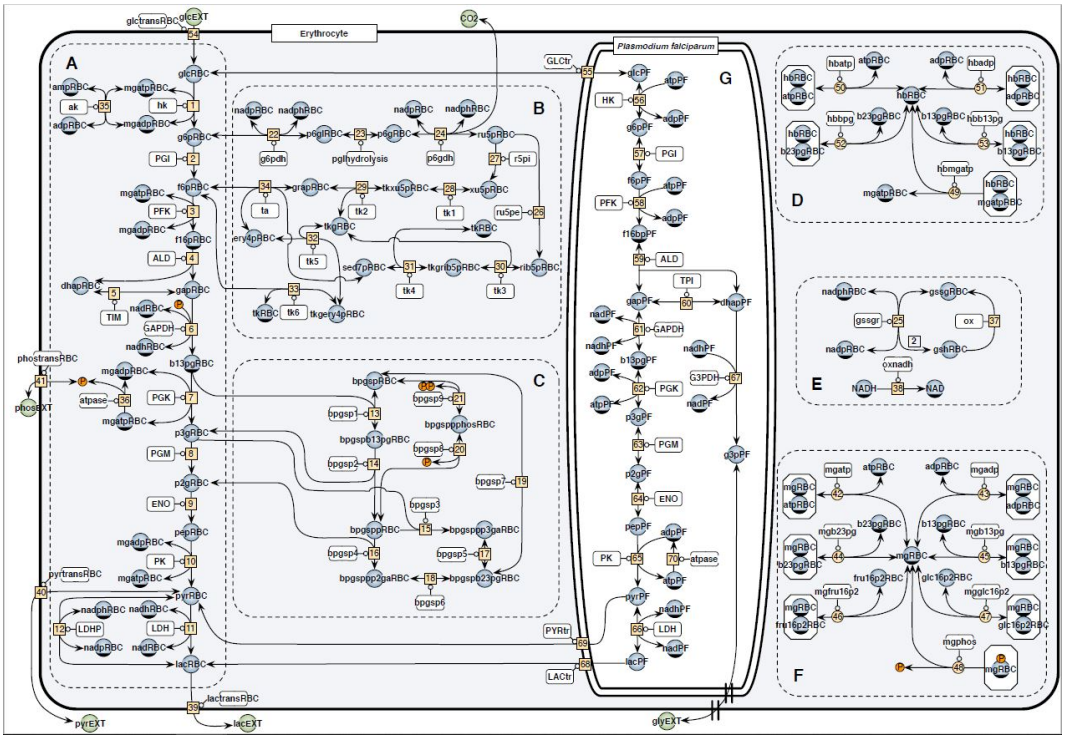


**Figure 4.5:** Schematic of the du Toit model of glucose metabolism in *P. falciparum*-infected erythrocytes.

Following the analysis of the model with the package and modular decomposition as described, it was determined that the steady state condition was upheld, as expected. Violations of the control theorems were, however, detected as shown in Table 4.7. These violations were determined to be the result of metabolites with low concentrations at steady state as well as reactions with fluxes at or near zero.

**Table 4.7:** Steady state condition and control theorem output following analysis of the du Toit model with the package.

```
In[19]:= ModularControlAnalysis[pathway, orderinglist]
{{"Steady State Condition"}, {True}}
{{"Concentration Summation-Unnormalised"}, {True}}
{{"Concentration Summation-Normalised"}, {True}}
{{"Concentration Connectivity-Unnormalised"}, {False}}
{{"Concentration Connectivity-Normalised"}, {False}}
{{"Flux Summation-Unnormalised"}, {True}}
{{"Flux Summation-Normalised"}, {True, False}}
{{"Flux Connectivity-Unnormalised"}, {True, False}}
{{"Flux Connectivity-Normalised"}, {False, False}}
```

The concentration connectivity and flux summation control theorem violations shown in Table 4.7 are similar to those observed during the analysis of the model with 0 fluxes at steady state, Appendix B.4, with the violations of the unnormalised forms of these control theorems the result of a large number of fluxes with magnitudes of less than $10^{-7}$ with several fluxes having a magnitude of $10^{-13}$ or smaller. These fluxes with small magnitudes, in conjunction with a number of module 2 metabolites with concentrations below $10^{-6}$, with the concentrations of some metabolites as low as $10^{-10}$, contribute to the remaining violations observed in the package output for the control theorem tests following the analysis of the du Toit model. The normalised flux summation for module 1 was determined to be valid, this is due to the reactions within module 1 not having zero or near-zero fluxes, whereas the normalised flux summation for module 2 was determined to be invalid, with the violation the result of a number of reactions with fluxes near, or at, zero at steady state. The flux connectivity violations are the result of inaccuracies caused by the fluxes with very small magnitudes. The violations are not the result of an inability to calculate the results, instead the results do not correspond to the expected output.

The understanding that the violations of the theorems are the result of both concentrations and fluxes with very small magnitudes, including zero for the fluxes, was confirmed following the determination of traditional control coefficients for the du Toit model as well as calculation of the traditional control theorems. The determined traditional control theorems had similar violations owing to inaccuracies arising from the small magnitude fluxes and metabolite concentrations as well as the 0 fluxes present. The overall control coefficients for module 1 were manually determined using a perturbation method where all internal and bridging reactions for module 1 were perturbed and the control coefficients determined. These control coefficients were subsequently compared

to the controls determined by the package. The control coefficients were accuarate to a magnitude of $10^{-7}$ with the exception of metabolites and fluxes with near zero magnitudes at steady state, which, as discussed in Appendix B.5, are forced to 0. In this way, the accuracy of the control coefficients determined by the package were validated, despite the violations observed in the control theorems.

The number of metabolites and fluxes in module 2 makes the inclusion of the control coefficient matrices impractical, however, specific control coefficients will be discussed. Selected overall concentration control coefficients for the parasite on module 2 metabolites are shown in Table 4.8. The control of the parasite on the metabolites of module 2 is low for the majority of metabolites, yet specific metabolites appear to experience considerable control such as the lactate concentration in the infected erythrocyte, lacRBCi, with an overall concentration control coefficient by module 1 of 0.989. The control of the parasite on the concentration of pyruvate in the erythrocyte, pyrRBCi, was also considerable. This suggests the parasite exerts a high degree of control on the concentrations of glycolysis end products in the erythrocyte, likely due to the high rate of glycolysis occurring in the parasite, which contributes to these metabolites. Despite the considerable control of the parasite on the concentrations of pyruvate and lactate in the erythrocyte, the control on the concentration of glucose, glcRBCi, was minimal. This suggests that despite the consumption of erythrocyte glucose, following transport into the parasite, the transport of glucose into the erythrocyte is enough to almost completely compensate.

**Table 4.8:** Overall concentration control coefficients for the parasite on specific module 2 metabolites.

| | Control of module 1a | |
|---|---|---|
| glcRBCi[t] | -0.00515 | glcRBCi[t] |
| lacRBCi[t] | 0.989 | lacRBCi[t] |
| pyrRBCi[t] | 0.692 | pyrRBCi[t] |
| nadRBCi[t] | -0.000399 | nadRBCi[t] |
| nadhRBCi[t] | 0.307 | nadhRBCi[t] |
| dhapRBCi[t] | 0.245 | dhapRBCi[t] |
| | Control of module 1a | |

The flux control coefficients of the parasite on the bridging fluxes were considerable and are shown in Table 4.9. The control of the parasite on the transport of glucose into the parasite, vPFvGLCtr, was determined to be 1. The control on the transport of lactate and pyruvate out of the parasite into the erythrocyte, reactions vPFvLACtr and vPFvPYRtr, were determined to be 1

and 0.991, respectively. The control of the parasite on the transport of glycerol out of the parasite and into the external environment, reaction vPFvGLYtr, was determined to be 0.991. These overall flux control coefficients demonstrate the high degree of control exerted by the parasite on the flux into and out of the parasite, with the control of the erythrocyte being minimal. This is due to the glucose concentration in the erythrocyte being constant and the effect of lactate and pyruvate on the parasite being small, which leads to the parasite having a control of 1 on its own flux. This is confirmed by the flux control coefficient matrix *fullnormCjBa2*, the matrix of flux control coefficients describing the control of module 2 reactions on the bridging fluxes.

**Table 4.9:** Overall flux control coefficients for the parasite on the bridging fluxes.

| | Control of module 1a | |
|---|---|---|
| vPFvGLCtr | 1. | vPFvGLCtr |
| vPFvLACtr | 1. | vPFvLACtr |
| vPFvPYRtr | 0.991 | vPFvPYRtr |
| vPFvGLYtr | 0.991 | vPFvGLYtr |
| | Control of module 1a | |

The matrix of overall flux control coefficients, *fullnormCj2ra_star*, contains the overall flux control coefficients of the parasite on the module 2 fluxes. Due to the number of reactions included in module 2, specific overall flux control coefficients were selected, with those of large magnitude shown in Table 4.10. The control on the transport of glucose into the erythrocyte, vRBCivGLCTRANSPORT, was considerable, with a control coefficient of 0.989. This quantitatively shows the parasite has a high degree of control on the glucose flux into the erythrocyte. The overall flux control coefficients of the parasite on the fluxes of reactions vRBCivLACTRANSPORT and vRBCivPYRTRANSPORT, were determined to be 0.989 and 0.998 respectively. This demonstrates the high degree of control the parasite has on the transport of both lactate and pyruvate out of the erythrocyte. In this way, it has been shown the parasite exerts a high degree of control on glucose flux through infected erythrocytes, as shown by the large flux control coefficients on the transport of glucose into the erythrocyte as well as the transport of both lactate and pyruvate out of the erythrocyte.

**Table 4.10:** Overall flux control coefficients for the parasite on specific module 2 fluxes.

| | Control of module 1a | |
|---|---|---|
| vRBCivGLCTRANSPORT | 0.989 | vRBCivGLCTRANSPORT |
| vRBCivLACTRANSPORT | 0.989 | vRBCivLACTRANSPORT |
| vRBCivPYRTRANSPORT | 0.998 | vRBCivPYRTRANSPORT |
| | Control of module 1a | |

This analysis demonstrated the application of both the package and the modular control analysis framework on a complex, biologically relevant model. In this case a single type 1 module was present and this might be limiting real life applications. For this reason, the package was extended to include multiple type 1 modules. First 2 type 1 modules were defined in the du Toit [12] model.

### 4.2.3 Analysis of glucose metabolism in *P. falciparum*-infected erythrocytes with two type 1 modules

The du Toit model of glucose metabolism in *P. falciparum*-infected erythrocytes [12] was decomposed such that 2 type 1 modules were defined and labeled as modules a and b as shown in Figure 4.6. Module 1a is identical to the module used during the modular analysis of the Penkler model in section 4.2.1, with the module encompassing the aldolase branch point of glycolysis in the parasite. Module 1b is defined such that the metabolites, $\mathbf{S}^{1b}$, are pepPF, p2gPF, and p3gPF. The module b internal reactions, $\mathbf{V}^{1b}$, are reactions vPFvENO and vPFvPGM, with the bridging reactions vPFvPGK and vPFvPK.

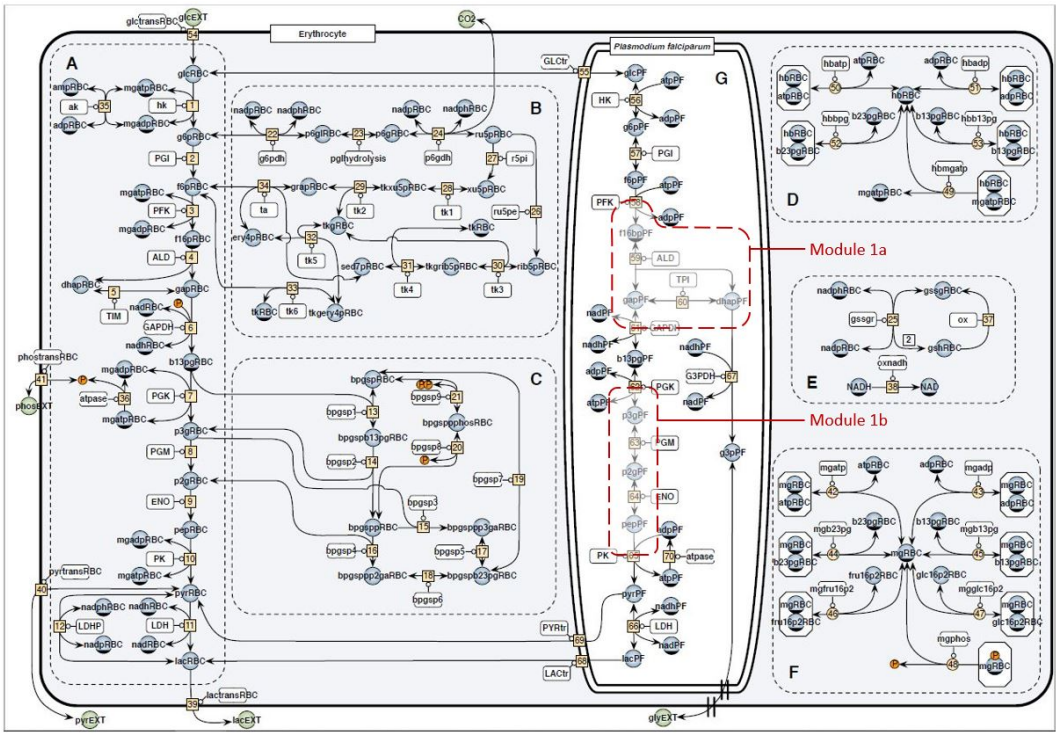


**Figure 4.6:** Schematic of the modular decomposition of the du Toit model of glucose metabolism in *P. falciparum*-infected erythrocytes with 2 type 1 modules defined and annotated as Module 1a and Module 1b.

The inclusion of a second type 1 module necessitates changes to the analysis framework to account for the additional type 1 module. This is achieved in a manner similar to that shown by Schuster and colleagues [1], where the analysis of a system with two type 1 modules was demonstrated, however, the modules were separated by metabolites alone, such that no reactions were present in module 2. This simplified the analysis as a number of components, which otherwise would need to be accounted for, could be reduced out of the equations. The decomposition chosen for the current analysis enables the stoichiometry matrix to be constructed,

$$\mathbf{N} = \left[\begin{array}{cc|cc|c} \mathbf{N_{1^a,1^a}} & 0 & \mathbf{N_{1^a,B^a}} & 0 & 0 \\ 0 & \mathbf{N_{1^b,1^b}} & 0 & \mathbf{N_{1^b,B^b}} & 0 \\ \hline 0 & 0 & \mathbf{N_{2,B^a}} & \mathbf{N_{2,B^b}} & \mathbf{N_{2,2}} \end{array}\right] \tag{4.1}$$

with the superscript $^{a}$ and $^{b}$ denoting modules 1a and 1b respectively and B the bridging reactions. The submatrices $\mathbf{N_{1^a,1^b}}$, $\mathbf{N_{1^b,1^a}}$, $\mathbf{N_{1^a,B^b}}$ and $\mathbf{N_{1^b,B^a}}$ have been replaced with 0 as metabolites in the type 1 modules may not be directly involved in the internal or bridging reactions of the other type 1 modules. While the metabolites of the different type 1 modules may not be directly involved in the reactions of other type 1 modules, they may act as allosteric effectors or otherwise indirectly influence the reactions of the other

type 1 module, such as is the case in this analysis where pepPF, a metabolite in module 1b, allosterically influences reaction vPFvTPI, a reaction of module 1a. The interaction is the result of pep acting as a competitive inhibitor of TPI. This interaction is allowed as the overall elasticities are determined such that both type 1 modules are allowed to attain a steady state, as described by Schuster and colleagues [1]. This is achieved by fixing the metabolites in module 2, while the metabolites in the type 1 modules remain unfixed, and then individually perturbing the module 2 metabolites enabling the determination of the overall elasticities of both type 1 modules. In this way, a matrix of overall elasticities is constructed for each type 1 module, such as ${}^*\epsilon_{B^a,2}$ and ${}^*\epsilon_{B^b,2}$ for the unnormalised overall elasticities of modules 1a and 1b respectively. As with the overall elasticity submatrices, a $\mathbf{Q}$ matrix is determined for each type 1 module, such that $\mathbf{Q}^a$ and $\mathbf{Q}^b$ are constructed and used in downstream equations. Due to the addition of a type 1 module, the number of control matrices determined during the analysis increases, from 6 control matrices, 2 for concentration control coefficients, and 4 for flux control coefficients as demonstrated in previous analyses, to 12 matrices. Three concentration control matrices, one for each module, as well as 9 flux control matrices. The concentration control matrices contain the concentration control coefficients for module 1a, module 1b, and module 2 reactions on module 2 metabolites. The 9 flux control matrices are such that 3 matrices encompass the control of modules 1a, 1b and module 2 reactions, on the bridging fluxes of modules 1a and 1b, as well as on the module 2 fluxes, accounting for the 9 flux control matrices. The steady state condition was also extended to account for the second type 1 module, with the adjusted steady state condition determined as such

$$\frac{d\overline{\mathbf{S}^2}}{dt} = \overbrace{\overline{\mathbf{N}}_{2,B^a} \cdot \mathbf{Q^a} \cdot {}^*\mathbf{J}^{Ra}}^{\text{module a interacting with module 2}} + \overbrace{\overline{\mathbf{N}}_{2,B^b} \cdot \mathbf{Q^b} \cdot {}^*\mathbf{J}^{Rb}}^{\text{module b interacting with module 2}} + \overbrace{\overline{\mathbf{N}}_{2,2} \cdot {}^*\mathbf{J}^2}^{\text{interactions within module 2}} = \mathbf{0} \tag{4.2}$$

with ${}^*\mathbf{J}^{Ra}$ and ${}^*\mathbf{J}^{Rb}$ the independent bridging fluxes for modules 1a and 1b, respectively. The control matrices are determined in a manner similar to that of the previous analyses. The control theorems must also be extended to account for the additional type 1 module. The theorems remain largely identical, with the component of the equations corresponding to the type 1 module now split into 2 components, that of modules 1a and 1b. An example of this extension is shown for the normalised concentration connectivity theorem, as shown in equation 3.52, when applied to a system decomposed such that two type 1 modules are present,

$$\begin{aligned}&({}^*\mathbf{C}^S_{2,Ra} \cdot {}^*\varepsilon_{R^a,2} + {}^*\mathbf{C}^S_{2,Rb} \cdot {}^*\varepsilon_{R^b,2} + \mathbf{C}^S_{2,2} \cdot \varepsilon_{2,2}) \cdot (dg\mathbf{S}^2)^{-1} \cdot \mathbf{L^2} \\ &= -(dg\mathbf{S}^2)^{-1} \cdot \mathbf{L^2}\end{aligned} \tag{4.3}$$

with ${}^*\mathbf{C}^S_{2,Ra}$ and ${}^*\mathbf{C}^S_{2,Rb}$ the normalised concentration control coefficient matrices for modules 1a and 1b, respectively. As with previous analyses, the link matrix $\mathbf{L}^2$ used in these calculations is an identity matrix due to the analysis being performed on the stoichiometrically reduced form of the model/system and as such can be removed from the equation for the purposes of the analyses performed using the package. The control coefficients for the dependent metabolites are only determined for the final matrices accessible by the user.

The addition of a component related to the additional module is not always applicable when determining the control theorems. In this case, the additional type 1 module is accounted for by a separate calculation in the normalised flux summation and flux connectivity theorems. The normalised flux connectivity theorem for 3 modules is determined as follows,

$$({}^*\mathbf{C}^J_{\mathrm{Ra,a}} \cdot {}^*\varepsilon_{\mathrm{R^a},2} + {}^*\mathbf{C}^J_{\mathrm{Ra,b}} \cdot {}^*\varepsilon_{\mathrm{R^b},2} + \mathbf{C}^J_{\mathrm{Ra},2} \cdot \varepsilon_{2,2}) \cdot (dg\mathbf{S^2})^{-1} \cdot \mathbf{L^2} = \mathbf{0} \quad (4.4)$$

$$({}^*\mathbf{C}^J_{\mathrm{Rb,a}} \cdot {}^*\varepsilon_{\mathrm{R^a},2} + {}^*\mathbf{C}^J_{\mathrm{Rb,b}} \cdot {}^*\varepsilon_{\mathrm{R^b},2} + \mathbf{C}^J_{\mathrm{Rb},2} \cdot \varepsilon_{2,2}) \cdot (dg\mathbf{S^2})^{-1} \cdot \mathbf{L^2} = \mathbf{0} \quad (4.5)$$

$$({}^*\mathbf{C}^J_{\mathrm{2,Ra}} \cdot {}^*\varepsilon_{\mathrm{R^a},2} + {}^*\mathbf{C}^J_{\mathrm{2,Rb}} \cdot {}^*\varepsilon_{\mathrm{R^b},2} + \mathbf{C}^J_{2,2} \cdot \varepsilon_{2,2}) \cdot (dg\mathbf{S^2})^{-1} \cdot \mathbf{L^2} = \mathbf{0} \quad (4.6)$$

where the flux connectivity theorem is applied to each module separately with 3 modules being present in the analysis, 2 type 1 modules and a single type 2 module. ${}^*\mathbf{C}^J_{\mathrm{Ra,a}}$ is the matrix of flux control coefficients of module 1a on the independent bridging fluxes of module 1a, ${}^*\mathbf{C}^J_{\mathrm{Ra,b}}$ the matrix of flux control coefficients of module 1b on the independent bridging fluxes of module 1a, and $\mathbf{C}^J_{\mathrm{Ra},2}$ the matrix of flux control coefficients for module 2 reactions on the independent bridging fluxes of module 1a. This naming pattern is consistent and applied to equations 4.5 and 4.6 in a similar manner. As a result of the changes made to the control theorems, an additional output can be seen in Table 4.11 for the normalised flux summation as well as the flux connectivity theorems. This table shows the steady state condition and control theorem outputs for the analysis of the du Toit model with the two type 1 modules indicated previously. The additional outputs for the normalised flux summation and the flux connectivity theorems correspond to the aditional type 1 module such that the output for module 1a, module 1b, and module 2 respectively, are shown. The second function argument, *orderinglist*, contains 2 lists corresponding to the 2 type 1 modules, each with three sublists. The composition of the sublists is identical to those used for analyses with a single type 1 module present, however, each type 1 module has its own metabolites, internal reactions, and bridging reactions populating the sublists.

**Table 4.11:** Steady state condition and control theorem outputs as determined by the package for the du Toit analysis with 2 type 1 modules.

```
In[6]:= ModularControlAnalysis[pathway, orderinglist]
{{"Steady State Condition"}, {True}}
{{"Concentration Summation-Unnormalised"}, {True}}
{{"Concentration Summation-Normalised"}, {True}}
{{"Concentration Connectivity-Unnormalised"}, {False}}
{{"Concentration Connectivity-Normalised"}, {False}}
{{"Flux Summation-Unnormalised"}, {True}}
{{"Flux Summation-Normalised"}, {{True, True, False}}}
{{"Flux Connectivity-Unnormalised"}, {{True, True, False}}}
{{"Flux Connectivity-Normalised"}, {{False, False, False}}}
```

A number of control theorem violations were determined for this analysis. While these violations may initially appear problematic, the violations correspond to those observed during the analysis of the du Toit model with a single type 1 module, the results of which were confirmed to be accurate. Similarly, the control coefficients determined during this analysis were confirmed by perturbation of the appropriate reactions. In this way, the control coefficients were determined manually and compared to the output provided by the package, with the control coefficients determined to be accurate despite the violations observed for the control theorems, as with the previous analysis of the du Toit model.

The overall flux control coefficients for both type 1 modules on the bridging fluxes of each type 1 module are shown in Table 4.12. The control exerted by module 1a on vPFvG3PDH was determined to be 0.589. This is of interest as the control of this module in the Penkler model was determined to be 0.725, as shown in Table 4.6b. There is an evident decrease in the control of module 1a on its bridging fluxes when comparing the controls determined during the analysis of the Penkler model to that of the du Toit model. This suggests that the control of the aldolase branch point reactions of the parasite on the glycolytic pathway of *P. falciparum* is greater in isolation, with an evident decrease in control following infection of a human erythrocyte. Table 4.12 shows the low degree of control exerted by module 1b on the bridging fluxes of both type 1 modules, with near zero flux control coefficients determined. This suggests that module 1b exerts minimal control over the flux through both type 1 modules.

**Table 4.12:** Overall flux control coefficients of modules 1a and 1b on the bridging fluxes of modules 1a and 1b.

```
In[7]:= fullnormCjBara_star // DispMat
Out[7]//MatrixForm=
                Control of module 1a
vPFvPFK              0.382              vPFvPFK
vPFvG3PDH            0.589              vPFvG3PDH
vPFvGAPDH            0.376              vPFvGAPDH
                Control of module 1a
```

```
In[8]:= fullnormCjBarb_star // DispMat
Out[8]//MatrixForm=
                Control of module 1b
vPFvPFK              0.00508            vPFvPFK
vPFvG3PDH           -0.0287             vPFvG3PDH
vPFvGAPDH            0.00612            vPFvGAPDH
                Control of module 1b
```

**(a)** Overall flux control coefficients for modules 1a and 1b on the bridging fluxes of module 1a.

```
In[9]:= fullnormCjBbra_star // DispMat
Out[9]//MatrixForm=
                Control of module 1a
vPFvPGK              0.376              vPFvPGK
vPFvPK               0.376              vPFvPK
                Control of module 1a
```

```
In[10]:= fullnormCjBbrb_star // DispMat
Out[10]//MatrixForm=
                Control of module 1b
vPFvPGK              0.00612            vPFvPGK
vPFvPK               0.00612            vPFvPK
                Control of module 1b
```

**(b)** Overall flux control coefficients for modules 1a and 1b on the bridging fluxes of module 1b.

The overall control coefficients for module 1a on the fluxes and metabolites in module 2 are contained in matrices accessible with the variables *fullnormCj2ra_star* and *fullnormCs2ra_star* respectively. Due to the number of reactions and metabolites included in module 2, specific overall control coefficients have been selected and are shown in Table 4.13. The overall flux control coefficients shown for module 1a identify the module as exerting considerable control over several fluxes in module 2, with specific reference to the fluxes of transporter reactions enabling the transport of glucose, lactate, pyruvate, and glycerol between the parasite, the infected erythrocyte, and the external environment. This suggests the aldolase branch point of the glycolytic pathway in the parasite, contributes a considerable degree of the control exerted by the parasite as a whole, determined in section 4.2.2.

The control of module 1a on a number of module 2 metabolites is shown in Table 4.13, with the control on metabolites f6pPF and b13pgPF being considerable. The control coefficient for f6pPF is negative due to its consumption by module 1a, with b13pgPF produced by module 1a. Module 1a exerts considerable control over the concentration of glucose in the parasite, with a concentration control coefficient of -0.423, however, minimal control is observed for the concentration of glucose in the erythrocyte. This corresponds well with the minimal control of the parasite on the glucose concentration in the infected erythrocyte determined in section 4.2.2. Table 4.13 illustrates that module 1a is responsible for a considerable degree of the control determined for the parasite on metabolites in the erythrocyte.

**Table 4.13:** Overall control coefficients for module 1a on specific fluxes and metabolites in module 2.

| | Control of module 1a | |
|---|---|---|
| vPFvGLCtr | 0.382 | vPFvGLCtr |
| vPFvGLYtr | 0.589 | vPFvGLYtr |
| vPFvLACtr | 0.369 | vPFvLACtr |
| vPFvPYRtr | 0.589 | vPFvPYRtr |
| vRBCivGLCTRANSPORT | 0.378 | vRBCivGLCTRANSPORT |
| vRBCivLACTRANSPORT | 0.365 | vRBCivLACTRANSPORT |
| vRBCivPYRTRANSPORT | 0.592 | vRBCivPYRTRANSPORT |
| | Control of module 1a | |

| | Control of module 1a | |
|---|---|---|
| b13pgPF[t] | 1.02 | b13pgPF[t] |
| f6pPF[t] | −0.907 | f6pPF[t] |
| g3pPF[t] | 0.589 | g3pPF[t] |
| g6pPF[t] | −0.865 | g6pPF[t] |
| glcPF[t] | −0.423 | glcPF[t] |
| glcRBCi[t] | −0.00197 | glcRBCi[t] |
| lacPF[t] | 0.413 | lacPF[t] |
| lacRBCi[t] | 0.365 | lacRBCi[t] |
| pyrPF[t] | 0.739 | pyrPF[t] |
| pyrRBCi[t] | 0.411 | pyrRBCi[t] |
| adpPF[t] | −0.425 | adpPF[t] |
| | Control of module 1a | |

Identical overall flux and concentration control coefficients were selected for module 1b (relative to those shown for module 1a) and are shown in Table 4.14. Module 1b exerts minimal control over the fluxes and metabolite concentrations in module 2. An exception to the minimal control exerted by module 1b is the control of the module on the concentration of b13pg in the parasite, with a concentration control coefficient of -1.25. This large negative concentration control coefficient for module 1b is expected as module 1b includes reactions directly downstream of b13pg in the glycolytic pathway within the parasite, which result in the consumption of b13pg.

**Table 4.14:** Overall control coefficients for module 1b on specific fluxes and metabolites in module 2.

| | Control of module 1b | |
|---|---|---|
| vPFvGLCtr | 0.00508 | vPFvGLCtr |
| vPFvGLYtr | −0.0287 | vPFvGLYtr |
| vPFvLACtr | 0.00723 | vPFvLACtr |
| vPFvPYRtr | −0.0287 | vPFvPYRtr |
| vRBCivGLCTRANSPORT | 0.00502 | vRBCivGLCTRANSPORT |
| vRBCivLACTRANSPORT | 0.00715 | vRBCivLACTRANSPORT |
| vRBCivPYRTRANSPORT | −0.0288 | vRBCivPYRTRANSPORT |
| | Control of module 1b | |

| | Control of module 1b | |
|---|---|---|
| b13pgPF[t] | −1.25 | b13pgPF[t] |
| f6pPF[t] | −0.0115 | f6pPF[t] |
| g3pPF[t] | −0.0287 | g3pPF[t] |
| g6pPF[t] | −0.011 | g6pPF[t] |
| glcPF[t] | −0.00561 | glcPF[t] |
| glcRBCi[t] | −0.0000262 | glcRBCi[t] |
| lacPF[t] | 0.00671 | lacPF[t] |
| lacRBCi[t] | 0.00715 | lacRBCi[t] |
| pyrPF[t] | −0.0218 | pyrPF[t] |
| pyrRBCi[t] | −0.0199 | pyrRBCi[t] |
| adpPF[t] | −0.00833 | adpPF[t] |
| | Control of module 1b | |

In this way, module 1a exerts considerable control, while module 1b exerts minimal control over the components of module 2. The control exerted by module 1a and 1b does not account for the control coefficients with magnitudes of approximately 1 determined for the parasite as a whole. This indicates the flux control is distributed among the reactions in the parasite. In this way, the final objective of this thesis, the application of modular control analysis to

complex, biologically relevant models (more specifically glucose metabolism in *P. falciparum*-infected erythrocytes) has been achieved.

The application of the framework to the model of glucose metabolism in *P. falciparum*-infected erythrocytes has revealed that the parasite exerts complete control on the flux through itself and the infected erythrocyte. The control of the parasite on the concentration of the glycolytic end products lactate and pyruvate was also considerable. Further application of the framework revealed that while the aldolase branch point accounts for a considerable degree of the control exerted by the parasite, the control is not localised to a single portion of the pathway.

While the analysis of a system with 2 type 1 modules is beneficial, the analysis of systems with multiple type 1 modules may be desired. For this reason, the package has been constructed such that analyses with multiple type 1 modules may be performed.

# Chapter 5

# General Discussion and Conclusion

The overall aim presented in this thesis was to determine the control of the *P. falciparum* parasite on glucose metabolism in an infected erythrocyte. This analysis would then act as a case study demonstrating the benefits of applying modular control analysis on larger models including whole-body models of disease states. This aim was achieved through the completion of a number of objectives: i) the selection of an appropriate theoretical framework, ii) formulation of modular control analysis in the Wolfram Mathematica® coding context, iii) performing analyses on core models that demonstrate components that may be present in biological systems, iv) development of a Wolfram Mathematica® package automating analyses, and v) analysing complex models of glycolysis in the malaria parasite in isolation as well as glucose metabolism within *P. falciparum*-infected human erythrocytes.

Modular control analysis was selected as the theoretical framework for the analyses as the framework is more generally applicable than the top-down and hierarchical control analysis frameworks. The two main constraints of this framework concern the definition of the modules, with modules of two types being defined. Type 1 modules, for which the overall control coefficients are determined, include the components of a system which are not under direct observation, while a type 2 module includes the components of the system which can be directly observed/measured. The two types of modules are linked by bridging reactions which can also be directly observed. The first constraint for defining a type 1 module is that conserved moiety cycles may not link components of type 1 modules with components of type 2 modules. Secondly, components of type 1 modules may not act as allosteric effectors for components of module 2. While these constraints limit what may be defined as modules when analysing biochemical systems, the impact of such constraints can be reduced through the analysis of systems with multiple type 1 modules as components of type 1 modules may act as allosteric effectors of components of other type 1 modules; thereby reducing the limitation imposed by the second constraint for defining type 1 modules. Alternatively, the modular

decomposition may be restructured such that the desired portions of the pathways may be defined as type 1 modules. In this way, while modular control analysis imposes constraints on modules, and subsequently analyses, these constraints can usually be accommodated, making this framework a powerful tool.

Despite the benefits of applying modular control analysis, this analysis framework has not been extensively used to analyse biochemical systems or the models thereof. This limited usage may be the result of the complexity of the mathematics inherent in the framework limiting widespread implementation and application, as well as the difficulty of experimental determination of the overall elasticities required [24]. Section 2.6.1 discusses two examples of the application of modular control analysis to biochemical systems. The first described the application of modular control analysis to slipping enzymes, whereby slipping enzymes are considered type 1 modules [34]. The second application of modular control analysis that was discussed concerned the determination of the control of membrane processes, such as membrane located enzymes, on the growth rate of the yeast *K. marxianus* [35]. The analysis provided insight into the high degree of control membrane processes exert on the growth rate, however, the analysis was performed such that two modules were defined, both of which were treated as type 1 modules for which the overall control coefficients of the modules on the maximum specific growth rate were determined. As such, no specific linking intermediate or bridging reactions were identified. In this way, modular control analysis was adapted such that it could be applied to achieve the aim of the study. These studies demonstrate benefits of applying modular control analysis, and adaptations thereof, however, they do not really apply modular control analysis to its full and/or intended capability/usage. Since the application of the framework may have been limited due to its complexity, we started the development of a package automating the application of modular control analysis to models of biochemical systems, enabling more widespread use as the user needs only limited knowledge of the framework to be able to utilise the package. In this way, this is one of the first studies enabling modular control analysis to be used to analyse models of large, complex biochemical systems.

Following the selection of modular control analysis as the framework to be utilised, analyses were performed on a number of core models including simple linear and branched systems, as described in the formalisation of the framework [1]. The framework was then applied to systems with moiety conserved cycles present. This inclusion resulted in added complexity due to the dependence of the dependent metabolites on the independent metabolites during the determination of the steady state concentrations. This is not specific to modular control analysis and must also be addressed when performing traditional metabolic control analysis using a perturbation approach to determine elasticities. This was addressed through the reduction of the model such

that dependent metabolites are expressed in terms of independent metabolites. These reduced models were then analysed enabling the determination of the independent concentration control coefficients. The independent concentration control coefficients enabled the determination of the control coefficients for the dependent metabolites present in the original model, in doing so enabling the analyses to quantify the control distribution within the original model despite the presence of dependent metabolites. Following the successful analysis of branched systems as well as systems with moiety conserved cycles present, less common components/states were considered and subsequently incorporated into core models and analysed, including the presence of fluxes at or near 0 at steady state, as well as metabolites with 0 or near 0 concentrations at steady state. These were addressed and subsequently analyses can be performed on a wide range of models of biochemical systems, assuming the modular decomposition has been performed correctly. In this way, application of the framework was simplified, enabling the analysis of complex, biologically relevant models, specifically the Penkler model of glycolysis in a *P. falciparum* parasite [11] and the du Toit model of glucose metabolism in *P. falciparum*-infected erythrocytes [12].

The Penkler and du Toit models [11; 12] were analysed, with these analyses demonstrating the application of the package on more complex, biologically relevant models of biochemical systems. The analyses of these biological models demonstrated the benefits of modular control analysis, as well as the package automating the analyses. The overall flux control coefficients determined for the parasite confirm the understanding that the *P. falciparum* parasite exerts considerable control on the flux through the infected erythrocyte, with the control quantified and determined to be near complete. The control of the parasite on the metabolites in the infected erythrocyte was also determined. The control of the parasite on glucose concentration in the erythrocyte was determined to be near zero, despite the high degree of control of the parasite on the transport of glucose. The control of the parasite on lactate and pyruvate concentrations in the erythrocyte was considerable. The high degree of control of the parasite on the concentration of lactate, in conjunction with the high degree of control on the transport of lactate out of the erythrocyte, suggests the parasite may be responsible for a considerable contribution to the increase in lactic acid observed in patients with severe malaria infections.

Analysing large models with a single type 1 module may provide the desired insight into the control distribution within a system, however, analyses with multiple type 1 modules may be required. Performing analyses on large models such as that of whole-body models of disease states may benefit from decomposition into multiple type 1 modules. The hierarchical whole-body model of glucose metabolism in malaria patients [3] is an example of a model where decomposition with multiple type 1 modules would be desirable such that the

overall control of organs as well as other compartments may be determined in a single analysis. For this reason the package was developed such that these multi-module analyses are supported. A function was developed supporting analyses with 'n' number of type 1 modules, ModularControlAnalysis. This extension of the package further streamlines the application of modular control analysis to models of biochemical systems as only limited knowledge of modular decomposition is required. The package has been constructed such that a degree of error checking is included, designed to assist the user to identify the cause of erroneous modular decomposition if present. In this way, the application of modular control analysis to models has been simplified, enabling such analyses to be performed without intimate knowledge of the framework.

As such, the aim of this thesis has been achieved and this thesis has contributed to answering the research question: Can the contribution of organs and molecular compartments of interest to certain disease states be quantified using established theoretical frameworks? While the contribution of compartments of interest to disease states has not been explicitly determined, the contribution of the malaria parasite to glucose metabolism in infected erythrocytes has been determined. Such an analysis can be considered a first step to the application of an established theoretical framework to determine the contribution of compartments (such as organs) to disease states. The developed package supports the use of modular control analysis to perform analyses on whole-body models of disease states by making it easier to perform the analysis. A logical next step for future research is to focus on the control of the malaria parasite to glucose metabolism in malaria patients. Analyses on a whole-body model of glucose metabolism in malaria patients may provide insight into the extent to which the malaria parasite, in terms of percentage parasitaemia, controls the glucose flux in the host. The control of the parasite on concentrations of glucose and lactate in the blood could be quantified, possibly providing insight into the development or maintenance of lactic acidosis and hypoglycaemia in malaria patients. Applying modular control analysis to a model of glucose metabolism in a patient with type 2 diabetes may also be an interesting progression. Such an analysis could provide insight into the control of muscle on glucose metabolism as well as various other organs and compartments of interest. The use of modular control analysis on models of disease states may aid the identification of compartments with high control, possibly aiding in the treatment of a number of diseases including malaria and type 2 diabetes.

# Appendices

# Appendix A

# Core models

## A.1 Linear Pathway

### A.1.1 ODEs

The variable metabolites present in this model are $x1, x2, x3$ and $x4$ with the following ODEs:

$$x1'(t) = 1.vs - 1.v1 \tag{A.1}$$
$$x2'(t) = 1.v1 - 1.v2 \tag{A.2}$$
$$x3'(t) = 1.v2 - 1.v3 \tag{A.3}$$
$$x4'(t) = 1.v3 - 1.v4 \tag{A.4}$$

### A.1.2 Rate Equations

$$vs = ksf \cdot S - ksr \cdot x1(t) \tag{A.5}$$
$$v1 = k1f \cdot x1(t) - k1r \cdot x2(t) \tag{A.6}$$
$$v2 = k2f \cdot x2(t) - k2r \cdot x3(t) \tag{A.7}$$
$$v3 = k3f \cdot x3(t) - k3r \cdot x4(t) \tag{A.8}$$
$$v4 = k4f \cdot x4(t) - k4r \cdot P \tag{A.9}$$

### A.1.3 Parameters

$$k1f = 3.0 \quad s^{-1} \tag{A.10}$$
$$k1r = 1.0 \quad s^{-1} \tag{A.11}$$
$$k2f = 1.5 \quad s^{-1} \tag{A.12}$$
$$k2r = 0.5 \quad s^{-1} \tag{A.13}$$
$$k3f = 2.0 \quad s^{-1} \tag{A.14}$$
$$k3r = 1.0 \quad s^{-1} \tag{A.15}$$
$$k4f = 2.0 \quad s^{-1} \tag{A.16}$$
$$k4r = 0.5 \quad s^{-1} \tag{A.17}$$
$$ksf = 2.0 \quad s^{-1} \tag{A.18}$$
$$ksr = 1.0 \quad s^{-1} \tag{A.19}$$
$$P = 1.0 \quad mmol \tag{A.20}$$
$$S = 1.0 \quad mmol \tag{A.21}$$
$$\text{Volume} = 1.0 \quad L \tag{A.22}$$

### A.1.4 Initial Values

$$x1(0) = 1.0 \quad mmol \tag{A.23}$$
$$x2(0) = 1.0 \quad mmol \tag{A.24}$$
$$x3(0) = 1.0 \quad mmol \tag{A.25}$$
$$x4(0) = 1.0 \quad mmol \tag{A.26}$$

## A.2 Branched pathway

### A.2.1 ODEs

The variable metabolites present in this model are $x1, x2, x3, x4, x5$ and $x6$ with the following ODEs:

$$x1'(t) = 1.v1 - 1.v2 \tag{A.27}$$
$$x2'(t) = 1.v2 - 1.v3 - 1.v4 \tag{A.28}$$
$$x3'(t) = 1.v3 - 1.v5 \tag{A.29}$$
$$x4'(t) = 1.v4 - 1.v6 \tag{A.30}$$
$$x5'(t) = 1.v5 - 1.v7 \tag{A.31}$$
$$x6'(t) = 1.v6 - 1.v8 \tag{A.32}$$

### A.2.2 Rate Equations

$$v1 = k1f \cdot s - k1r \cdot x1(t) \tag{A.33}$$
$$v2 = k2f \cdot x1(t) - k2r \cdot x2(t) \tag{A.34}$$
$$v3 = k3f \cdot x2(t) - k3r \cdot x3(t) \tag{A.35}$$
$$v4 = k4f \cdot x2(t) - k4r \cdot x4(t) \tag{A.36}$$
$$v5 = k5f \cdot x3(t) - k5r \cdot x5(t) \tag{A.37}$$
$$v6 = k6f \cdot x4(t) - k6r \cdot x6(t) \tag{A.38}$$
$$v7 = k7f \cdot x5(t) - k7r \cdot p1 \tag{A.39}$$
$$v8 = k8f \cdot x6(t) - k8r \cdot p2 \tag{A.40}$$

### A.2.3 Parameters

$$k1f = 1.0 \quad s^{-1} \tag{A.41}$$
$$k1r = 1.0 \quad s^{-1} \tag{A.42}$$
$$k2f = 1.0 \quad s^{-1} \tag{A.43}$$
$$k2r = 1.0 \quad s^{-1} \tag{A.44}$$
$$k3f = 1.2 \quad s^{-1} \tag{A.45}$$
$$k3r = 1.0 \quad s^{-1} \tag{A.46}$$
$$k4f = 1.0 \quad s^{-1} \tag{A.47}$$
$$k4r = 1.0 \quad s^{-1} \tag{A.48}$$
$$k5f = 1.1 \quad s^{-1} \tag{A.49}$$
$$k5r = 1.0 \quad s^{-1} \tag{A.50}$$
$$k6f = 1.0 \quad s^{-1} \tag{A.51}$$
$$k6r = 1.0 \quad s^{-1} \tag{A.52}$$
$$k7f = 1.0 \quad s^{-1} \tag{A.53}$$
$$k7r = 1.0 \quad s^{-1} \tag{A.54}$$
$$k8f = 1.0 \quad s^{-1} \tag{A.55}$$
$$k8r = 1.0 \quad s^{-1} \tag{A.56}$$
$$p1 = 1.0 \quad mmol \tag{A.57}$$
$$p2 = 1.0 \quad mmol \tag{A.58}$$
$$s = 5.0 \quad mmol \tag{A.59}$$
$$\text{Volume} = 1.0 \quad L \tag{A.60}$$

### A.2.4 Initial Values

$$x1(0) = 1.0 \quad mmol \tag{A.61}$$
$$x2(0) = 1.0 \quad mmol \tag{A.62}$$
$$x3(0) = 1.0 \quad mmol \tag{A.63}$$
$$x4(0) = 1.0 \quad mmol \tag{A.64}$$
$$x5(0) = 1.0 \quad mmol \tag{A.65}$$
$$x6(0) = 1.0 \quad mmol \tag{A.66}$$

## A.3 Complex pathway

### A.3.1 ODEs

The variable metabolites present in this model are $x1, x2, x3, x4, x5, x8, x9$ and $x10$ with the following ODEs:

$$X1'(t) = 1.v_1 - 1.v_4 - 1.v_3 \tag{A.67}$$
$$X10'(t) = 1.v_7 - 1.v_9 \tag{A.68}$$
$$X2'(t) = 1.v_2 - 1.v_1 \tag{A.69}$$
$$X3'(t) = 1.v_1 - 1.v_2 \tag{A.70}$$
$$X4'(t) = 1.v_3 - 1.v_5 \tag{A.71}$$
$$X5'(t) = 1.v_4 - 1.v_6 \tag{A.72}$$
$$X8'(t) = 1.v_5 - 1.v_7 \tag{A.73}$$
$$X9'(t) = 1.v_6 - 1.v_8 \tag{A.74}$$

### A.3.2 Rate Equations

$$v_1 = k1f \cdot X0 \cdot X2(t) - k1r \cdot X1(t) \cdot X3(t) \tag{A.75}$$
$$v_2 = k2f \cdot X6 \cdot X3(t) - k2r \cdot X7 \cdot X2(t) \tag{A.76}$$
$$v_3 = k3f \cdot X1(t) - k3r \cdot X4(t) \tag{A.77}$$
$$v_4 = k4f \cdot X1(t) - k4r \cdot X5(t) \tag{A.78}$$
$$v_5 = k5f \cdot X4(t) - k5r \cdot X8(t) \tag{A.79}$$
$$v_6 = k6f \cdot X5(t) - k6r \cdot X9(t) \tag{A.80}$$
$$v_7 = k7f \cdot X8(t) - k7r \cdot X10(t) \tag{A.81}$$
$$v_8 = k8f \cdot X9(t) - k8r \cdot P2 \tag{A.82}$$
$$v_9 = k9f \cdot X10(t) - k9r \cdot P1 \tag{A.83}$$

### A.3.3 Parameters

$$k1f = 1.0 \quad s^{-1} \tag{A.84}$$
$$k1r = 1.0 \quad s^{-1} \tag{A.85}$$
$$k2f = 1.0 \quad s^{-1} \tag{A.86}$$
$$k2r = 1.0 \quad s^{-1} \tag{A.87}$$
$$k3f = 1.1 \quad s^{-1} \tag{A.88}$$
$$k3r = 1.0 \quad s^{-1} \tag{A.89}$$
$$k4f = 1.0 \quad s^{-1} \tag{A.90}$$
$$k4r = 1.0 \quad s^{-1} \tag{A.91}$$
$$k5f = 1.0 \quad s^{-1} \tag{A.92}$$
$$k5r = 1.0 \quad s^{-1} \tag{A.93}$$
$$k6f = 1.0 \quad s^{-1} \tag{A.94}$$
$$k6r = 1.0 \quad s^{-1} \tag{A.95}$$
$$k7f = 1.0 \quad s^{-1} \tag{A.96}$$
$$k7r = 1.0 \quad s^{-1} \tag{A.97}$$
$$k8f = 1.0 \quad s^{-1} \tag{A.98}$$
$$k8r = 1.0 \quad s^{-1} \tag{A.99}$$
$$k9f = 1.0 \quad s^{-1} \tag{A.100}$$
$$k9r = 1.0 \quad s^{-1} \tag{A.101}$$
$$P1 = 1.0 \quad mmol \tag{A.102}$$
$$P2 = 1.0 \quad mmol \tag{A.103}$$
$$X0 = 10.0 \quad mmol \tag{A.104}$$
$$X6 = 5.0 \quad mmol \tag{A.105}$$
$$X7 = 1.0 \quad mmol \tag{A.106}$$
$$\text{Volume} = 1.0 \quad L \tag{A.107}$$

### A.3.4 Initial Values

$$X1(0) = 1.0 \quad mmol \tag{A.108}$$
$$X10(0) = 1.0 \quad mmol \tag{A.109}$$
$$X2(0) = 1.0 \quad mmol \tag{A.110}$$
$$X3(0) = 1.0 \quad mmol \tag{A.111}$$
$$X4(0) = 2.0 \quad mmol \tag{A.112}$$
$$X5(0) = 1.0 \quad mmol \tag{A.113}$$
$$X8(0) = 1.0 \quad mmol \tag{A.114}$$
$$X9(0) = 1.0 \quad mmol \tag{A.115}$$

## A.4 Pathway with equilibrium reactions

The variable metabolites present in this model are $x1, x2, x3, x4, x5, x6$ and $p2$ with the following ODEs:

### A.4.1 ODEs

$$p2'(t) = 1.v8 \tag{A.116}$$
$$x1'(t) = 1.v1 - 1.v2 \tag{A.117}$$
$$x2'(t) = 1.v2 - 1.v4 - 1.v3 \tag{A.118}$$
$$x3'(t) = 1.v3 - 1.v5 \tag{A.119}$$
$$x4'(t) = 1.v4 - 1.v6 \tag{A.120}$$
$$x5'(t) = 1.v5 - 1.v7 \tag{A.121}$$
$$x6'(t) = 1.v6 - 1.v8 \tag{A.122}$$

### A.4.2 Rate Equations

$$v1 = k1f \cdot s - k1r \cdot x1(t) \tag{A.123}$$
$$v2 = k2f \cdot x1(t) - k2r \cdot x2(t) \tag{A.124}$$
$$v3 = k3f \cdot x2(t) - k3r \cdot x3(t) \tag{A.125}$$
$$v4 = k4f \cdot x2(t) - k4r \cdot x4(t) \tag{A.126}$$
$$v5 = k5f \cdot x3(t) - k5r \cdot x5(t) \tag{A.127}$$
$$v6 = k6f \cdot x4(t) - k6r \cdot x6(t) \tag{A.128}$$
$$v7 = k7f \cdot x5(t) - k7r \cdot p1 \tag{A.129}$$
$$v8 = k8f \cdot x6(t) - k8r \cdot p2(t) \tag{A.130}$$

### A.4.3 Parameters

$$k1f = 1.0 \quad s^{-1} \tag{A.131}$$
$$k1r = 1.0 \quad s^{-1} \tag{A.132}$$
$$k2f = 1.0 \quad s^{-1} \tag{A.133}$$
$$k2r = 1.0 \quad s^{-1} \tag{A.134}$$
$$k3f = 1.2 \quad s^{-1} \tag{A.135}$$
$$k3r = 1.0 \quad s^{-1} \tag{A.136}$$
$$k4f = 1 \times 10^{-8} \quad s^{-1} \tag{A.137}$$
$$k4r = 1 \times 10^{-8} \quad s^{-1} \tag{A.138}$$
$$k5f = 1.1 \quad s^{-1} \tag{A.139}$$
$$k5r = 1.0 \quad s^{-1} \tag{A.140}$$
$$k6f = 6.5 \times 10^{-7} \quad s^{-1} \tag{A.141}$$
$$k6r = 2 \times 10^{-7} \quad s^{-1} \tag{A.142}$$
$$k7f = 1.0 \quad s^{-1} \tag{A.143}$$
$$k7r = 1.0 \quad s^{-1} \tag{A.144}$$
$$k8f = 1.0 \quad s^{-1} \tag{A.145}$$
$$k8r = 1.0 \quad s^{-1} \tag{A.146}$$
$$p1 = 1.0 \quad mmol \tag{A.147}$$
$$s = 5.0 \quad mmol \tag{A.148}$$
$$\text{Volume} = 1.0 \quad L \tag{A.149}$$

### A.4.4 Initial Values

$$p2(0) = 1.0 \quad mmol \tag{A.150}$$
$$x1(0) = 1.0 \quad mmol \tag{A.151}$$
$$x2(0) = 1.0 \quad mmol \tag{A.152}$$
$$x3(0) = 1.0 \quad mmol \tag{A.153}$$
$$x4(0) = 1.0 \quad mmol \tag{A.154}$$
$$x5(0) = 1.0 \quad mmol \tag{A.155}$$
$$x6(0) = 1.0 \quad mmol \tag{A.156}$$

# Appendix B

# Package Guide

## B.1 Application of the Package

This section is intended to guide a user through using the package to perform modular control analyses on models of biochemical systems. Initially, the package needs to be loaded by the Wolfram Mathematica® notebook. This can be done using the *Needs* function with "ModularControlAnalysis`" as the required context. Additionally, the file location of the package must be entered as the second argument for the *Needs* function if the package is not located in the same folder as the notebook. Unprotect[Print] is used so that Print = Null can be run. This suppresses print statements present in several package functions:

**Needs**["**ModularControlAnalysis`** ", "*File location of Package*"];
**Unprotect**[**Print**];
**Print** = **Null**

Secondly, the model information must be included/saved in the notebook, preferably as a variable such as 'pathway'. The model description can be obtained by selecting a model from JWS Online (models can be added by the user if the desired model is not available). The website can be accessed by going to `https://jjj.bio.vu.nl/`.

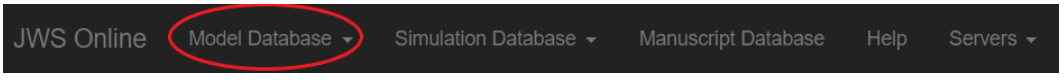


Select the Model Database tab to see a list of the models available under the Curated Models tab. Filters may be applied to search for a specific curated Model. Alternatively, a model can be uploaded or created in the Session Models tab. Models that are uploaded will only be saved if the user is signed into the website. This can be done by creating an account on the home page.

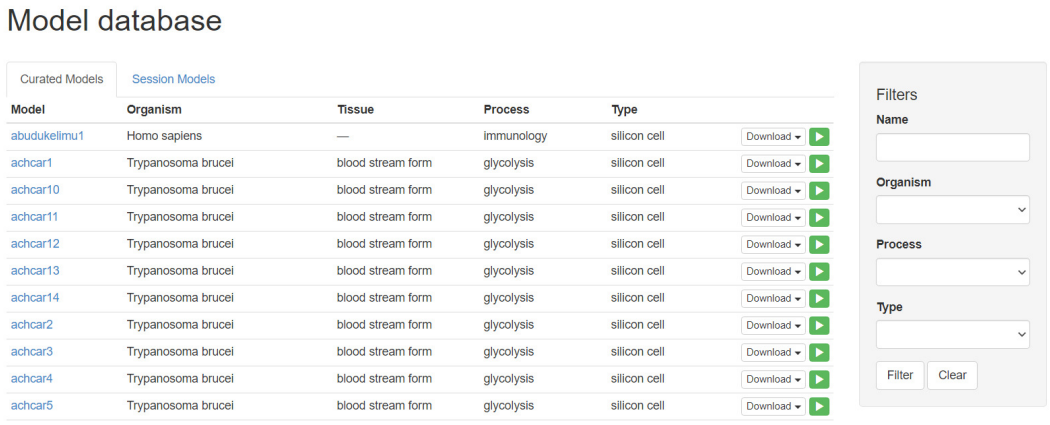


The user can then select the desired model to analyse.

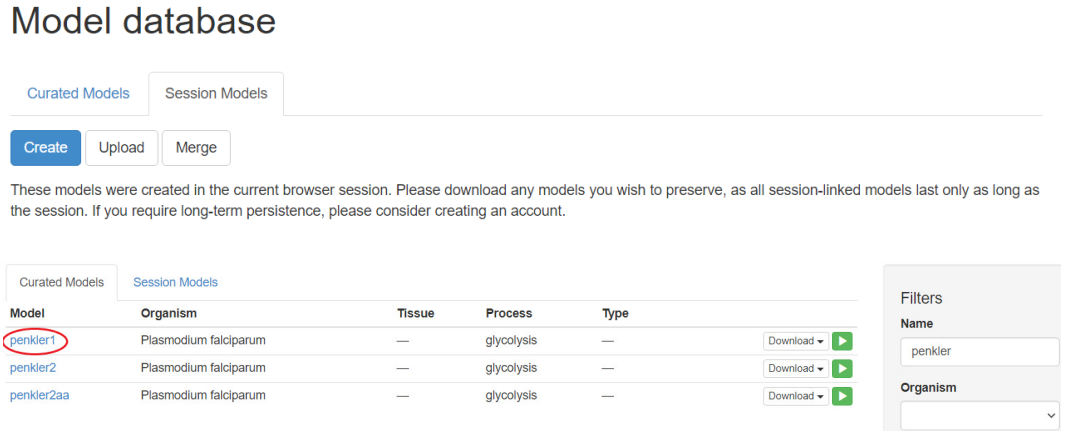


Once the model has been selected, the user can go to the address bar at the top of the screen and add 'mfu' to the url. The addition of 'mfu' will result in the model description being displayed in the form required by the package analysis functions.

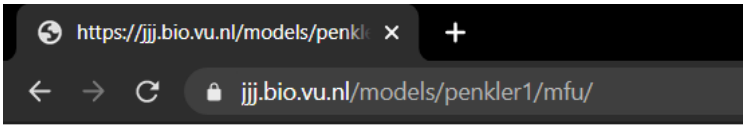


Once the model description is available, it can be copied using ctrl + a (to select the model description) and ctrl + c (to copy the model description). The model description can then be pasted into the notebook and saved as a variable, such as 'pathway', for ease of use. It is recommended the user removes all instances of 'model``' present in the model description as this improves the readability of the model components. The removal can be quickly achieved using ctrl + F and then entering 'model``' in the 'Find' bar, the 'Replace with' bar must be left empty/blank. Selecting 'Replace All' will promptly remove all instances of 'model``' from the model description.

In this way, *pathway* = { *Full model description as obtained from JWS Online using /mfu in the url* }.

The list of metabolites can be obtained with pathway[[1]][[1]], where the first [[1]] indicates the stoichiometry matrix of the model and the second indicates the row headers, with the rows headers being the metabolites for the stoichiometry matrix.

The components of the type 1 module(s) can then be determined and saved as a variable, such as 'orderinglist'. The list should be constructed such that there are 3 sublists for each list and 1 list for each type 1 module. The sublists are ordered such that the metabolites are first, the internal module 1 reactions second, and thirdly the bridging reactions. An example analysis will be performed on the Penkler model [11] with module 1 metabolites, dhapPF, f16bpPF and gapPF. The module 1 internal reactions are vPFvALD and vPFvTPI, with the bridging reactions vPFvGAPDH, vPFvG3PDH and vPFvPFK. The metabolites must be added to the list as present in the model description, this means the '[t]' must be included. The orderinglist would then be:

$$\begin{aligned} \textit{orderinglist} = &\{\{\{\text{dhapPF}[t], \text{f16bpPF}[t], \text{gapPF}[t]\}, \\ &\{\text{vPFvALD}, \text{vPFvTPI}\}, \\ &\{\text{vPFvGAPDH}, \text{vPFvG3PDH}, \text{vPFvPFK}\}\}\}; \end{aligned}$$

The modular control analysis function can then be called using the model description and module 1 component list as function arguments. A general function, ModularControlAnalysis, can be used for analysis with 1 or multiple type 1 modules.

**ModularControlAnalysis**[*pathway*, *orderinglist*]
{{Steady State Condition}, {True}}
{{Concentration Summation-Unnormalised}, {True}}
{{Concentration Summation-Normalised}, {True}}
{{Concentration Connectivity-Unnormalised}, {True}}
{{Concentration Connectivity-Normalised}, {True}}
{{Flux Summation-Unnormalised}, {True}}
{{Flux Summation-Normalised}, {True, True}}
{{Flux Connectivity-Unnormalised}, {True, True}}
{{Flux Connectivity-Normalised}, {True, True}}

The output of the function is the result of the steady state and control theorem tests for the modular analysis. The desired output for each is True, however a False output for the control theorem checks does not immediately

invalidate the analysis. This is due to the possible inclusion of metabolites with very small concentrations at steady state as well as reactions with fluxes of zero or near-zero at steady state, which can result in the control theorems being violated despite the determined control coefficients being accurate.

The overall control coefficients for the type 1 module can be accessed using specific variables determined by the package. For an analysis with a single type 1 module using ModularControlAnalysis, the variables are *fullnormCs2ra_star*, *fullnormCjBara_star*, and *fullnormCj2ra_star* for the concentration control matrix, flux control on the bridging fluxes, and the flux control on the module 2 fluxes respectively. The DispMat function can be applied to the control coefficient matrices, with the resulting display shown and with the columns exerting the determined control on the rows in the matrix.

*fullnormCs2ra_star//DispMat*
*fullnormCj2ra_star//DispMat*
*fullnormCjBara_star//DispMat*

| | Control of Module 1a | |
|---|---|---|
| atpPF[$t$] | 0.0817 | atpPF[$t$] |
| b13pgPF[$t$] | 1.03 | b13pgPF[$t$] |
| f6pPF[$t$] | −0.969 | f6pPF[$t$] |
| g3pPF[$t$] | 0.521 | g3pPF[$t$] |
| g6pPF[$t$] | −0.927 | g6pPF[$t$] |
| glcPF[$t$] | −0.451 | glcPF[$t$] |
| lacPF[$t$] | 0.0625 | lacPF[$t$] |
| nadPF[$t$] | 0.00285 | nadPF[$t$] |
| p2gPF[$t$] | 0.514 | p2gPF[$t$] |
| p3gPF[$t$] | 0.539 | p3gPF[$t$] |
| pepPF[$t$] | 0.654 | pepPF[$t$] |
| pyrPF[$t$] | 0.582 | pyrPF[$t$] |
| adpPF[$t$] | −0.411 | adpPF[$t$] |
| nadhPF[$t$] | −0.146 | nadhPF[$t$] |
| | Control of Module 1a | |

$$\begin{pmatrix} \_ & \text{Control of Module 1a} & \_ \\ \text{vPFvATPASE} & 0.388 & \text{vPFvATPASE} \\ \text{vPFvENO} & 0.402 & \text{vPFvENO} \\ \text{vPFvGLCtr} & 0.415 & \text{vPFvGLCtr} \\ \text{vPFvGLYtr} & 0.725 & \text{vPFvGLYtr} \\ \text{vPFvHK} & 0.415 & \text{vPFvHK} \\ \text{vPFvLACtr} & 0.388 & \text{vPFvLACtr} \\ \text{vPFvLDH} & 0.388 & \text{vPFvLDH} \\ \text{vPFvPGI} & 0.415 & \text{vPFvPGI} \\ \text{vPFvPGK} & 0.402 & \text{vPFvPGK} \\ \text{vPFvPGM} & 0.402 & \text{vPFvPGM} \\ \text{vPFvPK} & 0.402 & \text{vPFvPK} \\ \text{vPFvPYRtr} & 0.725 & \text{vPFvPYRtr} \\ \_ & \text{Control of Module 1a} & \_ \end{pmatrix}$$

$$\begin{pmatrix} \_ & \text{Control of Module 1a} & \_ \\ \text{vPFvGAPDH} & 0.402 & \text{vPFvGAPDH} \\ \text{vPFvG3PDH} & 0.725 & \text{vPFvG3PDH} \\ \text{vPFvPFK} & 0.415 & \text{vPFvPFK} \\ \_ & \text{Control of Module 1a} & \_ \end{pmatrix}$$

The module 2 control coefficients can be accessed using the variables *fullnormCs22*, *fullnormCjBa2*, and *fullnormCj22* for the module 2 concentration control coefficients, the flux control coefficients on the bridging fluxes and on the module 2 fluxes, respectively, in a manner similar to that which has been shown for the overall control coefficients. Analyses with multiple type 1 modules results in the determination of numerous control coefficient matrices, each saved as and accessible via a specific variable. The variable names provide an indication of the meaning of the control coefficients therein, for example, the variable *fullnormCj2rb_star* is the matrix of overall flux control coefficients of module 1B on the module 2 fluxes. Cj denotes a flux control coefficient matrix, with 2 identifying what is being controlled and rb identifying what is exerting the control, with rb used to represent the overall control of module 1B. Overall control coefficients of a type 1 module are indicated by *_star*.

## B.2 Error Checking mechanisms within the Package

The package discussed herein reduces the complexity of applying modular control analysis to models of biochemical systems however, a requirement is the decomposition of the system in a manner that conforms to the constraints and assumptions inherent in the framework of modular control analysis. As such,

decomposition in a manner that violates these assumptions and constraints results in the determination of erroneous control coefficients. Consequently, a number of error checking mechanisms have been implemented within the package that aim to identify erroneous decomposition as well as the specific metabolites and reactions causing the violations. Once identified, the user is then informed as to which metabolites and reactions are violating the constraints of the framework. This allows the user to revise the decomposition that was selected, knowing the reason for which the decomposition was identified as problematic/erroneous. The error checking mechanisms have been constructed such that computation of the control coefficients is aborted if the decomposition is identified to be erroneous. This was implemented as it limits the risk of the user interpreting the results as correct when this is not the case, as well as reducing the computation time before the user is informed of the problematic decomposition.

Examples of the output returned by analyses with erroneous modular decomposition will be provided, using the model of glycolysis in the *P. falciparum* parasite constructed by Penkler and colleagues [11], the model analysed in section B.1. Two analyses will be presented, each demonstrating the output returned by the function performing the analysis if the decomposition is determined to be incorrect. The following is the output provided by the package function using the modular decomposition as described by the variable, *orderinglist*.

```
In[5]:= orderinglist = {{{pepPF[t], p2gPF[t], p3gPF[t]}, {vPFvENO, vPFvPGM}, {vPFvPGK, vPFvPK}}};

In[6]:= ModularControlAnalysis[pathway, orderinglist]

Out[6]= {pepPF[t], is directly involved in reaction(s), {vPFvTPI},
          currently designated as being in module 2. This is a violation of the constraints
            imposed in modular control analysis and subsequently the analysis has been aborted.}
```

This decomposition is erroneous as the module 1 metabolite pepPF interacts with the module 2 reaction vPFvTPI through a means other than the bridging reactions. In this case, the interaction is the result of pep competitively inhibiting TPI. This is a violation of the constraints of modular control analysis as the decomposition should be constructed such that the matrices $\varepsilon_{2,1}$ and $\mathbf{N}_{1,2}$ are equal to 0. The interaction of module 1 metabolites with module 2 reactions is the first error type identified by the package functions. The second error type identified concerns the stoichiometric interaction of module 2 metabolites with module 1 reactions, as the matrix $\mathbf{N}_{2,1}$ is expected to equal 0. The following is an example of such a situation:

```
In[5]:= orderinglist1 = {{{glcPF[t], g6pPF[t]}, {vPFvHK}, {vPFvGLCtr, vPFvPGI}},
          {{p2gPF[t], p3gPF[t]}, {vPFvPGM}, {vPFvENO, vPFvPGK}}};

In[6]:= ModularControlAnalysis[pathway, orderinglist1]

Out[6]= {{{Module 2 metabolite, adpPF[t], is metabolized by a module 1 reaction: vPFvHK}
         {Module 2 metabolite, atpPF[t], is metabolized by a module 1 reaction: vPFvHK}},
         Computation has been terminated due to the presence of stoichiometric
            interactions between module 2 metabolites and module 1 reactions as described.}
```

The analysis depicted above was aborted with the message displayed due to the presence of stoichiometric interactions between the module 2 metabolites adpPF and atpPF with module 1 reaction vPFvHK. Such interactions are not permitted by the modular control analysis framework and as such the control coefficients determined would be erroneous. In this way, the functions available in the package facilitate the application of modular control analysis to models of biochemical systems as well as the troubleshooting of erroneous decomposition.

Performing analyses using the functions available in this package requires knowledge of the functions as well as the variables made accessible to the user, subsequently a number of functions and variables accessible to the user will be discussed.

## B.3 Overview of accessible functions and variables

The use of the functions available in this package for performing modular control analysis on biochemical system requires a number of variables to be defined and made accessible to the user, with some of these variables having been mentioned previously however, for the purpose of providing clarity a list of variables and functions of interest has been compiled.

$$ModularControlAnalysis[pathway\_\,, orderinglist\_\,]$$

The function argument *orderinglist* must be provided such that the information of the type 1 modules is in the form of a list containing a separate list for each type 1 module, as has been demonstrated in this package guide. Analyses with 2 or more type 1 modules results in additional lists being present in the main list, each with 3 sublists corresponding to the components of the individual type 1 modules.

Calling this function results in a number of variables being defined. The naming pattern used for the control coefficient matrices is such that each type 1 module is labelled using a letter of the alphabet from "a" to "z". The Q matrices are an exception to this naming scheme, with the Q matrices accessible using the variable *Qmatrices*, which is a list of all the Q matrices determined for the type 1 modules. In this way, if there are five type 1 modules there will be five Q matrices contained in the list. While the control coefficient matrices are accessible as described, the current naming scheme supports up to 26 type 1 modules. As such, the control coefficient matrices determined are also made accessible using the following variables: *full-*

*normCs2r_starMatrices*, *fullnormCjbr2Matrices*, *fullnormCjbr_starMatrices*, and *fullnormCj2r_starMatrices* such that the current naming scheme need not be a limitation as these variables contain all the determined control coefficients pertaining to the type 1 modules. A selection of the variables accessible to the user are:

*Qmatrices* : This contains the Q matrices determined for the type 1 modules.

*fullnormCs22* : Concentration control coefficient matrix for module 2 reactions on module 2 metabolites.

*fullnormCj22* : Flux control coefficient matrix for module 2 reactions on their fluxes.

*fullnormCjBa2* : Flux control coefficient matrix for module 2 reactions on the bridging fluxes of module 1a.

*fullnormCs2ra_star* : Concentration control coefficient matrix for module 1a on module 2 metabolites.

*fullnormCj2ra_star* : Flux control coefficient matrix for module 1a on module 2 fluxes.

*fullnormCjBara_star* : Flux control coefficient matrix for module 1a on the bridging fluxes of module 1a.

*fullnormCjBb2* : Flux control coefficient matrix for module 2 reactions on module 1b's bridging fluxes.

*fullnormCs2rb_star* : Concentration control coefficient matrix for module 1b on module 2 metabolites.

*fullnormCjBarb_star* : Flux control coefficient matrix for module 1b on module 1a's bridging fluxes.

*fullnormCjBbra_star* : Flux control coefficient matrix for module 1a on module 1b's bridging fluxes.

*fullnormCjBbrb_star* : Flux control coefficient matrix for module 1b on module 1b's bridging fluxes.

*fullnormCj2rb_star* : Flux control coefficient matrix for module 1b on module 2 fluxes.

with variables following the alphabetic progression defined and accessible to the user if analyses with more than 2 type 1 modules are defined. Additional functions are included in the package which are accessible to the user including *ststSolMatFormR*, enabling the determination of steady state concentrations and fluxes of a pathway using the FindRoot Mathematica function, and *DispMat*, which enables matrices with row and column headers to be visualised in a more legible format.

## B.4 Model with 0 fluxes at steady state

The analysis was performed on a simple branched model shown in Figure B.1. The model was constructed such that the lower branch consisting of reactions v4, v6 and v8 is allowed to reach equilibrium. This was achieved by not fixing metabolite p2, essentially making the lower branch a "dead-end" branch where metabolites will accumulate until the flux through the branch declines to 0 where it remains at steady state. The modular decomposition was chosen such that metabolites x2 and x3 are considered components of module 1, reaction v3 is the only reaction within module 1, and the bridging reactions consist of reactions v2, v4 and v5, as shown in Figure B.1. The model components including ODEs, rate equations, parameters, and initial values are located in section A.4. Three significant digits will be displayed for the determined control coefficients.

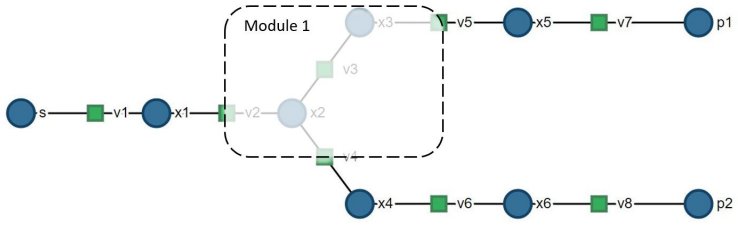


**Figure B.1:** Simple branched model with one branch allowed to reach equilibrium. Subsequently, the branch at equilibrium exhibits a 0 flux at steady state. The modular decomposition is as shown, with the type 1 module annotated as Module 1.

The presence of 0 fluxes results in numerical errors if left unaddressed prior to normalising the determined matrices, both manually and with the package. The numerical errors arise as a result of the need to invert steady state fluxes during the normalisation of several matrices, such as the flux control coefficient matrices. The inversion results in an error if the flux has a magnitude of 0 at steady state. Therefore, it was decided that the 0 fluxes were to be addressed during the construction of the inverse of the diagonal matrices where appropriate. This was achieved by checking the values of the fluxes at steady state to be added to the diagonal matrices and if the value is equivalent to 0,

including a value of 0 into the diagonal matrix of inverted values. If, however, the flux was not equivalent to 0 then the value was inverted and incorporated into the diagonal matrix. Inclusion of 0 was chosen as equilibrium reactions exert no control on fluxes and metabolite concentrations at steady state.

Following analysis of the model using the package, it was determined that not all modular control theorems were upheld, specifically the normalised concentration connectivity and normalised flux summation control theorems as can be seen in Table B.1.

**Table B.1:** The result for the steady state condition and modular control theorems as determined by the package following analysis of the model with 0 fluxes present.

```
{{"Steady State Condition"}, {True}}
{{"Concentration Summation-Unnormalised"}, {True}}
{{"Concentration Summation-Normalised"}, {True}}
{{"Concentration Connectivity-Unnormalised"}, {True}}
{{"Concentration Connectivity-Normalised"}, {False}}
{{"Flux Summation-Unnormalised"}, {True}}
{{"Flux Summation-Normalised"}, {False, False}}
{{"Flux Connectivity-Unnormalised"}, {True, True}}
{{"Flux Connectivity-Normalised"}, {True, True}}
```

Despite the control theorem violations being of concern, the control coefficients determined using the package were compared to those of the appropriate traditional control coefficients. This comparison proved beneficial despite the violations as it was determined that the control coefficients determined by the package achieved a maximum absolute difference in the order of magnitude of $10^{-10}$ from those determined using traditional MCA. This degree of accuracy is more than sufficient and subsequently the control theorems for the traditional control coefficients were also determined, with the aim of identifying if the control theorem violations observed during the modular control analysis were the result of the modular analysis alone, or if similar violations occur during MCA. The traditional control theorems exhibited identical violations to those identified in the modular control analysis. The normalised concentration connectivity theorem was determined to be violated as a result of the metabolites in the branch with a flux of 0 at steady state, namely metabolites $p2, x4, x6$ for the modular analysis. The normalised concentration connectivity theorem for the traditional MCA was determined to be similarly violated. The evaluation of the normalised flux summation theorem can be trivially upheld for the traditional control coefficients if performed using the normalised K matrix: $\mathbf{C}_I^J \cdot \mathbf{K} = \mathbf{K}$ where $\mathbf{C}_I^J$ is the matrix of normalised independent flux control

coefficients and $\mathbf{K}$ is the normalised K matrix. However, if the alternative method using multiplication by a vector of 1's is used, $\mathbf{C}_I^J \cdot \mathbf{1} = \mathbf{1}$, with $\mathbf{1}$ denoting a unit vector of 1 of appropriate length, then the flux summation theorem is determined to be violated. The method used in the package makes use of the unit vector of 1's and subsequently the normalised flux summation theorem is determined to be violated.

The control coefficients determined by the package are shown in Table B.2. Table B.2a shows the control coefficients determined for components of module 2, while Table B.2b shows the overall control coefficients determined for module 1.

**Table B.2:** Control coefficients determined by the package following analysis of the branched pathway with 0 fluxes present.

```
In[7]:= fullnormCs22 // DispMat
        fullnormCj22 // DispMat
        fullnormCjBa2 // DispMat
```

Out[7]//MatrixForm=

| _ | v1 | v6 | v7 | v8 | _ |
|---|---|---|---|---|---|
| p2[t] | 0.173 | 0. | -0.111 | 0. | p2[t] |
| x1[t] | 0.187 | 0. | -0.0422 | 0. | x1[t] |
| x4[t] | 0.173 | 0. | -0.111 | 0. | x4[t] |
| x5[t] | 0.114 | 0. | -0.408 | 0. | x5[t] |
| x6[t] | 0.173 | 0. | -0.111 | 0. | x6[t] |
| _ | v1 | v6 | v7 | v8 | _ |

Out[8]//MatrixForm=

| _ | v1 | v6 | v7 | v8 | _ |
|---|---|---|---|---|---|
| v1 | 0.23 | 0. | 0.174 | 0. | v1 |
| v6 | 0. | 0. | 0. | 0. | v6 |
| v7 | 0.23 | 0. | 0.174 | 0. | v7 |
| v8 | 0. | 0. | 0. | 0. | v8 |
| _ | v1 | v6 | v7 | v8 | _ |

Out[9]//MatrixForm=

| _ | v1 | v6 | v7 | v8 | _ |
|---|---|---|---|---|---|
| v2 | 0.23 | 0. | 0.174 | 0. | v2 |
| v4 | 0. | 0. | 0. | 0. | v4 |
| v5 | 0.23 | 0. | 0.174 | 0. | v5 |
| _ | v1 | v6 | v7 | v8 | _ |

**(a)** Module 2 control coefficients

```
In[10]:= fullnormCs2ra_star // DispMat
         fullnormCj2ra_star // DispMat
         fullnormCjBara_star // DispMat
```

Out[10]//MatrixForm=

| _ | Control of module 1a | _ |
|---|---|---|
| p2[t] | -0.0613 | p2[t] |
| x1[t] | -0.144 | x1[t] |
| x4[t] | -0.0613 | x4[t] |
| x5[t] | 0.294 | x5[t] |
| x6[t] | -0.0613 | x6[t] |
| _ | Control of module 1a | _ |

Out[11]//MatrixForm=

| _ | Control of module 1a | _ |
|---|---|---|
| v1 | 0.596 | v1 |
| v6 | 0. | v6 |
| v7 | 0.596 | v7 |
| v8 | 0. | v8 |
| _ | Control of module 1a | _ |

Out[12]//MatrixForm=

| _ | Control of module 1a | _ |
|---|---|---|
| v2 | 0.596 | v2 |
| v4 | 0. | v4 |
| v5 | 0.596 | v5 |
| _ | Control of module 1a | _ |

**(b)** Module 1 overall control coefficients

The reactions with fluxes of 0 at steady state were determined to have no control over any module 2 metabolites nor on the bridging and module 2 reactions. Similarly, neither the other module 2 reactions nor module 1 exert control on the reactions with 0 fluxes, which is to be expected. In this way, the package is capable of accurately analysing models with 0 fluxes at steady state. A similar problem which has been addressed is that of near-zero fluxes at steady state, as well as near-zero metabolite concentrations. While the inversion of numbers approaching zero (with magnitudes of $10^{-6}$

or lower) can be performed, the accuracy may not be maintained throughout the necessary calculations, particularly as reactions can be determined to be of magnitudes up to or smaller than $10^{-20}$ in some models. The concentration of metabolites may also be determined to be of magnitudes approaching zero further contributing to the accuracy concern. The cause for this accuracy concern is due to the numerical precision, however, this situation has been addressed and is described in the following section.

## B.5 Addressing near zero fluxes and metabolites

Near zero fluxes and metabolites pose an accuracy concern due to the numerical precision of the package, which is limited to machine precision equivalent to $10^{-16}$. For this reason it is possible control coefficients for reactions and metabolites with small magnitudes at steady state may not be accurate as they may require a greater degree of precision than is available.

Due to the accuracy of the control coefficients corresponding to fluxes and/or metabolites with near zero reaction rates or concentrations, respectively, being of concern, it was decided that a threshold of $10^{-6}$ would be used for the final control coefficients accessible by the user. Throughout the determination of the control coefficient matrices there are two instances where the construction of a diagonal matrix of the inverse of fluxes or metabolite concentrations is required and applied to the determined control coefficients. The first instance is during the normalisation of the control coefficient matrices. The diagonal matrices of the inverses of the fluxes or metabolite concentrations (as appropriate) are constructed while checking for equivalence to 0. If the flux or metabolite concentration is equivalent to zero, then 0 is included in the diagonal matrix, otherwise the inverse of the value is incorporated. The equivalence to zero is used at this point due to the downstream extension of the control coefficient matrices such that the controls on the independent bridging fluxes are extended to encompass all bridging fluxes. A similar extension is performed for the concentration control coefficients such that the control coefficients for all metabolites in module 2 are determined, as opposed to solely those corresponding to independent metabolites. As such, if the threshold is implemented at this point, rather than checking for equivalence to zero, the accuracy of control coefficients for dependent fluxes and metabolites may be negatively impacted if they are affected by reactions or metabolites with fluxes or concentrations below the threshold, despite themselves being above the threshold.

The second instance where the construction of a diagonal matrix of the

inverse of reaction rates and metabolite concentrations is required for the control coefficient matrices is during the extension of the independent control coefficients such that the control coefficients of all module 2 and bridging components are expressed. This is achieved during the normalisation of the Q matrix as well as the module 2 link matrix. In this way, the application of the threshold enables the flux and concentration control coefficients for reactions and metabolites with fluxes and concentrations below the threshold to be forced to zero, addressing the accuracy concern, while leaving the control coefficients of components with magnitudes above the threshold unaltered. This incorporation of the threshold results in the flux control coefficient matrices describing the control of module 2 reactions on their fluxes, as well as the type 1 module on module 2 fluxes, without the threshold having been implemented. This is due to a K matrix not being applied during the analysis. Therefore, a diagonal matrix is constructed and populated with either 1, or 0 along the diagonal, with 1 corresponding to module 2 reactions with fluxes with magnitudes above the threshold at steady state and 0 corresponding to fluxes with magnitudes below the threshold. The diagonal matrix is then multiplied by the matrices of flux control coefficients of module 2 reactions on their own fluxes, as well as the overall flux control coefficients of module 1 on module 2 fluxes. In this way, the flux control coefficients for reactions with near zero fluxes, as determined by the threshold, are treated in a manner comparable to the other flux and concentration control coefficients. As a result, the normalised control coefficients, as well as the normalised elasticity matrices, used during the control theorem calculations have been subjected to an equivalence check to 0, as required for the construction of the diagonal matrices of the inverse of fluxes and metabolites as appropriate. The full, normalised control coefficient matrices accessible to the user have been treated utilising the threshold as described. In this way, the treatment has been applied in a consistent manner for the control theorem tests as well as in a separate, consistent manner for the final, normalised control coefficient matrices describing the control of all components in module 2 as well as those bridging type 1 modules to module 2. A message is also presented to the user stating the fluxes and/or metabolites that have been affected by the incorporation of the threshold. In this way, the affected control coefficients are expressed as 0, with an accompanying message stating for which metabolites and fluxes the control coefficients were forced to 0. As such, the presence of metabolites and fluxes with near zero magnitudes at steady state has been addressed, enabling the package to perform analyses on models with such components present.

# List of References

[1] Schuster, S., Kahn, D. and Westerhoff, H.V.: Modular analysis of the control of complex metabolic pathways. *Biophys. Chem.*, vol. **48**, no. 1, pp. 1–17, 1993.

[2] Kang, H., Han, K. and Choi, M.Y.: Mathematical model for glucose regulation in the whole-body system. *Islets*, vol. 4, no. 2, pp. 84–93, 2012. ISSN 19382014.

[3] Snoep, J.L., Green, K., Eicher, J., Palm, D.C., Penkler, G., du Toit, F., Walters, N., Burger, R., Westerhoff, H.V. and van Niekerk, D.D.: Quantitative analysis of drug effects at the whole-body level: a case study for glucose metabolism in malaria patients. *Biochem. Soc. T.*, vol. **43**, no. 6, pp. 1157–1163, 11 2015.

[4] Xu, K., Morgan, K.T., Gehris, A.T., Elston, T.C. and Gomez, S.M.: A whole-body model for glycogen regulation reveals a critical role for substrate cycling in maintaining blood glucose homeostasis. *PLoS Comput. Biol.*, vol. 7, no. 12, 2011. ISSN 1553734X.

[5] Kacser, H. and Burns, J.A.: The control of flux. *Symposia of the Society for Experimental Biology*, vol. 27, pp. 65–104, 1973. ISSN 00811386.

[6] Brown, G.C., Hafner, R.P. and Brand, M.D.: A "top-down" approach to the determination of control coefficients in metabolic control theory. *Eur. J. Biochem.*, vol. **188**, no. 2, pp. 321–325, 1990.

[7] Hofmeyr, J.H.S. and Westerhoff, H.V.: Building the cellular puzzle: Control in multi-level reaction networks. *Journal of Theoretical Biology*, vol. 208, no. 3, pp. 261–285, 2001. ISSN 00225193.

[8] WHO: *World malaria report 2019*. World Health Organization, 2019.

[9] White, N.J., Pukrittayakamee, S., Hien, T.T., Faiz, M.A., Mokuolu, O.A. and Dondorp, A.M.: Malaria. *The Lancet*, vol. 383, no. 9918, pp. 723–735, 2014. ISSN 1474547X.

[10] Leopold, S.J., Ghose, A., Allman, E.L., Kingston, H.W.F., Hossain, A., Dutta, A.K., Plewes, K., Chotivanich, K., Day, N.P.J., Tarning, J., Winterberg, M., White, N.J., Llinás, M. and Dondorp, A.M.: Identifying the Components of Acidosis in Patients With Severe *Plasmodium falciparum* Malaria Using Metabolomics. *The Journal of Infectious Diseases*, vol. **219**, pp. 1766–1776, 2019.

[11] Penkler, G., Du Toit, F., Adams, W., Rautenbach, M., Palm, D.C., Van Niekerk, D.D. and Snoep, J.L.: Construction and validation of a detailed kinetic model of glycolysis in *Plasmodium falciparum*. *FEBS J.*, vol. **282**, no. 8, pp. 1481–1511, 2015.

[12] du Toit, F.: *Modeling glycolysis in Plasmodium-infected erythrocytes*. Ph.D. thesis, University of Stellenbosch, 2015.

[13] Geenen, S., Taylor, P.N., Snoep, J.L., Wilson, I.D., Kenna, J.G. and Westerhoff, H.V.: Systems biology tools for toxicology. *Archives of Toxicology*, vol. 86, no. 8, pp. 1251–1271, 2012. ISSN 03405761.

[14] Nielsen, J.: Systems Biology of Metabolism. *Annual Review of Biochemistry*, vol. 86, no. 1, pp. 245–275, 2017. ISSN 0066-4154.

[15] Orth, Jeffrey D., Ines Thiele, B.Ø.P.: What is flux balance analysis? *Nat. Biotechnol.*, vol. 28, no. 3, pp. 245–248, 2010. ISSN 1546-1696.

[16] Zanghellini, J., Ruckerbauer, D.E., Hanscho, M. and Jungreuthmayer, C.: Elementary flux modes in a nutshell: Properties, calculation and applications. *Biotechnol. J.*, vol. 8, no. 9, pp. 1009–1016, 2013. ISSN 18606768.

[17] Fell, D.A.: Metabolic control analysis: A survey of its theoretical and experimental development. *Biochemical Journal*, vol. 286, no. 2, pp. 313–330, 1992. ISSN 02646021.

[18] Jensen, P.R., Van Der Weijden, C.C., Jensen, L.B., Westerhoff, H.V. and Snoep, J.L.: Extensive regulation compromises the extent to which DNA gyrase controls dna supercoiling and growth rate of Escherichia coli. *European Journal of Biochemistry*, vol. 266, no. 3, pp. 865–877, 1999. ISSN 00142956.

[19] Hofmeyr, J.-H.S.: Metabolic control analysis in a nutshell. *Proc. 2nd Int. Conf. Syst. Biol.*, , no. ii, pp. 291–300, 2001.
Available at: `http://www.siliconcell.net/sica/NWO-CLS/CellMath/OiOvoer/Hofmeyr_nutshell.pdf`

[20] Moreno-Sanchez, R., Saavedra, E., Rodriguez-Enriquez, S. and Olin, M.: Metabolic control analysis: A tool for designing strategies to manipulate

metabolic pathways. *Journal of biomedicine & biotechnology*, vol. 2008, p. 597913, 07 2008.

[21] Heinrich, R. and Rapoport, T.A.: A Linear Steady-State Treatment of Enzymatic Chains: General Properties, Control and Effector Strength. *European Journal of Biochemistry*, vol. 42, no. 1, pp. 89–95, 1974. ISSN 14321033.

[22] Bakker, B.M., Michels, P.A., Opperdoes, F.R. and Westerhoff, H.V.: What controls glycolysis in bloodstream form Trypanosoma brucei? *Journal of Biological Chemistry*, vol. 274, no. 21, pp. 14551–14559, 1999. ISSN 00219258.

[23] Smallbone, K., Messiha, H.L., Carroll, K.M., Winder, C.L., Malys, N., Dunn, W.B., Murabito, E., Swainston, N., Dada, J.O., Khan, F., Pir, P., Simeonidis, E., Spasić, I., Wishart, J., Weichart, D., Hayes, N.W., Jameson, D., Broomhead, D.S., Oliver, S.G., Gaskell, S.J., McCarthy, J.E., Paton, N.W., Westerhoff, H.V., Kell, D.B. and Mendes, P.: A model of yeast glycolysis based on a consistent kinetic characterisation of all its enzymes. *FEBS Letters*, vol. 587, no. 17, pp. 2832–2841, 2013. ISSN 00145793.

[24] Brand, M.D.: Top down metabolic control analysis. *Journal of Theoretical Biology*, vol. 182, no. 3, pp. 351–360, 1996. ISSN 00225193.

[25] Simpson, T.W., Shimizu, H. and Stephanopoulos, G.: Experimental determination of group flux control coefficients in metabolic networks. *Biotechnology and Bioengineering*, vol. 58, no. 2-3, pp. 149–153, 1998. ISSN 00063592.

[26] Kacser, H. and Small, J.R.: Responses of metabolic systems to large changes in enzyme activities and effectors. 2. The linear treatment of branched pathways and metabolite concentrations. Assessment of the general non-linear case. *European Journal of Biochemistry*, vol. 213, pp. 625–640, 1993.

[27] Ciapaite, J., Bakker, S.J.L., Van Eikenhorst, G., Wagner, M.J., Teerlink, T., Schalkwijk, C.G., Fodor, M., Ouwens, D.M., Diamant, M., Heine, R.J., Westerhoff, H.V. and Krab, K.: Functioning of oxidative phosphorylation in liver mitochondria of high-fat diet fed rats. *Biochimica et Biophysica Acta - Molecular Basis of Disease*, vol. 1772, no. 3, pp. 307–316, 2007. ISSN 09254439.

[28] Schuster, S.: Use and Limitations of Modular Metabolic Control Analysis in Medicine and Biotechnology. *Metab. Eng.*, vol. **1**, no. 3, pp. 232–242, 1999.

[29] Kahn, D. and Westerhoff, H.V.: Control theory of regulatory cascades. *Journal of Theoretical Biology*, vol. 153, no. 2, pp. 255–285, 1991. ISSN 10958541.

[30] Snoep, J.L., Van Der Weijden, C.C., Andersen, H.W., Westerhoff, H.V. and Jensen, P.R.: DNA supercoiling in Escherichia coli is under tight and subtle homeostatic control, involving gene-expression and metabolic regulation of both topoisomerase I and DNA gyrase. *European Journal of Biochemistry*, vol. 269, no. 6, pp. 1662–1669, 2002. ISSN 00142956.

[31] Westerhoff, H.V., Getz, W.M., Bruggeman, F., Hofmeyr, J.H.S., Rohwer, J.M. and Snoep, J.L.: ECA: Control in ecosystems. *Molecular Biology Reports*, vol. 29, no. 1-2, pp. 113–117, 2002. ISSN 03014851.

[32] Bruggeman, F.J., Snoep, J.L. and Westerhoff, H.V.: Control, responses and modularity of cellular regulatory networks: A control analysis perspective. In: *IET Systems Biology*, vol. 2, pp. 397–410. 2008.

[33] Heinrich, R. and Schuster, S.: *The Regulation of Cellular Systems*. Springer US, 2012.

[34] Schuster, S. and Westerhoff, H.V.: Modular control analysis of slipping enzymes. *BioSystems*, vol. 49, no. 1, pp. 1–15, 1999. ISSN 03032647.

[35] Groeneveld, P. and Westerhoff, H.: *Modular control analysis: are membranes or cytosol more important for growth for the industrial yeast Kluyweromyces marxianus?*, pp. 277–284. Stellenbosch University Press, 2000. Gebeurtenis: BTK-2000 Stellenbosch.

[36] Talapko, J., Škrlec, I., Alebić, T., Jukić, M. and Včev, A.: Malaria: The past and the present. *Microorganisms*, vol. 7, no. 6, 2019. ISSN 20762607.

[37] Mulquiney, P.J., Bubb, W.A. and Kuchel, P.W.: Model of 2,3-bisphosphoglycerate metabolism in the human erythrocyte based on detailed enzyme kinetic equations: In vivo kinetic characterization of 2,3-bisphosphoglycerate synthase/phosphatase using 13C and 31P NMR. *Biochemical Journal*, vol. **342**, no. 3, pp. 567–580, 1999. ISSN 02646021.

[38] Mulquiney, P.J. and Kuchel, P.W.: Model of 2,3-bisphosphoglycerate metabolism in the human erythrocyte based on detailed enzyme kinetic equations: Equations and parameter refinement. *Biochemical Journal*, vol. **342**, no. 3, pp. 581–596, 1999. ISSN 02646021.

[39] Mulquiney, P.J. and Kuchel, P.W.: Computer simulation and Metabolic Control Analysis. *Biochemical Journal*, vol. **342**, no. 3, pp. 597–604, 1999.

[40] Westerhoff, H.V., Groen, A.K. and Wanders, R.J.A.: The thermodynamic basis for the partial control of oxidative phosphorylation by the adenine-nucleotide translocator. *Biochem. Soc. T.*, vol. **11**, no. 1, pp. 90–91, 1983.

[41] Reder, C.: Metabolic control theory: A structural approach. *J. Theor. Biol.*, vol. 135, no. 2, pp. 175–201, 1988. ISSN 10958541.